AN ANALYSIS OF MULTIREFLECTOR OPTICAL RESONATORS

Thesis by

Peter Osgoode Clark

In Partial Fulfillment of the Requirements

For the Degree of

Doctor of Philosophy

California Institute of Technology

Pasadena, California

1964

(Submitted March 10, 1964)

ACKNOWLEDGEMENTS

The author would like to extend his sincere appreciation to Dr. Nicholas George for his guidance and encouragement throughout the course of this research.

The author wishes to thank Mrs. Olive List who typed the manuscript, Mrs. Martha Lamson who assisted with the computer programming and Mrs. Melanie Loosli who did the art work. The financial support of a California Institute of Technology scholarship and an IBM fellowship are gratefully acknowledged.

ABSTRACT

Geometrical optics and self-consistent field techniques are used to determine the properties of multireflector optical resonators in which the field distributions are multiply-reflected and travel in clockwise and counter-clockwise directions in the cavity. Two types of resonators are considered, a symmetric N-mirror resonator whose axis is a regular N-sided polygon and a nonsymmetric four-mirror resonator whose axis is a parallelogram.

The geometrical optics approach leads to sets of coupled nonlinear difference equations which describe the paths of optical rays in the resonators. Approximate solutions to the equations are obtained and a calculation of the first correction term is carried out in the case of the symmetric cavity. It is shown that the approximate analysis may also be formulated in a chain matrix representation. Stability conditions are obtained which determine the mirror curvatures and spacings for high or low-loss multireflector resonators. The set of difference equations may be reduced to recurrence relations which enable the path of an optical ray in the cavity to be calculated exactly using a digital computer.

Integral equations are obtained which determine the mode distributions in the symmetric N-mirror and nonsymmetric four-mirror cavities. The equations are not solved exactly except in the particular case of a "pseudo-confocal" symmetric resonator which has nonspherical mirrors. Solutions to the general integral equations are

determined in the zero wavelength limit. Resonance conditions and detailed descriptions of the field distributions are obtained for both the symmetric and nonsymmetric resonators. For the particular cases of the symmetric three and four-mirror resonators the diffraction losses are obtained by transforming the integral equations to a form such that existing numerical solutions may be used.

Two-mirror cavities are treated as simplifications of the multireflector theory. The results of other authors are obtained and extended. The expressions for the resonance condition and minimum mode volume for the symmetric nonconfocal resonator are found to differ slightly from those previously derived. Amplitude and phase distributions throughout the volume of a plane-parallel Fabry-Perot resonator are calculated numerically on an IBM 7090 computer.

TABLE OF CONTENTS

CHAPTER	SECTION	TITLE	PAGE
I		INTRODUCTION	1
	1.1	A Brief History of Laser Development	1
	1.2	A Survey of Previous Contributions to the Theory of Optical Resonators	3
	1.3	Content of this Paper	6
II		THE GEOMETRICAL OPTICS OF MULTIREFLECTOR OPTICAL RESONATORS	8
	2.1	The Symmetric N-Mirror Resonator	8
	2.1a	Mirror-Lens Equivalence	8
	2.1b	Difference Equation Formulation	10
	2.1c	Approximate Solutions and Stability Conditions	12
	2.1d	Derivation of the Stability Condition from a Consideration of Lens Astigmatism	15
	2.1e	Matrix Formulation of the Approximate Solution	16
	2.1f	Iterative Corrections to the Approximate Solutions	18
	2.1g	Exact Numerical Solution	20
	2.2	The Nonsymmetric Four-Mirror Resonator	20
	2.2a	Difference Equation Formulation	20
	2.2b	Approximate Solutions and Stability Conditions	22
	2.2c	Matrix Formulation of the Approximate Solutions	26

CHAPTER	SECTION	TITLE	PAGE
	2.2d	First Order Iterative Corrections to the Approximate Solutions	28
III		THE CONCEPT OF SELF-CONSISTENT FIELD ANALYSIS	29
	3.1	Formulation of the Problem	29
	3.1a	Description of the Fields in Terms of Travelling Waves	29
	3.1b	Boundary Conditions and Consideration of an Arbitrarily Polarized Field	29
	3.1c	Vector Green's Theorem Derivation of an Integral Equation for the Fields in a Symmetric Resonator	31
	3.1d	Integral Equation for the Fields in a Nonsymmetric Resonator	37
	3.2	Solutions of the Integral Equation	39
IV		THE SELF-CONSISTENT FIELD ANALYSIS OF MULTIREFLECTOR OPTICAL RESONATORS	42
	4.1	The Symmetric N-Mirror Resonator	42
	4.1.1	Formulation of the Problem	42
	4.1.2	Two Special Cases	46
	4.1.2a	$\ell \gg b$	46
	4.1.2b	Pseudo-Confocal Resonator	49
	4.1.3	General Case	53
	4.1.3a	Modes of the Resonator	53
	4.1.3b	Resonance Conditions	55
	4.1.3c	Electric Field at an Arbitrary Point in the Resonator	56
	4.1.3d	Nodal Surfaces	62

CHAPTER	SECTION	TITLE	PAGE
	4.1.3e	Mode Dimensions and Mode Volume	64
	4.1.3f	Numerical Solutions	65
	4.2	The Nonsymmetric Four-Mirror Resonator	72
	4.2a	Modes of the Resonator	72
	4.2b	Resonance Conditions	83
	4.2c	Electric Field at an Arbitrary Point in the Resonator	85
	4.2d	Nodal Surfaces	89
	4.2e	Mode Dimensions and Mode Volume	90
V		THE SELF-CONSISTENT FIELD ANALYSIS OF THE TWO-MIRROR RESONATOR	92
	5.1	Symmetric, Nonconfocal Resonator	92
	5.1a	Modes of the Resonator	92
	5.1b	Resonance Conditions and Diffraction Losses	94
	5.1c	Electric Field at an Arbitrary Point in the Resonator	96
	5.1d	Nodal Surfaces	99
	5.1e	Mode Dimensions and Mode Volume	103
	5.2	Confocal Resonator	105
	5.2a	Approximate Solution	105
	5.2b	Exact Solution	108
	5.3	Nonsymmetric, Nonconfocal Resonator	109
	5.3a	Modes of the Resonator	109
	5.3b	Resonance Conditions	112

CHAPTER	SECTION	TITLE	PAGE
	5.3c	Electric Field at an Arbitrary Point in the Resonator	113
	5.3d	Nodal Surfaces	116
	5.3e	Mode Dimensions and Mode Volume	118
	5.4	Plane-Parallel and Concentric Resonators	120
	5.4a	Equivalence of the Plane-Parallel and Concentric Resonators	120
	5.4b	Electric Field in the Plane-Parallel Resonator	122
VI		SUMMARY AND CONCLUSIONS	130
Appendix 1		First Order Iterative Corrections to the Approximate Solutions of the Difference Equations Governing the Path of a Ray in a Symmetric N-Mirror Resonator	133
Appendix 2		An Expression for the Vectors $\underline{\underline{E}}$ and $\underline{\underline{H}}$ at an Interior Point in Terms of the Values of $\underline{E}$ and $\underline{H}$ Over an Enclosing Surface (45)	136
Appendix 3		Propagation in Rotating Systems (47)	139
Appendix 4		Solution of the General Integral Equation	142
Appendix 5		Approximation to the Lowest Order Eigenvalue for the Symmetric, Nonconfocal Two-Mirror Resonator	145
References			148

CHAPTER I

INTRODUCTION

1.1 A Brief History of Laser Development

In 1958 Schawlow and Townes (1), Prokhorov (2), and Dicke (3) independently proposed that maser concepts (4) could be extended to the optical and infrared regions of the spectrum. They realized that at these high frequencies the extremely monochromatic radiation and coherent amplification which are characteristic of atomic and molecular oscillators and amplifiers would be great value in many areas of scientific interest.

Two years later Maiman (5,6) announced laser action ("microwave" is replaced by "light" in the acronym maser) in ruby at 6943 $\mathring{A}$. This was followed by the He-Ne laser (1.153μ) developed by Javan et al (7) in 1961. The same year Snitzer (8) obtained laser action at 1.06μ in Nd^{3+} - doped glass. The first semi-conductor laser (GaAs at 8400$\mathring{A}$) was announced almost simultaneously by three different groups in 1962 (9,10,11), a circumstance which clearly indicates the large amount of research being performed in the laser field.

The preceding examples represent the first optical masers in four different classes of materials : single crystals, gases, amorphous hosts, and semi-conductors. In each group the initial laser has been joined by many others. The rate of development in this area is so great that no attempt will be made here to list all known examples of laser action. The interested reader is referred to the recent

literature and to the many available review articles and bibliographies [see, for example, (12,13,14,15)].

Research in the laser field has not been restricted solely to the search for new "laser lines". Basic knowledge concerning the optical and infrared properties of matter has been obtained with the laser as well as because of it. A new field of physics, that of non-linear optics, has been opened up and Raman spectroscopy has received new interest. Gaseous lasers have made possible ultra-high resolution spectroscopy in the infrared range and have been proposed as precise measuring devices in gravitational and seismological experiments. The development of the giant-pulse or Q-switched laser (16) has led to new investigations of the interaction of high-energy light beams with matter. Naturally the commercial aspects of lasers have not been neglected. An extremely large portion of present research is devoted to optical communication systems and high resolution radars, and high-power pulsed lasers have been used in a variety of applications ranging from micro-welding and machining to an investigation of the destruction of cancer cells.

One could speculate indefinitely about the future of the optical maser. As a tool for basic research it will definitely achieve the status of the microwave and optical techniques which proceeded it. However the rate of development has been so great that no one can predict with certainty which will be the most important applications nor which will be of greatest commercial value.

1.2 A Survey of Previous Contributions to the Theory of Optical Resonators

The basic model for a laser is one in which light is coherently amplified as it travels through an active medium. The gain per unit length of such media is so small that in order to achieve appreciable amplification the path length would be prohibitively long. To avoid this the laser material is placed in a resonant structure such that the radiation passes through the same volume of material many times, each time being amplified, before it escapes from the resonator.

The resonant frequency of a cavity is determined by the requirement that characteristic dimensions of the cavity be of the order of a half wavelength. In the microwave and even the millimeter-wave regions the problems of constructing such a resonator are easily overcome. However at optical and infrared frequencies the cavity dimensions are of necessity very much greater than a wavelength and consequently the resonance condition is satisfied for a wide range of frequencies. Since the gain of the active medium is small it is necessary that the loss of the cavity be minimized. The narrow cavity linewidths which are associated with such low-loss or high-Q resonators are much less than the linewidths of the atomic or molecular transitions involved in the laser process. As a result it is possible for light at several closely spaced frequencies to simultaneously satisfy the resonance condition for the cavity and experience sufficient amplification to sustain oscillation. There may exist non-linearities which would allow the most favored mode to suppress oscillation in those which are less

favored. However the spacing of the modes is sufficiently small that very small changes in cavity dimensions or other characteristics may cause the oscillation to shift from one mode to another with accompanying changes in frequency.

The first considerations of the multiresonant properties of the electromagnetic fields in a closed resonator were made by Rayleigh in 1900 and Jeans in 1905. They independently showed that the number of modes of oscillation per unit volume in a wavelength interval $d\lambda$ is given by $\frac{8\pi d\lambda}{\lambda^4}$. The derivation of Planck's black-body radiation law follows directly from the representation of the electromagnetic field inside a cavity as a number of independent harmonic oscillators corresponding to the various normal modes of oscillation of the cavity and having the energy distribution determined by Planck in 1901.

The original proposals for infrared and optical masers (1,2,3) suggested the plane-parallel Fabry-Perot interferometer (17) as a resonator. In their paper Schawlow and Townes presented the initial analysis of such a multimode cavity and suggested methods of mode selection. In 1961 self-consistent numerical calculations by Fox and Li (18) showed that after light is reflected back and forth many times in the Fabry-Perot interferometer a state is reached in which the relative field distribution does not vary and the amplitude decays at an exponential rate. Such steady-state field distributions are regarded as normal modes of the resonator. It was found that the diffraction losses of low order modes of this type are significantly less than those arrived at by the Schawlow-Townes analysis.

At the same time Boyd and Gordon (19) presented an analytic description of an open resonator formed by two identical spherical reflectors separated by a distance equal to the common radius of curvature. The use of two confocal mirrors as an interferometer had previously been described by Connes (20,21). In their paper Boyd and Gordon also included a treatment of symmetric nonconfocal resonators.

The following year Boyd and Kogelnik (22) extended the analysis of resonators with spherical reflectors to nonsymmetric cases. Goubau and Schwering (23) had previously investigated the guided propagation of electromagnetic wave beams and some of their results are applicable to the analysis of open cavities. The nonconfocal resonator was also treated numerically by Fox and Li (24) and by Soohoo (25).

The self-consistent field analysis initiated by Fox and Li (18) leads to integral equations which cannot be solved in general. Tang (26) and Culshaw (27) attempted to apply variational techniques to these equations, however it was later pointed out that their results are inconclusive (28,29).

Several other approaches to the analysis of Fabry-Perot resonators have been followed. Kotik and Newstein (30) and Barone (31) have investigated the problem by describing the cavity fields in terms of plane-wave spectra (32). Vaĭnshteĭn (33) has developed an analysis for open resonators which is based on a rigorous theory of diffraction at the open end of a waveguide. Zimmerer (34) has shown that the spherical mirror Fabry-Perot resonator may be derived from an oblate spheroidal resonator and Specht (35) has completed an analysis of spherical

mirror cavities in an oblate spheroidal coordinate system which is valid at optical wavelengths.

For gas lasers the existing optical resonator theories have been entirely adequate but with solid state lasers in which the resonator is formed by depositing highly reflecting coatings on the plane parallel ends of the crystal there has been little consistent agreement between experimental observations of the field distributions and resonant frequencies and the theoretical predictions. Recent experiments by Evtuhov (36) provide an explanation for this discrepancy. He found that ruby crystals with nominally plane parallel faces appear to have curved surfaces when examined in a Twyman-Green interferometer. This effective curvature arises from the spatial variation of the refractive index throughout the crystals. Reinterpretation of the solid state resonator in terms of spherical rather than plane mirrors leads to close agreement between experiment and theory.

1.3 Content of this Paper

This paper extends the analysis of optical resonators to symmetric and nonsymmetric structures where the steady state field distributions are formed by the constructive interference of waves which are multiply-reflected and travel in clockwise and counterclockwise directions in the cavity rather than back and forth between two mirrors. Two approaches to the problem are presented, a geometrical optics method and a self-consistent field analysis.

In Chapter II the methods of geometrical optics are used to

describe the path of a ray in the resonator. This approach leads to a set of coupled, non-linear difference equations which, with one valid approximation, are easily linearized. This approximation also allows the description of the resonator to be written in a chain matrix representation. Relations among the resonator parameters which are necessary for stable operation are obtained.

A derivation of the integral equation for the fields in a symmetric multireflector resonator based on the vector Green's theorem is presented in Chapter III. The analysis is also extended to non-symmetric resonators. The integral equations are discussed and solutions are given.

Chapter IV contains analyses of symmetric N-mirror and non-symmetric four-mirror cavities based on the notions of Chapter III and valid for very small wavelengths. A complete description of the normal modes and resonator fields is obtained as well as the resonance conditions. The diffraction losses for symmetric three and four-mirror cavities are computed from available numerical solutions of the integral equations.

In Chapter V two-mirror resonators are treated as simplifications of the more complicated multireflector systems of Chapter IV. The results of Boyd and Gordon (19) and Boyd and Kogelnik (22) are obtained and extended. The field distribution in the plane parallel resonator which cannot be described analytically is computed numerically on an IBM 7090 computer.

CHAPTER II

THE GEOMETRICAL OPTICS OF MULTIREFLECTOR OPTICAL RESONATORS

2.1 The Symmetric N-Mirror Resonator

2.1a Mirror-Lens Equivalence

Several sections of a resonant structure using N identical, evenly-spaced, spherical reflectors are represented in Figure 2.1. The center-to-center spacing of the mirrors is ℓ and their common radius of curvature is b. The axis of the resonator is the N-sided regular polygon formed by a line joining the centers of consecutive mirrors. In order that the polygon be closed it is necessary that the tilt angle α, defined as the angle between the resonator axis and the normal to a reflector at its center, satisfy the condition

$$\alpha = \frac{N-2}{2N}\pi \tag{2.1}$$

For the usual situation in which the reflector separation is much greater than the reflector diameter, a spherical reflector with radius b and tilt angle α can be replaced by an equivalent lens. The distance to the point of intersection of a focussed ray and the lens axis is made equal to the distance to the point of intersection between the corresponding reflected ray and the axis in the reflector system. Distances are measured along the axes of the respective systems.

Figure 2.2 illustrates the geometry of the equivalent reflector and lens systems. Angles such that a ray must be rotated in a clockwise manner to coincide with the axis are defined as positive.

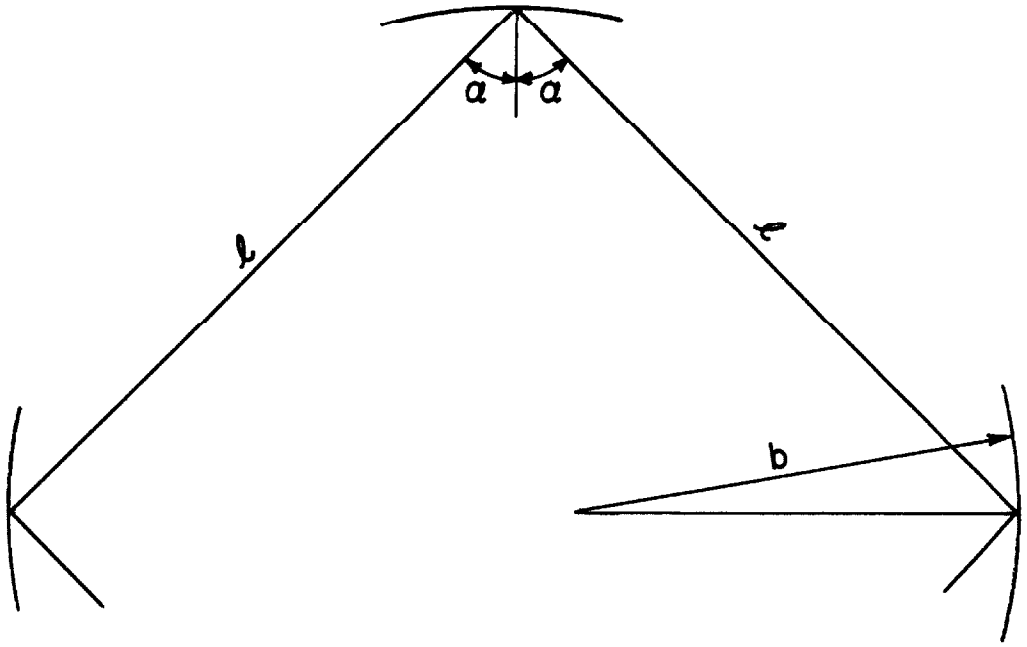

Fig. 2.1 A portion of a symmetric N-mirror resonator.

For paraxial rays the following relationships can easily be obtained from Figure 2.2:

$$\alpha + \frac{c}{b} = \gamma + \theta \tag{2.1a}$$

$$\alpha + \beta = \theta + \frac{c}{b} \tag{2.1b}$$

$$\beta = -\gamma' \tag{2.1c}$$

These equations are easily solved to give

$$\gamma - \gamma' = \frac{2c}{b} \tag{2.2}$$

A closed system with N identical, evenly spaced, spherical reflectors can now be represented as in Figure 2.3, where the oblique lines correspond to the positions of the equivalent lenses. ℓ is the center-to-center spacing; r_n and s_n are the heights of the ray at the reflector or lens surfaces measured perpendicular to the axis, and r_n' and s_n' are the slopes of the ray reflected from a mirror or emerging from an equivalent lens measured relative to the axis of the system.

2.1b Difference Equation Formulation

For small angles $\tan \gamma \simeq \gamma$ where $\tan \gamma$ is the slope of a ray previously defined as r_n' or s_n'. Also $c \cos \alpha = r_n$ or s_n. With the substitution of these relations into 2.2 one obtains from Figure 2.3 the following set of difference equations which describe the path of a

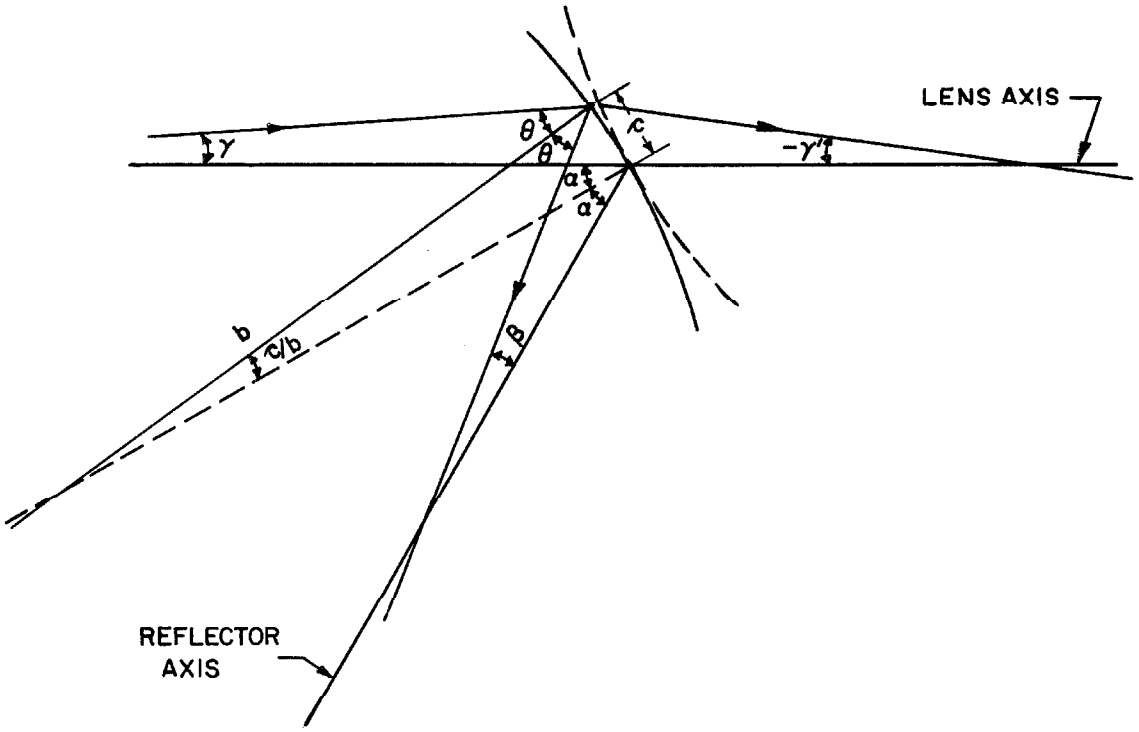

Fig. 2.2 Equivalent reflector and lens systems.

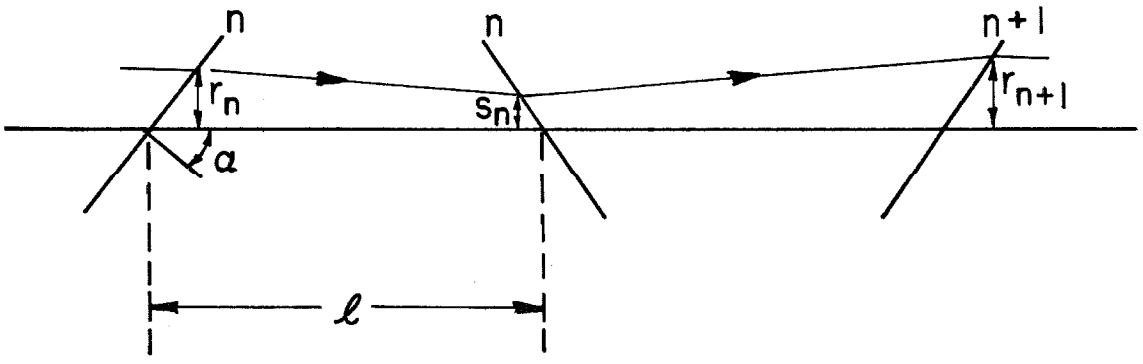

Fig. 2.3 Equivalent lens representation of the symmetric resonator.

ray in the cavity or through the equivalent lens system:

$$s_n - r_n = r'_n \left[\ell - (r_n + s_n) \tan \alpha \right] \tag{2.3a}$$

$$r_{n+1} - s_n = s'_n \left[\ell + (r_{n+1} + s_n) \tan \alpha \right] \tag{2.3b}$$

$$r'_n - s'_n = \frac{2s_n}{b \cos \alpha} \tag{2.3c}$$

$$s'_n - r'_{n+1} = \frac{2r_{n+1}}{b \cos \alpha} \tag{2.3d}$$

Exact analytical solutions to this set of simultaneous, non-linear difference equations have not been obtained.

2.1c Approximate Solutions and Stability Conditions

Since $\ell \gg (r_n + s_n) \tan \alpha$ a good approximation to the solution of the difference equations may be obtained by neglecting these terms in 2.3a and 2.3b:

$$s_n^{(o)} - r_n^{(o)} = r_n^{(o)'} \ell \tag{2.4a}$$

$$r_{n+1}^{(o)} - s_n^{(o)} = s_n^{(o)'} \ell \tag{2.4b}$$

$$r_n^{(o)'} - s_n^{(o)'} = \frac{2s_n^{(o)}}{b \cos \alpha} \tag{2.4c}$$

$$s_n^{(o)'} - r_{n+1}^{(o)'} = \frac{2r_{n+1}^{(o)}}{b \cos \alpha} \tag{2.4d}$$

Elimination of three variables leads directly to a linear, homogeneous difference equation for the approximate solution $r_n^{(o)}$:

$$r_{n+2}^{(o)} - 2\left[2\left(1 - \frac{\ell}{b \cos \alpha}\right)^2 - 1\right] r_{n+1}^{(o)} + r_n^{(o)} = 0 \qquad (2.5)$$

An identical equation for $s_n^{(o)}$ could also be written since omission of the last terms in 2.3a and 2.3b removes the distinction between $r_n^{(o)}$ and $s_n^{(o)}$.

Define

$$2\left(1 - \frac{\ell}{b \cos \alpha}\right)^2 - 1 = \cos \theta \qquad (2.6)$$

then $r_n^{(o)}$ will remain finite and have the form (37)

$$r_n^{(o)} = c_1^{(o)} \cos n\theta + c_2^{(o)} \sin n\theta \qquad (2.7)$$

provided that

$$0 \leq \left(1 - \frac{\ell}{b \cos \alpha}\right)^2 \leq 1 \qquad (2.8)$$

If convex mirrors are excluded 2.8 becomes

$$0 \leq \frac{\ell}{b \cos \alpha} \leq 2 \qquad (2.9)$$

The other quantities $s_n^{(o)}$, $s_n^{(o)'}$, $r_n^{(o)'}$ can be obtained in

terms of $s_n^{(o)}$:

$$s_n^{(o)} = \frac{r_n^{(o)} + r_{n+1}^{(o)}}{2 \cos \frac{\theta}{2}} \tag{2.10}$$

$$s_n^{(o)'} = \frac{s_{n+1}^{(o)} + (1-2 \cos \frac{\theta}{2})\, s_n^{(o)}}{2\ell \cos \frac{\theta}{2}} \tag{2.11}$$

$$r_n^{(o)'} = \frac{(2 \cos \frac{\theta}{2} - 1)\, s_n^{(o)} - s_{n-1}^{(o)}}{2\ell \cos \frac{\theta}{2}} \tag{2.12}$$

In order to complete the description of the ray path in the resonator it is necessary to include two boundary conditions. For example let $r_o^{(o)} = d_1$ and $s_o^{(o)} = d_2$. Then from 2.7 and 2.10

$$r_n^{(o)} = \frac{d_2 \sin n\theta - d_1 \sin (n - \frac{1}{2})\, \theta}{\sin \frac{\theta}{2}} \tag{2.13}$$

$$s_n^{(o)} = \frac{d_2 \sin (n + \frac{1}{2})\theta - d_1 \sin n\theta}{\sin \frac{\theta}{2}} \tag{2.14}$$

Provided that the stability condition 2.9 is satisfied these equations give the perpendicular distance of the ray from the axis as it is incident for the nth time on two consecutive mirrors in the resonator.

2.1d Derivation of the Stability Condition from a Consideration of Lens Astigmatism

The stability condition for the symmetric N-mirror resonator may be obtained without setting up the difference equations which describe the path of a ray in the resonator. This is accomplished by noting that an on-axis point in the resonator is an off-axis point for each mirror (or lens). The resonator axis and a normal to the reflector at its center correspond respectively to the oblique principal ray and the principal axis of the single lens.

The astigmatism of a lens (38) is specified relative to two principal planes, the tangential or primary plane described by the oblique principal ray and the principal axis and the sagittal or secondary plane which is perpendicular to the tangential plane. When rays from an off-axis point fall on the lens different amounts of convergence are introduced in the tangential and sagittal planes. As a consequence rays lying in the primary plane come to one focus and those lying in the secondary plane come to another.

If the angle between the oblique principal ray and the principal axis is α, it can be shown that for off-axis points the lens is characterized by two principal focal lengths:

tangential focal length $$f_t = f \cos \alpha \qquad (2.15)$$

sagittal focal length $$f_s = \frac{f}{\cos \alpha} \qquad (2.16)$$

where f is the focal length for on-axis object points.

Pierce (39) has shown that for stable propagation through a series of parallel lenses of focal length f and spacing ℓ it is necessary that

$$0 \leq \frac{\ell}{f} \leq 4 \tag{2.17}$$

It is evident from Figure 2.3 that the stability of the resonator will be determined by the behavior of a ray in the tangential plane (i.e. the plane of the diagram). A spherical reflector with radius of curvature b has a focal length of $\frac{b}{2}$ for on-axis object points, hence substitution of 2.15 into 2.17 gives

$$0 \leq \frac{\ell}{b \cos \alpha} \leq 2 \tag{2.9}$$

This is the same condition derived earlier in Section 2.1c from the requirement that solutions to the difference equations remain finite.

2.1e Matrix Formulation of the Approximate Solution

The linear equations 2.4a to 2.4b which result when the nonlinear terms in 2.3a and 2.3b are neglected may be written in matrix form,

$$\begin{pmatrix} r_n^{(o)} \\ r_n^{(o)'} \end{pmatrix} = \begin{pmatrix} 1 & \ell \\ -\frac{2}{b \cos \alpha} & 1 - \frac{2\ell}{b \cos \alpha} \end{pmatrix}^2 \begin{pmatrix} r_{n-1}^{(o)} \\ r_{n-1}^{(o)'} \end{pmatrix} \tag{2.18}$$

The transformation matrix appears as a squared matrix since the linearizing approximations have removed the difference between $r_n^{(o)}$ and $s_n^{(o)}$.

Since it relates "input" and "output" parameters the transformation matrix corresponds to the chain matrix of linear circuit theory (40) and displays similar properties. One of these properties is that the chain matrix for a cascaded series of quadrupoles is equal to the product of the chain matrices of the component quadrupoles, hence from equation 2.18

$$\begin{pmatrix} r_n^{(o)} \\ r_n^{(o)'} \end{pmatrix} = \begin{pmatrix} 1 & \ell \\ -\frac{2}{b \cos \alpha} & 1 - \frac{2\ell}{b \cos \alpha} \end{pmatrix}^{2n} \begin{pmatrix} r_o^{(o)} \\ r_o^{(o)'} \end{pmatrix} \qquad (2.19)$$

A second characteristic of a chain matrix is that it is unimodular, i.e. its determinant equals one. From the theory of matrices (41), the Nth power of a unimodular matrix M is

$$M^N = \begin{pmatrix} m_{11} U_{N-1}(a) - U_{N-2}(a) & m_{12} U_{N-1}(a) \\ m_{21} U_{N-1}(a) & m_{22} U_{N-1}(a) - U_{N-2}(a) \end{pmatrix} \qquad (2.20)$$

where

$$a = \frac{1}{2}(m_{11} + m_{22})$$

and U_N are the Chebyshev Polynomials of the second kind

$$U_N(a) = \frac{\sin\left[(N+1)\cos^{-1}a\right]}{\sqrt{1-a^2}}$$

Using 2.20 and the definition of θ given by 2.6, equation 2.19 reduces to

$$\begin{pmatrix} r_n^{(o)} \\ r_n^{(o)'} \end{pmatrix} = \frac{1}{\sin\frac{\theta}{2}} \begin{pmatrix} \sin n\theta - \sin(n-\frac{1}{2})\theta & \ell \sin n\theta \\ -\frac{2}{\ell}(1-\cos\frac{\theta}{2})\sin n\theta & (2\cos\frac{\theta}{2}-1)\sin n\theta - \sin(n-\frac{1}{2})\theta \end{pmatrix} \begin{pmatrix} r_o^{(o)} \\ r_o^{(o)'} \end{pmatrix} \tag{2.21}$$

If the initial conditions are given as $r_o^{(o)} = d_1$ and $s_o^{(o)} = d_2$ it is evident from Figure 2.3 that $r_o^{(o)'} = \frac{d_2 - d_1}{\ell}$ and 2.21 becomes

$$\begin{pmatrix} r_n^{(o)} \\ r_n^{(o)'} \end{pmatrix} = \frac{1}{\sin\frac{\theta}{2}} \begin{pmatrix} \sin n\theta - \sin(n-\frac{1}{2})\theta & \ell \sin n\theta \\ -\frac{2}{\ell}(1-\cos\frac{\theta}{2})\sin n\theta & (2\cos\frac{\theta}{2}-1)\sin n\theta - \sin(n-\frac{1}{2})\theta \end{pmatrix} \begin{pmatrix} d_1 \\ \frac{d_2-d_1}{\ell} \end{pmatrix} \tag{2.21'}$$

2.1f Iterative Corrections to the Approximate Solutions

An iterative procedure can be used to calculate corrections to the approximate solutions. This is done by substituting the approximate solutions into the terms in equations 2.3a and 2.3b which were

originally neglected. An inhomogeneous difference equation is obtained which can be solved for $r_n^{(1)}$; $s_n^{(1)}$, $r_n^{(1)'}$ and $s_n^{(1)'}$ can be expressed in terms of $r_n^{(1)}$. The procedure may be repeated to obtain $r_n^{(2)}$, and so on. In general the (m + 1)th approximations to r_n, s_n, r_n' and s_n' are obtained from the following set of equations:

$$r_{n+2}^{(m+1)} - 2\cos\theta\, r_{n+1}^{(m+1)} + r_n^{(m+1)} = (1-2\cos\tfrac{\theta}{2})(A_{n+1}^{(m)} + B_n^{(m)}) + A_n^{(m)} + B_{n+1}^{(m)} \tag{2.22a}$$

$$s_n^{(m+1)} = \frac{r_{n+1}^{(m+1)} + r_n^{(m+1)} - A_n^{(m)} - B_n^{(m)}}{2\cos\frac{\theta}{2}} \tag{2.22b}$$

$$r_n^{(m+1)'} = \frac{r_{n+1}^{(m+1)} + (1 - 2\cos\frac{\theta}{2})(r_n^{(m+1)} - A_n^{(m)}) - B_n^{(m)}}{2\ell\cos\frac{\theta}{2}} \tag{2.22c}$$

$$s_n^{(m+1)'} = \frac{-(1 - 2\cos\frac{\theta}{2})(r_{n+1}^{(m+1)} - B_n^{(m)}) - r_n^{(m+1)} + A_n^{(m)}}{2\ell\cos\frac{\theta}{2}} \tag{2.22d}$$

where $$A_n^{(m)} = r_n^{(m)'}(r_n^{(m)} + s_n^{(m)})\tan\alpha$$

$$B_n^{(m)} = s_n^{(m)'}(r_{n+1}^{(m)} + s_n^{(m)})\tan\alpha$$

The calculation of the first correction (m = o) is summarized in Appendix I.

2.1g Exact Numerical Solution

An exact, point by point, numerical calculation of r_n and s_n is possible. The elimination of r_n' and s_n' from the original set of simultaneous, non-linear difference equations 2.3a to 2.3d leads to two recurrence relations for r_{n+1} and s_{n+1}:

$$r_{n+1} = \frac{\ell\,(2s_n - r_n) - 2r_n s_n \tan\alpha - \frac{2s_n}{b\cos\alpha}\,(\ell + s_n\tan\alpha)\left[\ell - (r_n + s_n)\tan\alpha\right]}{\ell - 2s_n\tan\alpha + \frac{2s_n}{b\cos\alpha}\tan\alpha\left[\ell + (r_n + s_n)\tan\alpha\right]} \tag{2.23a}$$

$$s_{n+1} = \frac{\ell\,(2r_{n+1} - s_n) + 2r_{n+1}s_n\tan\alpha - \frac{2r_{n+1}}{b\cos\alpha}\,(\ell - r_{n+1}\tan\alpha)\left[\ell + (r_{n+1} + s_n)\tan\alpha\right]}{\ell + 2r_{n+1}\tan\alpha - \frac{2r_{n+1}}{b\cos\alpha}\tan\left[\ell + (r_{n+1} + s_n)\tan\alpha\right]} \tag{2.23b}$$

With initial conditions $r_o = d_1$ and $s_o = d_2$ and repeated use of 2.23a and 2.23b the path of a ray in the resonator can be calculated exactly. Such a computation is easily made using a digital computer.

2.2 The Nonsymmetric Four-Mirror Resonator (43)

2.2a Difference Equation Formulation

The four-mirror resonator has been chosen as an example in which the symmetry of the resonator using identical, evenly spaced mirrors is destroyed by using mirrors of different curvatures and different spacings (see Figure 2.4). However, for the example chosen, the

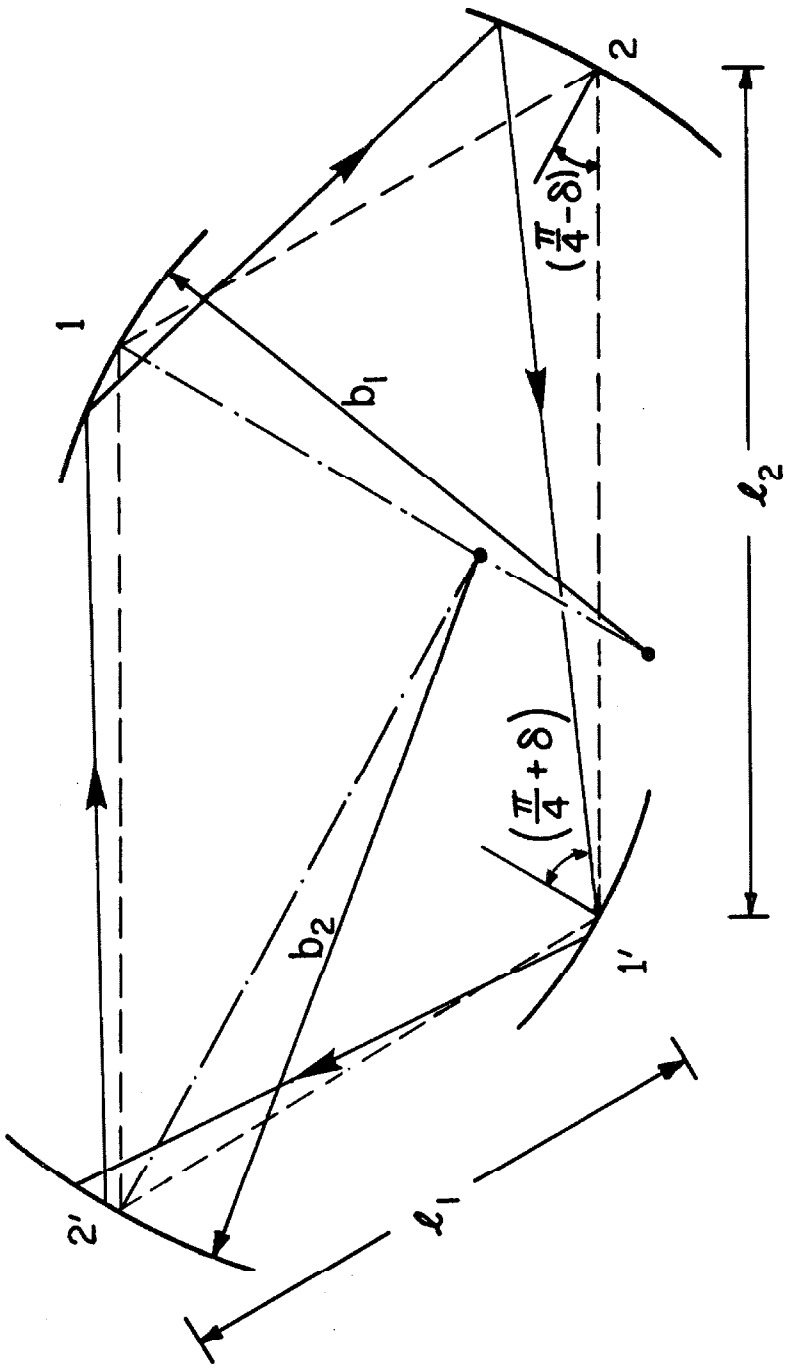

Fig. 2.4 Geometry of a particular nonsymmetric four mirror resonator.

symmetry about either of the diagonals allows the path of a ray in the cavity to be described by a set of four rather than eight difference equations:

$$s_n - r_n = r'_n \left[\ell_2 - r_n \tan \left(\frac{\pi}{4} - \delta\right) - s_n \tan \left(\frac{\pi}{4} + \delta\right) \right] \quad (2.24a)$$

$$r_{n+1} - s_n = s'_n \left[\ell_1 + s_n \tan \left(\frac{\pi}{4} + \delta\right) + r_{n+1} \tan \left(\frac{\pi}{4} - \delta\right) \right] \quad (2.24b)$$

$$r'_n - s'_n = \frac{2s_n}{b_1 \cos \left(\frac{\pi}{4} + \delta\right)} \quad (2.24c)$$

$$s'_n - r'_{n+1} = \frac{2r_{n+1}}{b_2 \cos \left(\frac{\pi}{4} - \delta\right)} \quad (2.24d)$$

r_n refers to the height of a ray at mirror 2 or 2' measured perpendicular to the axis, and r'_n refers to the slope of the ray reflected from mirror 2 or 2' measured relative to the axis. s_n and s'_n refer to the corresponding quantities measured at mirror 1 or 1'. The axis of the system is defined as the line joining the centers of consecutive mirrors, and the standard sign conventions of geometrical optics have been used. It should be noted that to describe a complete circuit about the resonator the equations must be applied twice.

2.2b Approximate Solutions and Stability Conditions

As was the case for the symmetrical cavity an approximate solution is obtained by neglecting the small terms in equations 2.24a and

2.24b. The resulting equation for $r_n^{(o)}$ is:

$$r_{n+2}^{(o)} - \ell_1 \ell_2 \left\{ \left[\frac{1}{\ell_1} + \frac{1}{\ell_2} - \frac{2}{b_1 \cos\left(\frac{\pi}{4} + \delta\right)} \right] \left[\frac{1}{\ell_1} + \frac{1}{\ell_2} - \frac{2}{b_2 \cos\left(\frac{\pi}{4} - \delta\right)} \right] - \left(\frac{1}{\ell_1^2} + \frac{1}{\ell_2^2} \right) \right\} r_{n+1}^{(o)} + r_n^{(o)} = 0 \qquad (2.25)$$

An identical equation for $s_n^{(o)}$ could also be written.

$r_n^{(o)}$ will remain finite and have the form (37)

$$r_n^{(o)} = a_1 \cos n\theta + a_2 \sin n\theta \qquad (2.26)$$

where

$$\theta = \cos^{-1} \frac{\ell_1 \ell_2}{2} \left\{ \left[\frac{1}{\ell_1} + \frac{1}{\ell_2} - \frac{2}{b_1 \cos\left(\frac{\pi}{4} + \delta\right)} \right] \left[\frac{1}{\ell_1} + \frac{1}{\ell_2} - \frac{2}{b_2 \cos\left(\frac{\pi}{4} - \delta\right)} \right] - \left(\frac{1}{\ell_1^2} + \frac{1}{\ell_2^2} \right) \right\} \qquad (2.27)$$

provided that

$$0 \leq \left[1 - \frac{\ell_1}{b_1 \cos\left(\frac{\pi}{4} + \delta\right)} \right] \left[1 - \frac{\ell_2}{b_2 \cos\left(\frac{\pi}{4} - \delta\right)} \right] + \left[1 - \frac{\ell_1}{b_2 \cos\left(\frac{\pi}{4} - \delta\right)} \right] \left[1 - \frac{\ell_2}{b_1 \cos\left(\frac{\pi}{4} + \delta\right)} \right] \leq 2 \qquad (2.28)$$

A graphical representation of the stability condition 2.28 can be easily obtained in two cases:

(a) $\ell_1 = \ell_2$

For the rhomboidal resonator equation 2.28 reduces to:

$$0 \leq \left[1 - \frac{\ell}{b_1 \cos\left(\frac{\pi}{4} + \delta\right)}\right]\left[1 - \frac{\ell}{b_2 \cos\left(\frac{\pi}{4} - \delta\right)}\right] \leq 1 \qquad (2.29)$$

The stability condition for the rhomboidal resonator is illustrated in Figure 2.5a.

(b) $b_1 = b_2$ and $\delta = 0$

For the rectangular resonator equation 2.28 reduces to:

$$0 \leq \left[1 - \frac{\sqrt{2}\ell_1}{b}\right]\left[1 - \frac{\sqrt{2}\ell_2}{b}\right] \leq 1 \qquad (2.30)$$

Figure 2.5b illustrates the conditions for stable operation of the rectangular cavity. Figures 2.5a and 2.5b the coordinates have been chosen to facilitate comparison with the stability conditions for the two mirror cavity investigated by Boyd and Kogelnik ([illegible]).

If the initial conditions are chosen as $r_o^{(o)} = d_1$ and $s_o^{(o)} = d_2$ then the approximate solutions for $s_n^{(o)}$ and $r_n^{(o)}$ are

$$r_n^{(o)} = a_1 \cos n\theta + a_2 \sin n\theta \qquad (2.31)$$

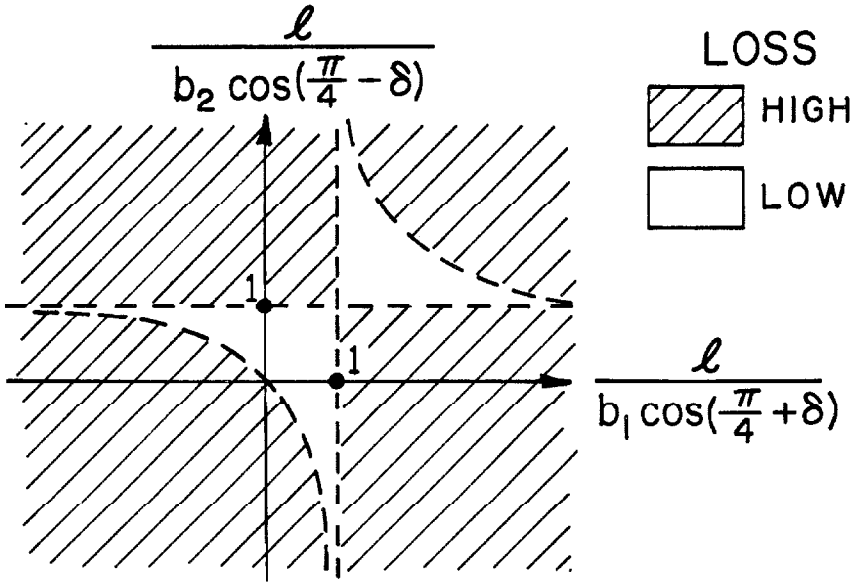

Fig. 2.5a High and low-loss regions for the rhomboidal resonator.

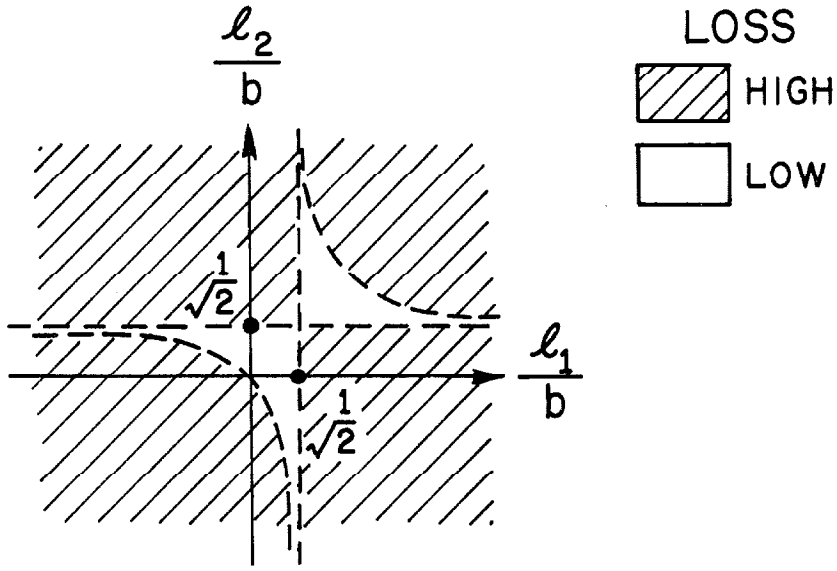

Fig. 2.5b High and low-loss regions for the rectangular resonator.

$$s_n^{(o)} = a_3 \left[\frac{\cos n\theta}{\ell_2} + \frac{\cos (n+1)\theta}{\ell_1} \right] + a_4 \left[\frac{\sin n\theta}{\ell_2} + \frac{\sin (n+1)\theta}{\ell_1} \right] \tag{2.32}$$

where

$$a_1 = d_1$$

$$a_2 = \frac{-d_1 \left(\cos\theta + \frac{\ell_1}{\ell_2} \right) + d_2 \ell_1 \left(\frac{1}{\ell_1} + \frac{1}{\ell_2} - \frac{2}{b_1 \cos \left(\frac{\pi}{4} + \delta \right)} \right)}{\sin \theta}$$

$$a_3 = \frac{a_1}{\frac{1}{\ell_1} + \frac{1}{\ell_2} - \frac{2}{b_1 \cos \left(\frac{\pi}{4} + \delta \right)}}$$

$$a_4 = \frac{a_2}{\frac{1}{\ell_1} + \frac{1}{\ell_2} - \frac{2}{b_1 \cos \left(\frac{\pi}{4} + \delta \right)}}$$

2.2c Matrix Formulation of the Approximate Solutions

After equations 2.24a to 2.24d are linearized by neglecting small terms they are easily rewritten in matrix form,

$$\begin{pmatrix} s_n^{(o)} \\ s_n^{(o)'} \end{pmatrix} = \begin{pmatrix} 1 & \ell_2 \\ \frac{-2}{b_1 \cos \left(\frac{\pi}{4} + \delta \right)} & 1 - \frac{2\ell_2}{b_1 \cos \left(\frac{\pi}{4} + \delta \right)} \end{pmatrix} \begin{pmatrix} r_n^{(o)} \\ r_n^{(o)'} \end{pmatrix} \tag{2.31a}$$

$$\begin{pmatrix} r_{n+1}^{(o)} \\ r_{n+1}^{(o)'} \end{pmatrix} = \begin{pmatrix} 1 & \ell_1 \\ \dfrac{-2}{b_2 \cos\left(\frac{\pi}{4} - \delta\right)} & 1 - \dfrac{2\ell_1}{b_2 \cos\left(\frac{\pi}{4} - \delta\right)} \end{pmatrix} \begin{pmatrix} s_n^{(o)} \\ s_n^{(o)'} \end{pmatrix} \quad (2.31b)$$

The equations may be combined in the form

$$\begin{pmatrix} r_n^{(o)} \\ r_n^{(o)'} \end{pmatrix} = M \begin{pmatrix} r_{n-1}^{(o)} \\ r_{n-1}^{(o)'} \end{pmatrix} \quad (2.32)$$

where M is the product of the transformation matrices of equations 2.31a and 2.31b.

Since M is unimodular it satisfies equation 2.20 and thus it follows from 2.32 that

$$\begin{pmatrix} r_n^{(o)} \\ r_n^{(o)'} \end{pmatrix} = \frac{1}{\sin\theta} \begin{pmatrix} \left(1 - \dfrac{2\ell_1}{b_1 \cos\left(\frac{\pi}{4} + \delta\right)}\right) \sin n\theta - \sin(n-1)\theta \\ -\left[\dfrac{2}{b_1 \cos\left(\frac{\pi}{4} + \delta\right)} + \left(\dfrac{2}{b_2 \cos\left(\frac{\pi}{4} - \delta\right)}\right)\left(1 - \dfrac{2\ell_1}{b_1 \cos\left(\frac{\pi}{4} + \delta\right)}\right)\right] \sin n\theta \end{pmatrix}$$

$$\begin{pmatrix} \left(\frac{1}{\ell_1} + \frac{1}{\ell_2} - \frac{2\ell_1\ell_2}{b_1\cos\left(\frac{\pi}{4}+\delta\right)}\right) \sin n\theta & \\ \left[-\frac{2\ell_2}{b_2\cos\left(\frac{\pi}{4}-\delta\right)} + \left(1-\frac{2\ell_1}{b_2\cos\left(\frac{\pi}{4}-\delta\right)}\right)\left(1-\frac{2\ell_2}{b_1\cos\left(\frac{\pi}{4}+\delta\right)}\right)\right]\sin n\theta - \sin(n-1)\theta & \end{pmatrix} \begin{pmatrix} r_o^{(o)} \\ \\ r_o^{(o)\prime} \end{pmatrix} \tag{2.33}$$

where θ is defined by equation 2.27.

If the initials conditions are $r_o^{(o)} = d_1$ and $s_o^{(o)} = d_2$, the column matrix on the right-hand side of equation 2.33 becomes

$$\begin{pmatrix} d_1 \\ \\ \dfrac{d_2 - d_1}{\ell_2} \end{pmatrix}$$

2.2d First Order Iterative Corrections to the Approximate Solutions

The first order corrections to the approximate solutions of equations 2.24a to 2.24d may be obtained by following a procedure similar to that outlined in Section 2.1f and Appendix 1 for the symmetric N-mirror resonator.

CHAPTER III

THE CONCEPT OF SELF-CONSISTENT FIELD ANALYSIS

3.1 Formulation of the Problem

3.1a Description of the Fields in Terms of Travelling Waves

To investigate the field distributions existing in resonators such as those illustrated by Figures 2.1 and 2.4 the method of analysis is to treat the fields as waves circulating around the resonator. The clockwise and counter-clockwise travelling waves may be considered independently. Since the wavelength at optical and infrared frequencies is much less than the mirror dimensions or spacings the travelling waves will be very closely TEM (transverse electromagnetic). Except for the reflectors the resonator is open, consequently it may be expected that if modes are to exist in the resonator the transverse spatial distribution of the travelling waves will be closely confined about a line joining the centers of consecutive mirrors.

3.1b Boundary Conditions and Consideration of an Arbitrarily Polarized Field

At each reflector the incident, reflected and transmitted fields are defined as $\underline{E}^{i(\pm)}$, $\underline{E}^{r(\pm)}$ and $\underline{E}^{t(\pm)}$. The superscripts $^{(+)}$ and $^{(-)}$ designate clockwise and counter-clockwise travelling waves respectively. At each reflector the boundary conditions to be satisfied by either the clockwise or the counter-clockwise circulating fields are

$$\begin{aligned} \underline{n} \times (\underline{E}^{i(\pm)} + \underline{E}^{r(\pm)}) &= \underline{n} \times \underline{E}^{t(\pm)} \\ \underline{n} \times (\underline{H}^{i(\pm)} + \underline{H}^{r(\pm)}) &= \underline{n} \times \underline{H}^{t(\pm)} \end{aligned} \qquad (3.1a)$$

The electric vector of an arbitrarily polarized wave can be resolved into two components, $\underline{E}_{\perp}$ perpendicular to the plane of incidence and $\underline{E}_{||}$ parallel to the plane of incidence. A consequence of the assumption that the waves are very nearly TEM is that the electric and magnetic fields satisfy the relation

$$\underline{H} = \frac{\underline{k} \times \underline{E}}{\omega\mu} \tag{3.2}$$

Thus the magnetic vector $\underline{H}_{||}$ corresponding to $\underline{E}_{||}$ is perpendicular to the plane of incidence and equations 3.1a and 3.1b become

$$\underline{E}_{\perp}^{i(\pm)} + \underline{E}_{\perp}^{r(\pm)} = \underline{E}_{\perp}^{t(\pm)} \tag{3.3a}$$

$$\underline{H}_{||}^{i(\pm)} + \underline{H}_{||}^{r(\pm)} = \underline{H}_{||}^{t(\pm)} \tag{3.3b}$$

The correspondence between $\underline{E}$ and $\underline{H}$ in Maxwell's equations (44), the similarity between the boundary conditions 3.3a and 3.3b, and the relation between $\underline{H}_{||}$ and $\underline{E}_{||}$ expressed by equation 3.2 imply that it is necessary to consider only one component of the field, e.g. $\underline{E}_{\perp}$.

For perfect reflection the boundary condition to be satisfied by $\underline{E}_{\perp}$ is

$$\underline{E}_{\perp}^{i(\pm)} + \underline{E}_{\perp}^{r(\pm)} = 0 \tag{3.4}$$

and for mirrors which are slightly transparent

$$\underline{E}_{\perp}^{i(\pm)} + \underline{E}_{\perp}^{r(\pm)} = \underline{E}_{\perp}^{t(\pm)} \tag{3.5}$$

where

$$\left|\underline{E}_{\perp}^{t(\pm)}\right| \ll \left|\underline{E}_{\perp}^{i(\pm)}\right| \simeq \left|\underline{E}_{\perp}^{r(\pm)}\right|$$

In the following analysis perfect reflection will always be assumed.* Occasional references to the field at a reflector will mean $\underline{E}_{\perp}^{t(\pm)}$, however the presence of this small component will always be neglected in determining the resonator field distributions.

3.1c Vector Green's Theorem Derivation of an Integral Equation for the Fields in a Symmetric Resonator

In Figure 3.1a the mirrors of a symmetric resonator are schematically represented as part of an arbitrary surface $S=A_1+A_2+A_3+S_1+S_2+S_3$ enclosing a volume V. The mirrors are assumed to be perfectly reflecting and so at each reflector the clockwise travelling fields in the resonator satisfy the condition

$$\underline{n} \times (\underline{E}^{i(+)} + \underline{E}^{r(+)}) = 0 \tag{3.6}$$

It is assumed that the fields are sufficiently confined about the resonator axis that they may be considered zero over the remainder of the surface.

---

* In the laboratory it is possible with the use of multi-layer dielectric films to achieve mirror transmission of less than 1% so that perfect reflection is a good approximation.

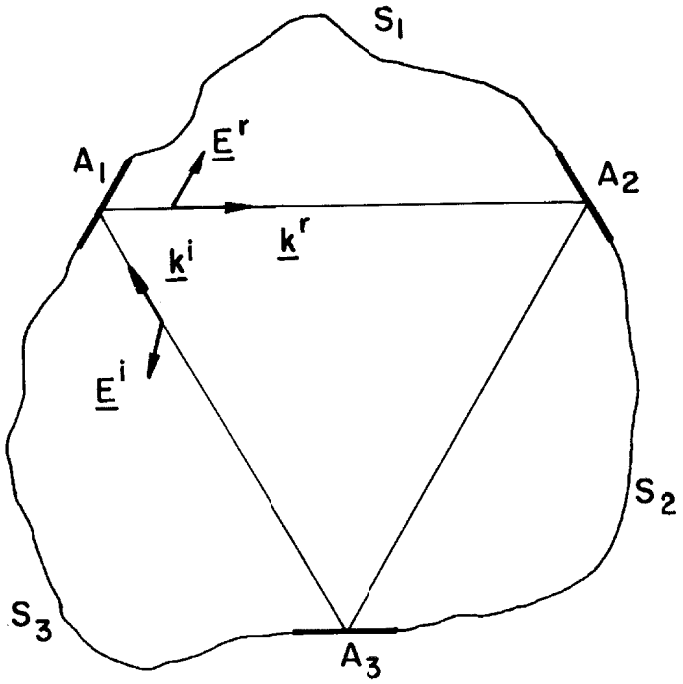

Fig. 3.1a A three-mirror symmetric resonator represented as a closed surface.

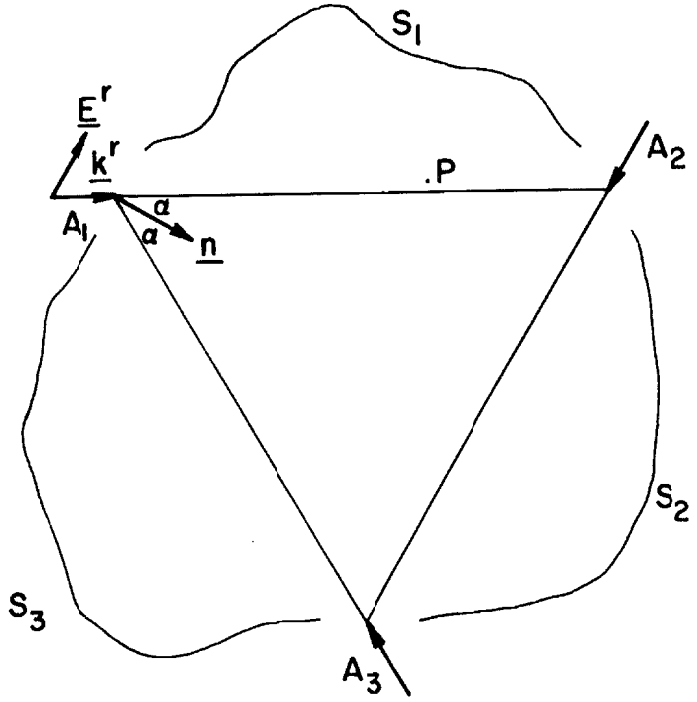

Fig. 3.1b The system of apertures analogous to the three-mirror symmetric resonator.

The analogy between reflection by a mirror and transmission through an aperture (similar to the mirror-lens equivalence discussed in the geometrical optics analysis of Section 2.1b) indicates that the situation illustrated schematically in Figure 3.1a is identical with that of Figure 3.1b. In this case the travelling waves are incident on the apertures from outside the volume V and have the direction indicated. Over the apertures A_1,A_2 and A_3 the electric field has the value $\underline{E}^{r(+)} = -\underline{E}^{i(+)}$ and the fields are negligible on the perfectly absorbing surfaces S_1,S_2 and S_3 which represent the open sides of the resonator.

The fields at an interior point of a volume V may be expressed in terms of the values of $\underline{E}$ and $\underline{H}$ over the enclosing surface S. Appendix 2 outlines a derivation of this relation which is based on an application of the vector Green's theorem to the field equations. For a source-free volume V the electric field at an arbitrary interior point P is

$$\underline{E}\,(P) = -\frac{1}{4\pi}\int_S dS\left[j\omega\mu\,(\underline{n}\times\underline{H})\varphi + (\underline{n}\times\underline{E})\times\nabla\varphi + (\underline{n}\cdot\underline{E})\nabla\varphi\right] \qquad (3.7)$$

where $\varphi = \frac{e^{-jkr}}{r}$ and r is measured from the surface element dS to the observation point P.

The assumption that the travelling waves are approximately TEM implies that over the apertures A_1,A_2 and A_3 the electric and magnetic vectors are related by equation 3.2 while on the perfectly absorbing surfaces S_1,S_2 and S_3 $\underline{E}$ and $\underline{H}$ are negligible. The directional properties of the aperture fields are such that the major

contribution to the electric field at the point P shown in Figure 3.1b comes from the field $\underline{E}^{r(+)}(1)$ in aperture A_1. Thus equation 3.7 may be rewritten as

$$\underline{E}^{(+)}(P) = \frac{1}{4\pi} \int_{A_1} dA_1 \frac{e^{-jkr}}{r} \Big\{ j\,(\underline{n}\cdot\underline{k})\,\underline{E}^{r(+)}(1) - j\,(\underline{n}\cdot\underline{E}^{r(+)}(1))\,\underline{k} + \left[(\underline{r}_o\cdot\underline{n})\,\underline{E}^{r(+)}(1) - (\underline{r}_o\cdot\underline{E}^{r(+)}(1))\,\underline{n} + (\underline{n}\cdot\underline{E}^{r(+)}(1))\,\underline{r}_o\right](jk+\frac{1}{r})\Big\} \quad (3.8)$$

where $\underline{r}_o$ is a unit vector in the direction of r, $\underline{n}$ is an inwardly-directed unit vector normal to A_1, and $\underline{k}$ is the propagation vector of the medium in resonator.

In Section 3.1b it was indicated that for an arbitrarily polarized electric field it is sufficient to consider the component parallel to the plane of the resonator (i.e. the plane of incidence) or the component perpendicular to the plane of the resonator. The latter component (i.e. $\underline{E}_1$) is arbitrarily chosen for consideration in the subsequent analysis. Since the fields are closely confined about the axis and since the aperture dimensions $\ll$ r, then $\underline{n}\cdot\underline{k} \simeq \underline{n}\cdot\underline{r}_o \simeq \cos\alpha$ and equation 3.8 simplifies to*

$$\underline{E}^{(+)}(P) = \underline{E}_1^{(+)}(P) = \frac{1}{4\pi} \int_{A_1} dA_1\, \underline{E}_1^{r(+)}(1)\, \frac{e^{-jkr}}{r}\,(2jk\cos\alpha + \frac{1}{r}) \quad (3.9)$$

---

* Smythe (46) derives this equation by considering what form of current distribution will give a tangential electric field over an area A of an infinite plane and zero over the remainder.

The first term on the right-hand side of equation 3.9 represents the field in the far zone of the aperture, the second term represents the near zone field. Since r is large, terms in $\frac{1}{r^2}$ can be neglected and equation 3.9 becomes

$$\underline{E}_{\perp}^{(+)}(P) = \frac{jk \cos \alpha}{2\pi} \int_{A_1} dA_1 \, \underline{E}_{\perp}^{r(+)}(1) \frac{e^{-jkr}}{r} \tag{3.10}$$

The vector notation may now be omitted since $\underline{E}_{\perp}^{i(+)}(P)$ and $\underline{E}_{\perp}^{r(+)}(1)$ have the same direction. When the observation point P is near the aperture A_2, $E_{\perp}^{(+)}(P)$ represents the field $E_{\perp}^{i(+)}(2)$ incident on aperture A_2, viz.

$$E_{\perp}^{i(+)}(2) = \frac{jk \cos \alpha}{2\pi} \int_{A_1} dA_1 \, E_{\perp}^{r(+)}(1) \frac{e^{-jkr_{12}}}{r_{12}} \tag{3.11}$$

where r_{12} is the distance from the source point on A_1 to the observation point on A_2.

Re-interpretation of equation 3.11 in terms of the electric field incident on a mirror and the application of the boundary condition for perfect reflection given by equation 3.4 lead to an equation for the electric field reflected from mirror 2 in terms of that reflected from mirror 1, i.e.

$$E_{\perp}^{r(+)}(2) = - \frac{jk \cos \alpha}{2\pi} \int_{A_1} dA_1 \, E_{\perp}^{r(+)}(1) \frac{e^{-jkr_{12}}}{r_{12}} \tag{3.12}$$

If normal modes or eigenfunctions are to exist in the resonator the spatial distribution of $E_{\perp}^{r(+)}(2)$ must be equal within a constant to that of $E_{\perp}^{r(+)}(1)$. If $E_{\perp}^{r(+)}$ is written as $E_{\perp}^{r(+)}(u,v)$ where u and v are coordinates describing the mirror surfaces, equation 3.12 becomes an integral equation for the spatial distribution of the clockwise travelling wave immediately following reflection (or preceding reflection since $E_{\perp}^{i(+)} = -E_{\perp}^{r(+)}$) from a mirror,

$$\sigma^{(+)} E_{\perp}^{r(+)}(u_2, v_2) = \frac{jk \cos \alpha}{2\pi} \int_{A_1} dA_1 \, E_{\perp}^{r(+)}(u_1, v_1) \frac{e^{-jkr_{12}}}{r_{12}} \qquad (3.13a)$$

The proportionality factor $\sigma^{(+)}$ will be generally complex. As well as including the phase shift on reflection, the phase angle of $\sigma^{(+)}$ gives the phase shift per transit which the field experiences in addition to the geometrical phase shift. For resonance it is necessary that the <u>total</u> phase shift in a round trip be an integer times 2π. The fractional energy loss per reflection due to diffraction effects is $1 - |\sigma^{(+)}|^2$.

Since the clockwise and counter-clockwise travelling waves may be treated separately an integral equation similar to 3.13 could be written for $E_{\perp}^{r(-)} = -E_{\perp}^{i(-)}$.

Once $E_{\perp}^{r(+)}(u,v)$ and $E_{\perp}^{r(-)}(u,v)$ have been determined the clockwise and counter-clockwise travelling waves at any point in the resonator may be calculated from equation 3.10. In a non-rotating resonator the

total field at a point will be the sum of the contributions of the two oppositely circulating fields.*

3.1d Integral Equation for the Fields in a Nonsymmetric Resonator

A nonsymmetric resonator with an arbitrary number of sides M may be treated in a manner similar to the analysis of Section 3.1c. The only requirement on the resonator geometry is that the optical ray joining the centers of consecutive mirrors and having its angle of incidence equal to its angle of reflection must close on itself after completing a circuit of the resonator.

The problem is approached by replacing only one of the mirrors by an aperture. On the remaining mirrors the total electric field is zero (perfect reflection) and on the absorbing surfaces the fields are negligible. A field $E_{(1)}^{r(+)}$ is considered to be incident on the aperture in the direction of the optical ray joining the center of the aperture to the center of the first mirror. The angle between a normal to the mirror (or aperture) and the optical ray joining their centers is defined as α_j, where the subscript j refers to the number of the mirror. Then the field reflected from mirror 2 may be calculated from equation 3.12,

---

* If the resonator is rotating the oppositely directed waves will experience a time delay per circuit of (refer Appendix 3)

$$\Delta t = \pm \frac{2\omega S \cos\theta}{c^2}$$

where ω is the angular rotation rate, S is the area enclosed by the circuit, and θ is the angle between a normal to S and the axis of rotation.

The oppositely circulating modes will differ in frequency by

$$\Delta\nu = \frac{4\omega S \cos\theta}{C\lambda}$$

where C is the perimeter of S.

$$E_{\perp}^{r(+)}(2) = \frac{-jk \cos \alpha_1}{2\pi} \int_{A_1} dA_1 \, E_{\perp}^{r(+)}(1) \, \frac{e^{-jkr_{12}}}{r_{12}} \qquad (3.12)$$

The field after subsequent reflections may be calculated in a similar manner, i.e.

$$E_{\perp}^{r(+)}(3) = \frac{-jk \cos \alpha_2}{2\pi} \int_{A_2} dA_2 \, E_{\perp}^{r(+)}(2) \, \frac{e^{-jkr_{23}}}{r_{23}}$$

$$E_{\perp}^{r(+)}(4) = \frac{-jk \cos \alpha_3}{2\pi} \int_{A_3} dA_3 \, E_{\perp}^{r(+)}(3) \, \frac{e^{-jkr_{34}}}{r_{34}}$$

$$E_{\perp}^{r(+)}(M) = \frac{-jk \cos \alpha_{M-1}}{2\pi} \int_{A_{M-1}} dA_{M-1} \, E_{\perp}^{r(+)}(M-1) \, \frac{e^{-jkr_{M-1,M}}}{r_{M-1,M}}$$

$$E_{\perp}^{i(+)}(1) = \frac{-jk \cos \alpha_M}{2\pi} \int_{A_M} dA_M \, E_{\perp}^{r(+)}(M) \, \frac{e^{-jkr_{M,1}}}{r_{M,1}}$$

$$= -E_{\perp}^{r(+)}(1)$$

If modes are to exist the fields must be equal within a constant after completing a circuit of resonator. The resulting integral equation for $E_{\perp}^{r(+)}(u_1, v_1)$ is

$$\sigma \, E_{\perp}^{(+)\,r(+)}(u_1', v_1') = \left(\frac{-jk}{2\pi}\right)^M \cos \alpha_1, \cos \alpha_2 \ldots \cos \alpha_M \int_{A_1} dA_1 \, E_{\perp}^{r(+)}(u_1, v_1) \, K_M(u_1, v_1, u_1', v_1') \qquad (3.13b)$$

where the kernel of the integral equation is given by

$$K_M(u_1,v_1;u_1',v_1') = \int_{A_2} dA_2 \cdots \int_{A_M} dA_M \frac{e^{-jk(r_{12}+r_{23}+\cdots r_{M,1})}}{r_{12}\, r_{23} \cdots r_{M,1}}$$

3.2 Solutions of the Integral Equation

It will be seen in the following sections that the integral equation 3.13a can always be reduced to the general form

$$\sigma_m f_m(z_2) = \frac{1}{\sqrt{2\pi}} \int_{-\sqrt{c}}^{\sqrt{c}} dz_1\, f_m(z_1)\, e^{j(\gamma z_1^2 + \gamma z_2^2 + z_1 z_2)} \qquad (3.13c)$$

This is a linear, homogeneous, Fredholm equation of the second kind. The kernel is complex and symmetric but non-Hermitian. In general this type of integral equation does not possess some of the familiar properties of integral equations with Hermitian kernels (29). A difference of particular interest is that the usual extremal principle by which the eigenvalues of a Hermitian kernel may be estimated using the Rayleigh-Ritz procedure does not apply to integral equations with complex symmetric kernels. This means that the use of variational techniques to estimate σ_m and hence the diffraction losses is invalid.

If distinct eigenvalues exist the corresponding eigenfunctions will be orthogonal in a non-Hermitian sense (43), i.e.

$$\int_{-\sqrt{c}}^{\sqrt{c}} dz\ f_m(z)\ f_n(z) = 0 \qquad m \neq n \qquad (3.14)$$

This type of orthogonality relation is characteristic of lossy systems.

Solutions exist for several forms of the integral equation 3.13c:

(a) $\gamma = 0$

An equation of the form

$$\sigma_m f_m(z_2) = \frac{1}{\sqrt{2\pi}} \int_{-\sqrt{c}}^{\sqrt{c}} dz_1\ f_m(z_1)\ e^{jz_1z_2} \qquad (3.15)$$

is often referred to as a finite Fourier transform. Slepian and Pollak (49) have shown solutions to be

$$f_m(z) \propto S_{0m}\left(c, \frac{z}{\sqrt{c}}\right) \qquad (3.16a)$$

$$\sigma_m = \sqrt{\frac{2c}{\pi}}\ j^m\ R_{0m}^{(1)}(c,1) \qquad m = 0,1,2\ \ldots \qquad (3.16b)$$

where $S_{0m}\left(c,\frac{z}{\sqrt{c}}\right)$ and $R_{0m}^{(1)}(c,1)$ are the angular and radial wave functions in prolate spheroidal coordinates defined by Flammer (50).

(b) $\gamma \neq 0$

Analytical solutions to equation 3.13c with $\gamma \neq 0$ and c finite have not been found. However some of the low order eigenfunctions have been obtained by iterative numerical computations (18, 24, 25).

Equation 3.13c can be solved when $c = \infty$. The kernel may be expanded as a sum of Gaussian-Hermite polynomials. These functions are

orthogonal over the interval $-\infty \leq z \leq \infty$. Thus it follows that the eigenfunctions $f_m(z)$ are Gaussian-Hermite functions. A detailed solution is given in Appendix 4. The results are

$$f_m(z) \propto He_m(\beta z)\, e^{-\frac{\beta^2 z^2}{2}} \tag{3.17a}$$

$$\sigma_m = e^{jm\frac{\pi}{2} + j\left(m+\frac{1}{2}\right)\tan^{-1}\frac{2\gamma}{\beta^2}} \tag{3.17b}$$

where $\beta = (1 - 4\gamma^2)^{\frac{1}{4}}$. The value $\gamma = \frac{1}{2}$ is not allowed. The significance of this will be discussed in Section 5.4a.

CHAPTER IV

THE SELF-CONSISTENT FIELD ANALYSIS OF MULTIREFLECTOR OPTICAL RESONATORS

4.1 The Symmetric N-Mirror Resonator

4.1.1 Formulation of the Problem

Two mirrors of a symmetric N-mirror optical cavity are illustrated in Figure 4.1. The perfectly reflecting mirrors are spherical with radius of curvature b. They are rectangular in cross-section with dimensions $2a_1$ perpendicular to the plane of the resonator and $2a_2$ in the plane of the resonator. The center-to-center separation is ℓ and the tilt angle is α.

Figure 4.1 indicates that the component of the electric field perpendicular to the plane of incidence corresponds to E_x. It is assumed that the reflected or incident field may be written as the product of a function of x and a function of y where x and y are the coordinates describing the mirror surface, viz.

$$E_x^{r(\pm)}(x,y) = -E_x^{i(\pm)}(x,y) = f_m^{(\pm)}(x)\, g_n^{(\pm)}(y) \tag{4.1}$$

The integral equation 3.13a for the electric field of the clockwise travelling wave immediately following reflection becomes

$$\sigma_m^{(+)}\, \sigma_n^{(+)}\, f_m^{(+)}(x_2)\, g_n^{(+)}(y_2) = \frac{jk\cos\alpha}{2\pi} \int_{-a_1}^{a_1} dx_1 \int_{-a_2}^{a_2} dy_1\, f_m^{(+)}(x_1)\, g_n^{(+)}(y_1)\, \frac{e^{-jkr_{12}}}{r_{12}} \tag{4.2}$$

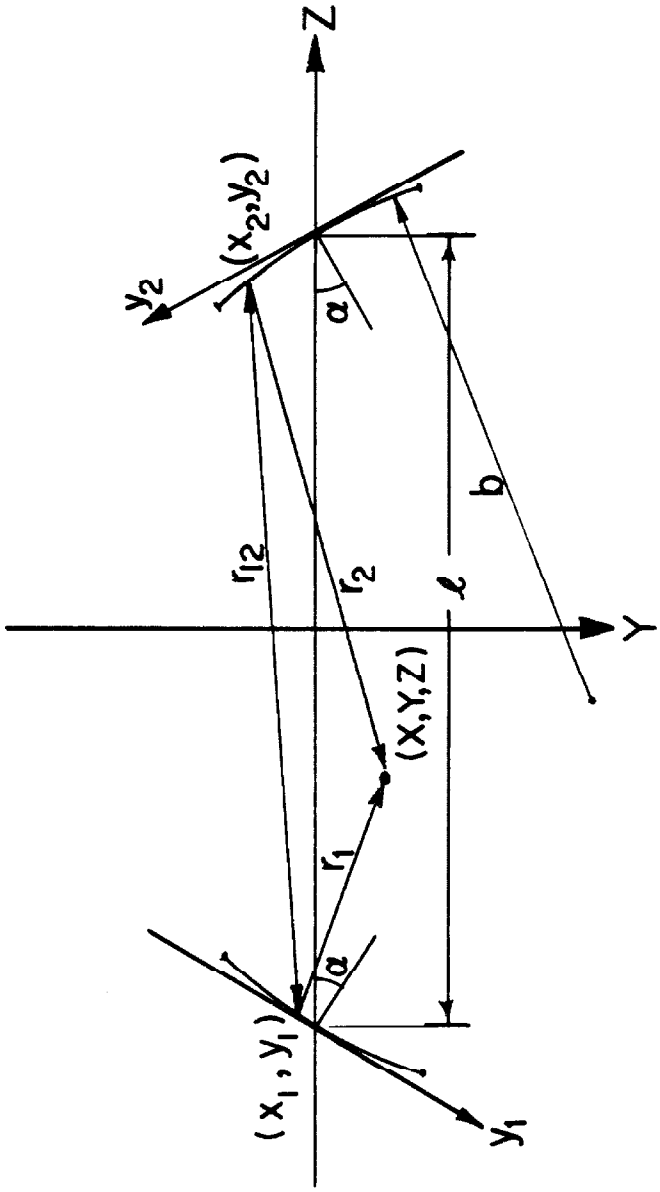

Fig. 4.1 Coordinate systems for the analysis of the symmetric M-mirror resonator.

For $b > a_1, a_2$ the distance r_{12} is given by

$$r_{12}^2 = (x_1-x_2)^2 + \left[(y_1+y_2)\cos\alpha + (x_1^2-x_2^2+y_1^2-y_2^2)\frac{\sin\alpha}{2b}\right]^2$$

$$+ \left[\ell + (y_1-y_2)\sin\alpha - (x_1^2+x_2^2+y_1^2+y_2^2)\frac{\cos\alpha}{2b}\right]^2 \qquad (4.3)$$

Providing that terms in x and y higher than second order make a negligible phase contribution they may be neglected (54). The necessary conditions are

$$\frac{a_1^2}{\ell\lambda} \ll \frac{\ell^2}{a_1^2}, \quad \frac{a_2^2}{\ell\lambda} \ll \frac{\ell^2}{a_2^2}$$

In the exponential r_{12} now becomes

$$r_{12} = \ell - \frac{(x_1x_2-y_1y_2\cos^2\alpha)}{\ell} + (y_1-y_2)\sin\alpha - (x_1^2+x_2^2)\left(\frac{\ell\cos\alpha-b}{2\ell b}\right)$$

$$- (y_1^2+y_2^2)\cos^2\alpha\left(\frac{\ell-b\cos\alpha}{2\ell b\cos\alpha}\right) \qquad (4.4)$$

In the denominator of the integrand r_{12} may be replaced by ℓ. It should be noted that to the accuracy of these approximations spherical and parabolic surfaces are indistinguishable.

With the substitutions

$$s = x\sqrt{\frac{k}{\ell}}$$

$$t = y\cos\alpha\sqrt{\frac{k}{\ell}}$$

$$c_1 = a_1^2 \frac{k}{\ell}$$

$$c_2 = a_2^2 \cos^2 \alpha \frac{k}{\ell}$$

$$\delta = \frac{\ell \cos \alpha - b}{2b}$$

$$\delta' = \frac{\ell - b \cos \alpha}{2b \cos \alpha}$$

the integral equation 4.2 for the normal modes becomes

$$\sigma_m^{(+)} \sigma_n^{(+)} F_m^{(+)}(s_2) G_n^{(+)}(t_2) = \frac{je^{-jk\ell}}{2\pi} \int_{-\sqrt{c_1}}^{\sqrt{c_1}} ds_1 \int_{-\sqrt{c_2}}^{\sqrt{c_2}} dt_1 F_m^{(+)}(s_1) G_n^{(+)}(t_1)$$

$$e^{j\left[s_1 s_2 - t_1 t_2 + \delta(s_1^2 + s_2^2) + \delta'(t_1^2 + t_2^2)\right]} \qquad (4.5)$$

where

$$F_m^{(+)}(s) \equiv f_m^{(+)}(x)$$

$$G_n^{(+)}(t) \equiv g_n^{(+)}(y)\, e^{-jky \sin\alpha}$$

The integral equation for the counter-clockwise travelling wave is identical to equation 4.5. However in this case

$$G_n^{(-)}(t) \equiv g_n^{(-)}(y)\, e^{+jky \sin\alpha}$$

Equation 4.5 is obviously separable into two equations, viz.

$$\chi_m^{(+)} F_m^{(+)}(s_2) = \frac{1}{\sqrt{2\pi}} \int_{-\sqrt{c_1}}^{\sqrt{c_1}} ds_1 \, F_m^{(+)}(s_1) \, e^{j\left[\delta(s_1^2+s_2^2)+ s_1 s_2\right]} \tag{4.6a}$$

$$\chi_n^{(+)} G_n^{(+)}(t_2) = \frac{1}{\sqrt{2\pi}} \int_{-\sqrt{c_2}}^{\sqrt{c_2}} dt_1 \, G_n^{(+)}(t_1) \, e^{j\left[\delta'(t_1^2+t_2^2)- t_1 t_2\right]} \tag{4.6b}$$

with

$$\sigma_m^{(+)} \sigma_n^{(+)} = j e^{-jk\ell} \chi_m^{(+)} \chi_n^{(+)}$$

4.1.2 Two Special Cases

Before proceeding to the general solutions of equations 4.6a and 4.6b it will be worthwhile to consider two special situations, namely the case in which $\ell \gg b$ and the "pseudo-confocal" case.

4.1.2a $\ell \gg b$

For the resonator in which $\frac{\ell}{b}$ is sufficiently large that

$$\delta (s_1^2 + s_2^2) \gg s_1 s_2$$

$$\delta'(t_1^2 + t_2^2) \gg t_1 t_2$$

and the exponentials $e^{js_1s_2}$ and $e^{-jt_1t_2}$ are close to unity for all values of s_1 and t_1, equation 4.5 becomes

$$\sigma_m^{(+)} \sigma_n^{(+)} F_m^{(+)}(s_2) G_n^{(+)}(t_2) \simeq \frac{je^{-jk\ell}}{2\pi} \int_{-\sqrt{c_1}}^{\sqrt{c_1}} ds_1 \int_{-\sqrt{c_2}}^{\sqrt{c_2}} dt_1 F_m^{(+)}(s_1) G_n^{(+)}(t_1) e^{j\left[\rho(s_1^2+s_2^2)+\rho'(t_1^2+t_2^2)\right]} \tag{4.7}$$

where

$$\rho = \frac{\ell \cos \alpha}{2b}$$

$$\rho' = \frac{\ell}{2b \cos \alpha}$$

It is obvious by inspection that the solution of equation 4.7 is

$$F^{(+)}(s)\, G^{(+)}(t) \propto e^{j(\rho s^2 + \rho' t^2)} \tag{4.8}$$

Thus the electric field distribution of the clockwise travelling wave just after reflection is

$$E_x^{r(+)}(x,y) = E_o\, e^{j\frac{k}{\ell}(\rho x^2 + \rho' y^2 \cos^2 \alpha + \ell y \sin \alpha)} \tag{4.9}$$

The corresponding field for the counter-clockwise travelling wave is just

$$E_x^{r(-)}(x,y) = E_o'\, e^{j\frac{k}{\ell}(\rho x^2 + \rho' y^2 - \ell y \sin \alpha)} \tag{4.10}$$

It is evident from equations 4.9 and 4.10 that an infinite set of modes cannot exist in the cavity if $\ell \gg b$. In fact in a non-rotating resonator in which the oppositely circulating fields have equal amplitudes, the resulting intensity distribution on a slightly non-perfect reflector will have the form

$$I(x,y) \propto \frac{\sin^2}{\cos^2}(ky \sin \alpha) \tag{4.11}$$

This is the intensity distribution of a double-slit interference pattern. The two neighboring mirrors act as the two coherently illuminated slits of the standard double-slit interference experiment. Both sine and cosine distribution are allowable since the oppositely circulating fields are entirely independent.

The eigenvalue corresponding to the solution 4.8 of the integral equation 4.7 is

$$\sigma^{(+)} = je^{-jk\ell}\, 2\frac{1}{\sqrt{\rho\rho'}}\, \varphi\left(\sqrt{\frac{2\rho c_1}{\pi}}\right)\, \varphi\left(\sqrt{\frac{2\rho' c_2}{\pi}}\right) \qquad (4.12)$$

where $\varphi(u) = C(u) + jS(u)$ is the complex Fresnel integral (55).

The energy loss per reflection due to diffraction at a mirror is given by

$$\alpha_D = 1 - |\sigma|^2$$

$$= 1 - \left|\frac{b}{\ell}\, \varphi\left(2a_1\sqrt{\frac{\cos\alpha}{\lambda b}}\right)\, \varphi\left(2a_2\sqrt{\frac{\cos\alpha}{\lambda b}}\right)\right|^2 \qquad (4.13)$$

The phase change between reflections is the phase angle of $\sigma^{(+)}$, viz.

$$k\ell - \frac{\pi}{2} + \tan^{-1}\left[\frac{C\left(2a_1\sqrt{\frac{\cos\alpha}{\lambda b}}\right)S\left(2a_2\sqrt{\frac{\cos\alpha}{\lambda b}}\right)+C\left(2a_2\sqrt{\frac{\cos\alpha}{\lambda b}}\right)S\left(2a_1\sqrt{\frac{\cos\alpha}{\lambda b}}\right)}{S\left(2a_1\sqrt{\frac{\cos\alpha}{\lambda b}}\right)S\left(2a_2\sqrt{\frac{\cos\alpha}{\lambda b}}\right)-C\left(2a_1\sqrt{\frac{\cos\alpha}{\lambda b}}\right)C\left(2a_2\sqrt{\frac{\cos\alpha}{\lambda b}}\right)}\right]$$

For resonance the total phase shift around the resonator must be an integral q times 2π, thus for the symmetric N-mirror resonator

$$\frac{4\ell}{\lambda}=\frac{4q}{N}+1-\frac{2}{\pi}\tan^{-1}\left[\frac{C(2a_1\sqrt{\frac{\cos\alpha}{\lambda b}})S(2a_2\sqrt{\frac{\cos\alpha}{\lambda b}})+C(2a_2\sqrt{\frac{\cos\alpha}{\lambda b}})S(2a_1\sqrt{\frac{\cos\alpha}{\lambda b}})}{S(2a_1\sqrt{\frac{\cos\alpha}{\lambda b}})S(2a_2\sqrt{\frac{\cos\alpha}{\lambda b}})-C(2a_1\sqrt{\frac{\cos\alpha}{\lambda b}})C(2a_2\sqrt{\frac{\cos\alpha}{\lambda b}})}\right] \tag{4.14}$$

For large values of its argument

$$\lim_{u\to\infty}\varphi(u)=\frac{1}{2}(1+j)$$

and thus at very short wavelengths diffraction loss and resonance conditions reduce to

$$\alpha_D = 1-\left(\frac{b}{2\ell}\right)^2 \tag{4.15}$$

$$\ell = \frac{q}{N}\lambda \tag{4.16}$$

Since $\ell \gg b$ equation 4.15 indicates that on each reflection nearly all of the incident energy is lost due to diffraction.

4.1.2b Pseudo-Confocal Resonator

Consider equations 4.6a and 4.6b once again. As noted in Section 3.2 this type of integral equation has not been solved for finite limits of integration. However solutions have been found when the

quadratic terms do not appear in the exponential. Unfortunately with spherical mirrors and non-zero α δ and δ' cannot be set equal to zero simultaneously. In view of this the requirement is for a symmetric N-mirror resonator in which each mirror has two radii of curvature, b in the x-z plane and b' in the y-z plane. The surface of the mirror is defined by the condition that the line of intersection between the surface and a plane containing the z-axis is a circular arc whose radius of curvature varies uniformly between b and b' as the plane rotates about the z-axis between the x-z and y-z planes. Under these conditions it is a simple matter to show that the distance r_{12} is given approximately by

$$r_{12} \simeq \ell - \frac{(x_1 x_2 - y_1 y_2 \cos^2\alpha)}{\ell} + (y_1 - y_2)\sin\alpha$$

$$- (x_1^2 + x_2^2)\left(\frac{\ell\cos\alpha - b}{2\ell b}\right) - (y_1^2 + y_2^2)\cos^2\alpha\left(\frac{\ell - b'\cos\alpha}{2\ell b'\cos\alpha}\right) \qquad (4.17)$$

For the "pseudo-confocal" geometry in which

$$b = \ell\cos\alpha$$

$$b' = \frac{\ell}{\cos\alpha}$$

Equations 4.6a and 4.6b reduce to

$$\chi_m^{(+)} F_m^{(+)}(s_2) = \frac{1}{\sqrt{2\pi}} \int_{-\sqrt{c_1}}^{\sqrt{c_1}} ds_1 \, F_m^{(+)}(s_1) \, e^{js_1 s_2} \tag{4.18a}$$

$$\chi_m^{(+)} G_n^{(+)}(t_2) = \frac{1}{\sqrt{2\pi}} \int_{-\sqrt{c_2}}^{\sqrt{c_2}} dt_1 \, G_n^{(+)}(t_1) \, e^{-jt_1 t_2} \tag{4.18b}$$

The eigenfunctions and eigenvalues for these equations are (refer Section 3.2).

$$F_m^{(+)}\left(c_1, \frac{s}{\sqrt{c_1}}\right) \propto S_{Om}\left(c_1, \frac{s}{\sqrt{c_1}}\right) \tag{4.19a}$$

$$G_n^{(+)}\left(c_2, \frac{t}{\sqrt{c_2}}\right) \propto S_{On}\left(c_2, \frac{t}{\sqrt{c_2}}\right) \tag{4.19b}$$

with $$\chi_m^{(+)} = \sqrt{\frac{2c_1}{\pi}} \, j^m \, R_{Om}^{(1)}(c_1, 1) \qquad m = 0,1,2 \ldots \tag{4.20a}$$

$$\chi_n^{(+)} = \sqrt{\frac{2c_2}{\pi}} \, (-j)^n \, R_{On}^{(1)}(c_2, 1) \qquad n = 0,1,2 \ldots \tag{4.20b}$$

where S_{Om} and $R_{Om}^{(1)}$ are the angular and radial wave functions in prolate spheroidal coordinates (49).

Therefore the electric field distribution of the clockwise travelling wave just after reflection is

$$E_x^{r(+)}(x,y) = E_o \, e^{+jky \sin\alpha} \, S_{Om}\left(\frac{a_1^2 k}{\ell}, \frac{x}{a_1}\right) \, S_{On}\left(a_2^2 \cos^2\alpha \, \frac{k}{\ell}, \frac{y \cos\alpha}{a_2}\right) \tag{4.21}$$

In a non-rotating resonator the field distribution at a

slightly transmitting mirror resulting from the interference of two oppositely travelling waves of equal amplitude is obtained by replacing the exponential factor in 4.21 by the interference factor $\frac{\sin}{\cos}(ky\sin\alpha)$ and E_o by $|E_t| \ll |E_o|$.

Information regarding phase changes and diffraction losses is obtained from the eigenvalues

$$\sigma_m^{(+)}\sigma_n^{(+)} = \frac{4a_1a_2\cos\alpha}{\ell\lambda}(-1)^n j^{m+n+1} e^{-jk\ell} R_{Om}^{(1)}\left(\frac{a_1^2k}{\ell}, 1\right) R_{On}\left(a_2^2\cos^2\alpha\,\frac{k}{\ell}, 1\right) \tag{4.22}$$

The phase change between two onsecutive reflections is given by the phase angle of $\sigma_m^{(+)}\sigma_n^{(+)}$. For resonance the total phase shift for a complete circuit of the resonator must be an integral multiple of 2π. Thus

$$2\pi q = N\left|(m + 3n + 1)\frac{\pi}{2} - k\ell\right| \qquad q = 0,1,2\ldots \tag{4.23}$$

With the substitution of equation 2.1 the resonance condition may be rewritten as

$$\frac{4\ell}{\lambda} = \left(1 - \frac{2\alpha}{\pi}\right)2q + (m + 3n + 1) \tag{4.24}$$

Equation 4.24 indicates that in general the resonator will not be frequency degenerate. An exception is when $\alpha = 0$, the case of the standard two-mirror confocal resonator which will be discussed in

Section 5.2.

Following the practice of other authors (18,19) the modes of the multi-mirror cavity will be designated as TEM_{mnq} since at least for small transverse wave numbers the axial electric and magnetic fields may be neglected.

At each reflection the fractional energy loss due to diffraction is

$$\alpha_D = 1 - \left[\frac{4a_1 a_2 \cos\alpha}{\ell\lambda} R_{0m}^{(1)}\left(\frac{a_1^2 k}{\ell}, 1\right) R_{0n}^{(1)}\left(a_2^2 \cos^2\alpha \frac{k}{\ell}, 1\right)\right]^2 \qquad (4.25)$$

Values of the function $R_{0m}^{(1)}(u)$ are given by Slepian and Pollak (48) for $u > 5$ and by Flammer for $u \leq 5$.

4.1.3 General Case

4.1.3a Modes of the Resonator

The solution of equation 4.6a and 4.6b for the general case in which δ and δ' are not zero is only possible in the limit of zero wavelength. With this approximation the limits of integration pass to infinity and the eigenfunctions and corresponding eigenvalues are (refer Section 3.2)

$$F_m^{(+)}(s) \propto He_m(\beta s)\, e^{-\frac{\beta^2 s^2}{2}} \qquad (4.26a)$$

$$G_n^{(+)}(t) \propto He_n(\beta' t)\, e^{-\frac{\beta'^2 t^2}{2}} \qquad (4.26b)$$

with

$$\chi_m^{(+)} = j^m e^{j(m + \frac{1}{2})\tan^{-1}\frac{2\delta}{\beta^2}} \qquad m = 0,1,2 \ldots \quad (4.27a)$$

$$\chi_n^{(+)} = j^{3n} e^{j(n + \frac{1}{2})\tan^{-1}\frac{2\delta'}{\beta'^2}} \qquad n = 0,1,2 \ldots \quad (4.27b)$$

where

$$\beta = (1 - 4\delta^2)^{\frac{1}{4}}$$

$$= \left(\frac{2\ell \cos\alpha}{b} - \frac{\ell^2 \cos^2\alpha}{b^2}\right)^{\frac{1}{4}}$$

$$\beta' = (1 - 4\delta'^2)^{\frac{1}{4}}$$

$$= \left(\frac{2\ell}{b\cos\alpha} - \frac{\ell^2}{b^2\cos^2\alpha}\right)^{\frac{1}{4}}$$

Thus the electric field distribution just following reflection from a mirror for a wave travelling in a clockwise manner is

$$E_x^{r(+)}(x,y) = E_o \frac{\Gamma(\frac{m}{2} + 1)\Gamma(\frac{n}{2} + 1)}{\Gamma(m+1)\Gamma(n+1)} e^{+jky\sin\alpha} e^{-\frac{k}{2\ell}(\beta^2x^2 + \beta'^2y^2\cos^2\alpha)}$$

$$He_m\left[(\tfrac{k}{\ell})^{1/2}\beta x\right] He_n\left[(\tfrac{k}{\ell})^{1/2}\beta' y\cos\alpha\right] \quad (4.28)$$

The normalization has been chosen so that $E_x^{r(+)}(0,0) = \pm E_o$ for m and n even. The observable interference field at a slightly imperfect reflector formed by two equal amplitude waves travelling in opposite

directions in a non-rotating resonator is obtained by replacing $e^{-jky \sin\alpha}$ with $\begin{matrix}\sin\\ \cos\end{matrix}(ky \sin\alpha)$ and E_o with $E_t \ll E_o$ in equation 4.28.

In order that the field distribution near the mirror decrease in the x and y directions it is evident from equation 4.28 that

$$\beta^2 > 0, \quad \beta'^2 > 0$$

The first condition leads to

$$0 \leq \frac{\ell \cos\alpha}{b} \leq 2$$

The second implies a more stringent requirement, i.e.

$$0 \leq \frac{\ell}{b \cos\alpha} \leq 2$$

These are the same stability conditions as obtained by the simple geometrical optics treatment of Section 2.1c.

4.1.3b Resonance Conditions

In this approximate analysis the eigenvalues obtained are purely imaginary, viz.

$$\sigma_m^{(+)}\sigma_n^{(+)} = e^{-j\left[k\ell - (m+3n+1)\frac{\pi}{2} - (m+\frac{1}{2})\tan^{-1}\frac{2\delta}{\beta^2} - (n+\frac{1}{2})\tan^{-1}\frac{2\delta'}{\beta'^2}\right]} \quad (4.30)$$

As expected the zero wavelength approximation leads to an absence of diffraction losses on reflection, however phase information is still present. For resonance the phase shift during a complete circuit of the resonator must be an integer q times 2π. Thus the phase shift per section of the symmetric N-mirror resonator is $\frac{2q\pi}{N}$ and the resonance condition is

$$\frac{2q\pi}{N} = \left| k\ell - (m + 3n + 1)\frac{\pi}{2} - (m+\tfrac{1}{2})\tan^{-1}\frac{2\delta}{\beta^2} - (n+\tfrac{1}{2})\tan^{-1}\frac{2\delta'}{\beta'^2} \right| \quad (4.31)$$

Substituting equation 2.1 into 4.31 leads to

$$\frac{4\ell}{\lambda} = (1-\frac{2\alpha}{\pi})2q + (m+3n+1) + \frac{2}{\pi}(m+\tfrac{1}{2})\tan^{-1}\frac{2\delta}{\beta^2} + \frac{2}{\pi}(n+\tfrac{1}{2})\tan\frac{2\delta'}{\beta'^2} \quad (4.32)$$

It is evident from equation 4.32 that no frequency degeneracy exists. The spectral range or mode separation is

$$\Delta(\frac{1}{\lambda}) = \frac{1}{4\ell}\left[(1-\frac{2\alpha}{\pi})\,2\Delta q + (1+\frac{2}{\pi}\tan^{-1}\frac{2\delta}{\beta^2})\Delta m + (3+\frac{2}{\pi}\tan^{-1}\frac{2\delta'}{\beta'^2})\Delta n\right] \quad (4.33)$$

As in Section 4.1.2b axial electric and magnetic fields are considered negligible and the modes are given the standard TEM_{mnq} designation.

4.1.3c Electric Field at an Arbitrary Point in the Resonator

The electric field traveling in a clockwise direction at an arbitrary point in the resonator between mirrors 1 and 2 (refer Figure 4.1) is obtained by calculating the integral of equation 3.10 with

$E_x^{r(+)}(x,y)$ given by 4.28. A lengthy integration leads to

$$E_x^{(+)}(X,Y,Z) = E_o \frac{\Gamma(\frac{m}{2}+1)\Gamma(\frac{n}{2}+1)}{\Gamma(m+1)\Gamma(n+1)} \sqrt{\frac{2}{\gamma\gamma'}} \; He_m\left(\sqrt{\frac{2k}{\ell}}\frac{\beta}{\gamma}X\right) \; He_n\left(\sqrt{\frac{2k}{\ell}}\frac{\beta'}{\gamma'}Y\right)$$

$$e^{-\frac{k}{\ell}\left(\frac{\beta^2}{\gamma^2}X^2 + \frac{\beta'^2}{\gamma'^2}Y^2\right)}$$

$$e^{-j\left[\frac{k\ell}{2}(1+\approx)+k\left(\frac{\cos\alpha}{b}\frac{X^2}{\gamma^2}+\frac{1}{b\cos\alpha}\frac{Y^2}{\gamma'^2}\right)\approx-(m+\frac{1}{2})(\frac{\pi}{2}-\varphi)-(n+\frac{1}{2})(\frac{\pi}{2}-\varphi')\right]}$$

(4.34)

where

$$\approx = \frac{2Z}{\ell}$$

$$\gamma = \left[2 - \frac{\ell\cos\alpha\,(1-\approx^2)}{b}\right]^{\frac{1}{2}}$$

$$\gamma' = \left[2 - \frac{\ell\,(1-\approx^2)}{b\cos\alpha}\right]^{\frac{1}{2}}$$

$$\varphi = \tan^{-1}\frac{2 - \frac{\ell\cos\alpha}{b}(1+\approx)}{\beta^2(1+\approx)}$$

$$\varphi' = \tan^{-1}\frac{2 - \frac{\ell}{b\cos\alpha}(1+\approx)}{\beta'^2(1+\approx)}$$

A similar integration in which $E_x^{r(-)}(x,y)$ is given by equation 4.28 with $e^{+jky\sin\alpha}$ replaced by $e^{-jky\sin\alpha}$ gives the counter-clockwise travelling-wave field at an arbitrary point in the resonator

between mirrors 1 and 2,

$$E_x^{(-)}(X,Y,Z) = (-1)^n E_o' \frac{\Gamma(\frac{m}{2}+1)\Gamma(\frac{n}{2}+1)}{\Gamma(m+1)\Gamma(n+1)} \sqrt{\frac{2}{\gamma\gamma'}}\, He_m\left(\sqrt{\frac{2k}{\ell}}\frac{\beta}{\gamma}X\right) He_n\left(\sqrt{\frac{2k}{\ell}}\frac{\beta'}{\gamma'}Y\right)$$

$$e^{-\frac{k}{\ell}\left(\frac{\beta^2}{\gamma^2}X^2 + \frac{\beta'^2}{\gamma'^2}Y^2\right)}$$

$$e^{-j\left[\frac{k\ell}{2}(1-\approx) - k\left(\frac{\cos\alpha}{b}\frac{X^2}{\gamma^2} + \frac{1}{b\cos\alpha}\frac{Y^2}{\gamma'^2}\right)\approx - (m+\frac{1}{2})(\frac{\pi}{2}-\chi) - (n+\frac{1}{2})(\frac{\pi}{2}-\chi')\right]} \qquad (4.35)$$

where

$$\chi = \tan^{-1}\frac{2 - \frac{\ell\cos\alpha}{b}(1-\approx)}{\beta^2(1-\approx)}$$

$$\chi' = \tan^{-1}\frac{2 - \frac{\ell}{b\cos\alpha}(1-\approx)}{\beta'^2(1-\approx)}$$

It is easily shown that the contributions to $E_x^{(+)}(X,Y,Z)$ and $E_x^{(-)}(X,Y,Z)$ due to back-scattering of the incident fields $E_x^{i(-)}(x_1,y_1)$ and $E_x^{i(+)}(x_2,y_2)$ at mirrors 1 and 2 respectively are reduced from the fields of equations 4.34 and 4.35 by the factor

$$e^{-\frac{k}{\ell}\left(\frac{\beta'\tan\alpha}{\gamma'}\right)^2}$$

Since this analysis is based on a zero-wavelength approximation the

back-scattered term can be neglected as long as $\beta' \neq 0$.

In a non-rotating resonator the oppositely directed travelling waves may be combined to give a resultant field distribution at each point in the cavity. Since each travelling wave independently satisfies the boundary conditions at the mirrors there is no condition on whether the two fields add or subtract. If the waves have equal amplitudes the total field at point (X,Y,Z) is

$$E_x(X,Y,Z) = E \frac{\Gamma(\frac{m}{2}+1)\Gamma(\frac{n}{2}+1)}{\Gamma(m+1)\Gamma(n+1)} \sqrt{\frac{2}{\gamma\gamma'}} He_m\left(\sqrt{\frac{2k}{\ell}}\frac{\beta}{\gamma}X\right) He_n\left(\sqrt{\frac{2k}{\ell}}\frac{\beta'}{\gamma'}Y\right)$$

$$e^{-\frac{k}{\ell}\left(\frac{\beta^2}{\gamma^2}X^2 + \frac{\beta'^2}{\gamma'^2}Y^2\right)}$$

$$\begin{matrix}\sin \\ \cos\end{matrix}\left[\frac{k\ell}{2}(1+\approx) + k\left(\frac{\cos\alpha}{b}\frac{X^2}{\gamma^2} + \frac{1}{b\cos\alpha}\frac{Y^2}{\gamma'^2}\right)\approx -(m+\tfrac{1}{2})(\tfrac{\pi}{2}-\varphi) - (n+\tfrac{1}{2})(\tfrac{\pi}{2}-\varphi)\right]$$

(4.36)

The arbitrary constant E has a different form for the sine and cosine distributions. In subsequent discussions the sine distribution is arbitrarily chosen for discussion.

The variation in amplitude of $\left[\frac{E_x(X,Y,Z)}{E}\right]$ for the TEM_{00q} mode in three and four-mirror resonators is illustrated in Figures 4.2a and 4.2b. The sine term has been suppressed.

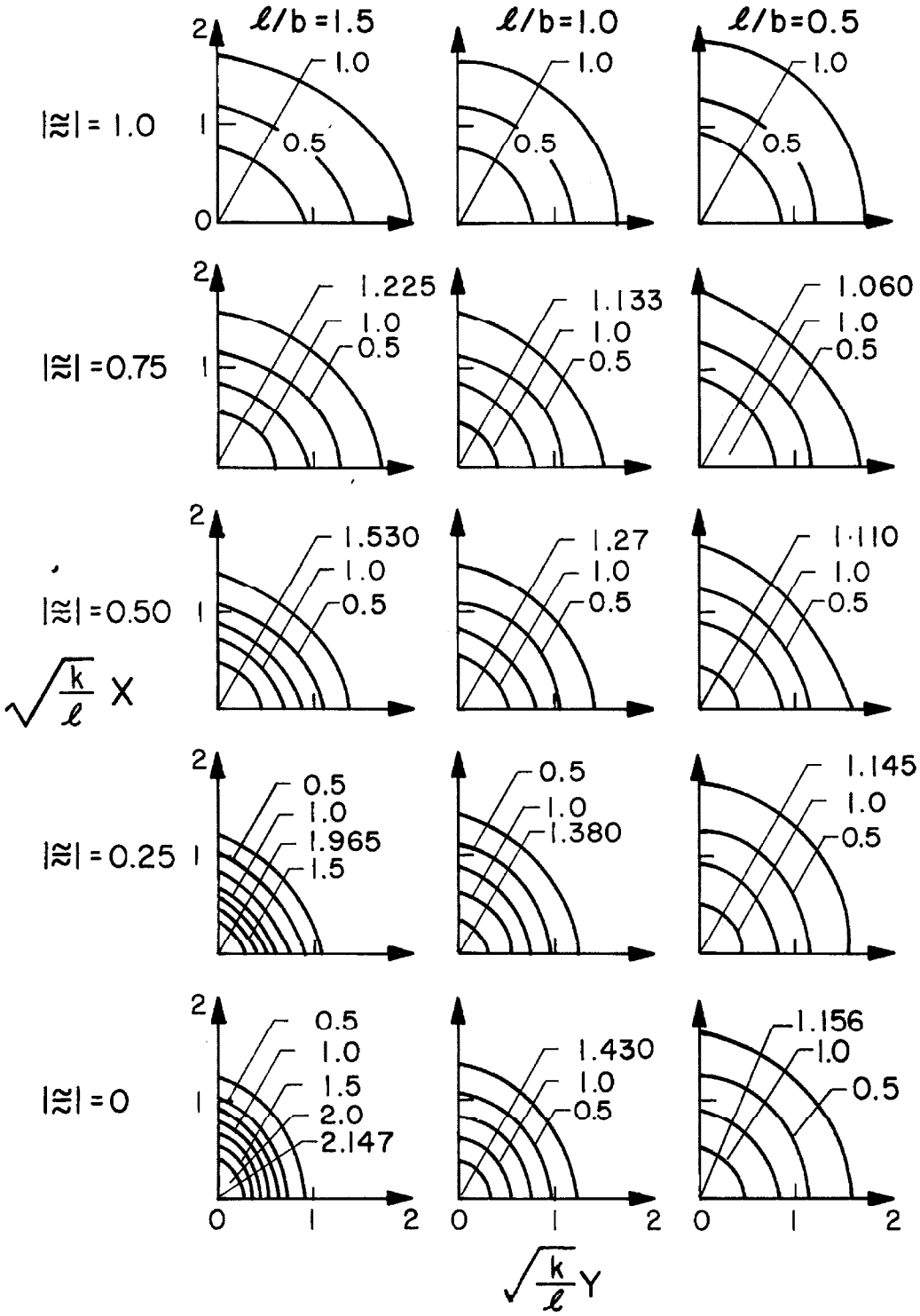

Fig. 4.2a Variation in amplitude of the TEM_{00q} mode in a symmetric three-mirror resonator for $\frac{\ell}{b} = 1.5, 1.0, 0.5$.

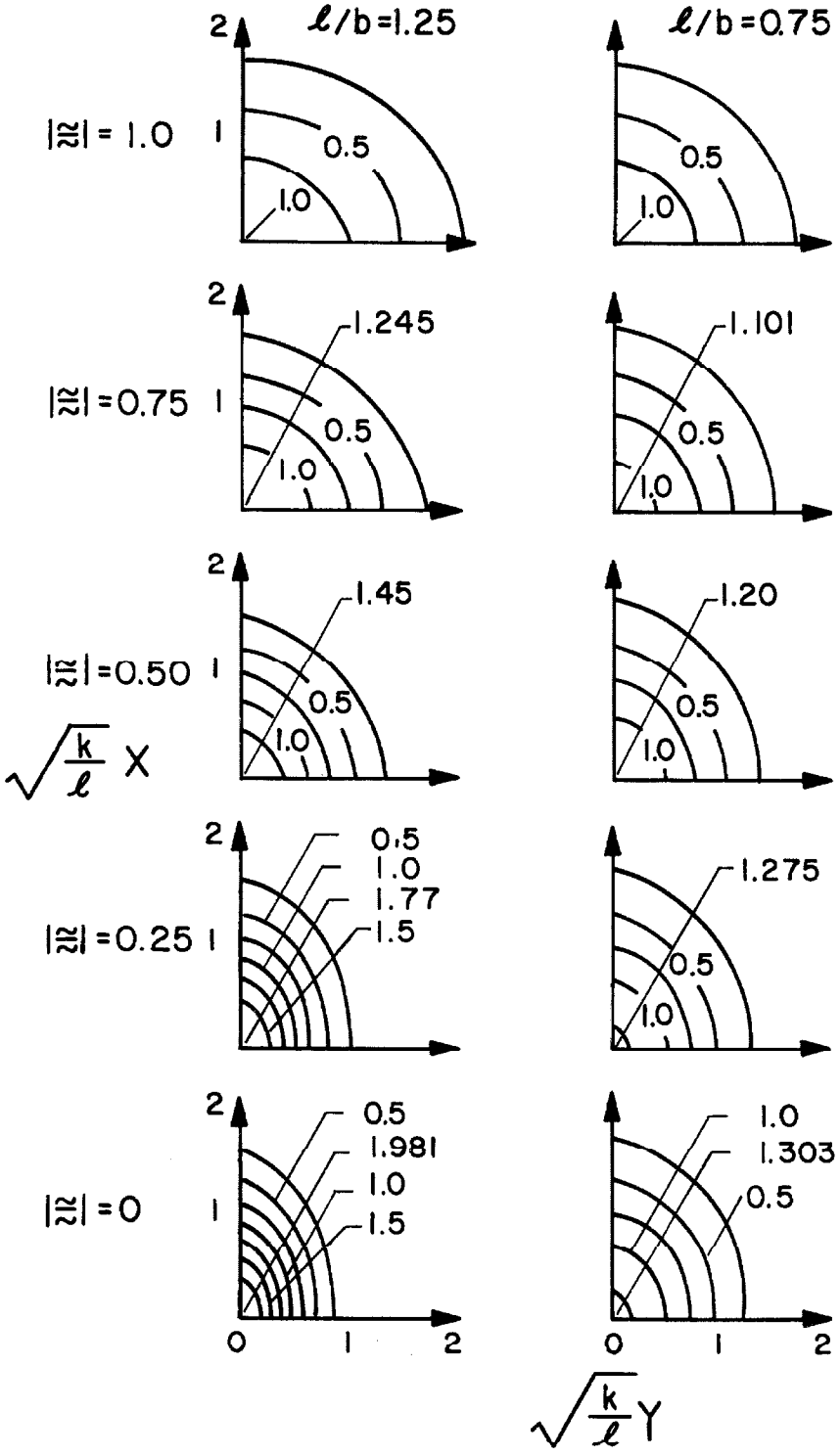

Fig. 4.2b Variation in amplitude of the TEM_{00q} mode in a symmetric four-mirror resonator for $\frac{\ell}{b}$ = 1.25, 0.75.

4.1.3d Nodal Surfaces

Nodal surfaces are defined as those surfaces on which the total electric field is zero. From equation 4.36 it is evident that this will be so when

$$\frac{k\ell}{2}\left(1+\approx\right)+k\left|\frac{\cos\alpha}{b}\frac{X^2}{r^2}+\frac{1}{b\cos\alpha}\frac{Y^2}{r'^2}\right|\approx-\left(m+\frac{1}{2}\right)\left(\frac{\pi}{2}-\varphi\right)-\left(n+\frac{1}{2}\right)\left(\frac{\pi}{2}-\varphi'\right)=p\pi \tag{4.37}$$

where p is an integer.

It is easily shown from equation 4.37 that to a good approximation the nodal surfaces in the far zone of the mirrors are defined by the condition that the line of intersection between the surfaces and a plane containing the Z-axis is a circular arc.

In the X-Z plane the radius of curvature of the curve is

$$\rho=\frac{b}{2}\left|\frac{r_o^2}{\approx_o\cos\alpha}\right| \tag{4.38}$$

and in the Y-Z plane

$$\rho'=\frac{b}{2}\left|\frac{r_o'^2\cos\alpha}{\approx_o}\right|$$

where Z_o ($\approx_o=\frac{2Z_o}{\ell}$) is the point of intersection of the nodal surface and the Z-axis and

$$r_o=\left[2-\frac{\ell\cos\alpha\,(1-\approx_o^2)}{b}\right]^{\frac{1}{2}}$$

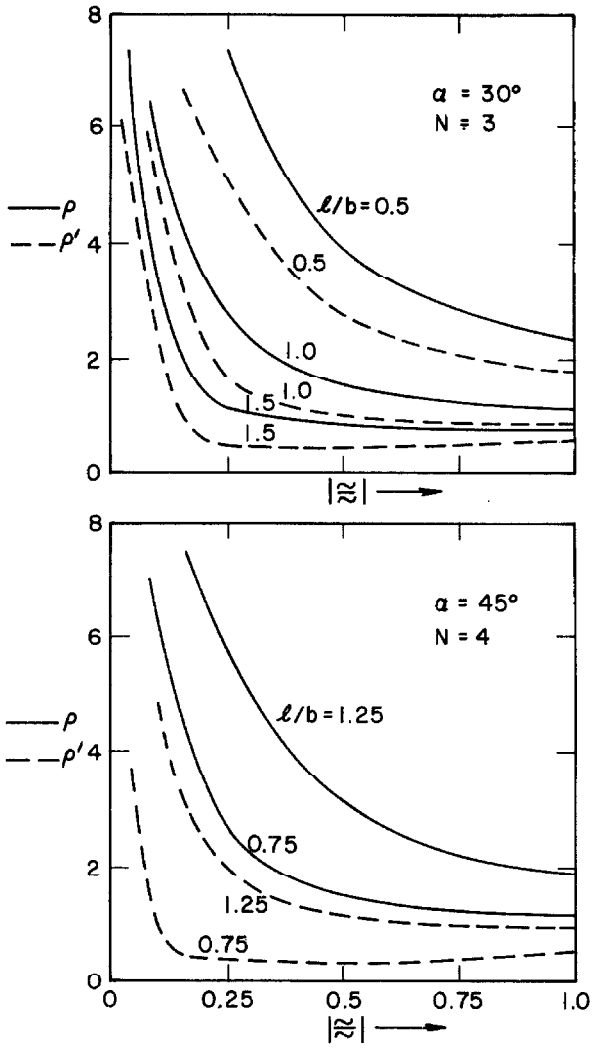

Fig. 4.3a

Variation of the nodal surface radii for symmetric three and four-mirror resonators.

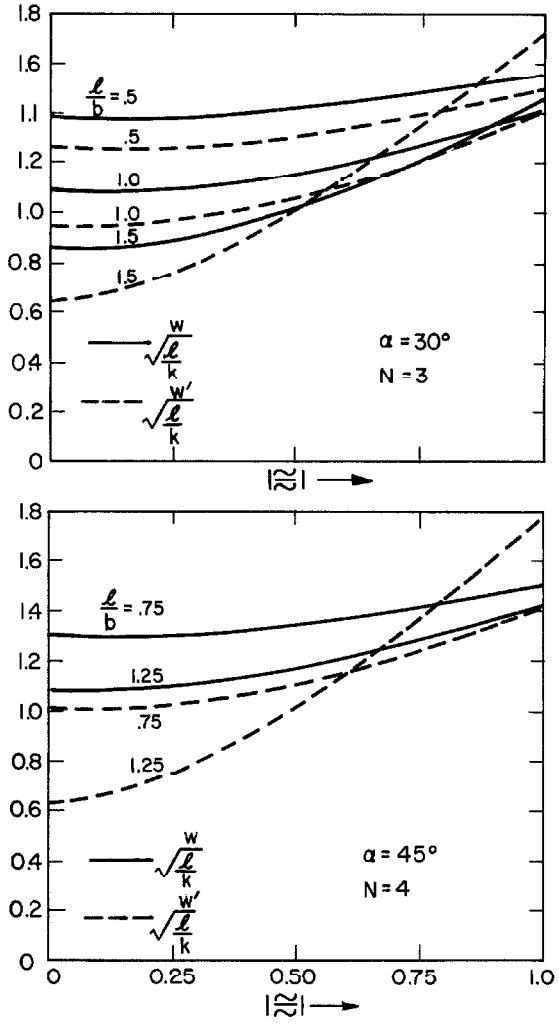

Fig. 4.3b

Variation of the characteristic mode dimensions for symmetric three and four-mirror resonators.

$$r_o' = \left[2 - \frac{\ell\,(1-\approx_o^2)}{b\cos\alpha}\right]^{\frac{1}{2}}$$

The variation of ρ and ρ' with $\approx_o$ is illustrated in Figure 4.3a for three and four-mirror resonators. The mirror spacing ℓ is chosen equal to unity.

4.1.3e Mode Dimensions and Mode Volume

The rate at which the amplitude of the field decays as the distance from the axis increases is determined by the exponential factor in equation 4.36. The constant amplitude locus of the exponential decay factor is an ellipse. Thus the field may be characterized by two dimensions w and w' which are defined as the distances along the X and Y-axes respectively at which the field amplitude decreases to e^{-1} of its value on the axis, viz.

$$w = \sqrt{\frac{\ell}{k}}\ \frac{r}{\beta} \qquad (4.40a)$$

$$w' = \sqrt{\frac{\ell}{k}}\ \frac{r'}{\beta'} \qquad (4.40b)$$

Figure 4.3b illustrates the variation of w and w' with $\approx$ for $\alpha = 30^o$ and 45^o and several values of the ratio $\frac{\ell}{b}$.

The incremental mode volume is defined as dZ times the cross-sectional area enclosed by the curve along which the amplitude has decreased to e^{-1} of its value on the axis, hence

$$dV = \pi\, w\, w'\, dZ$$

$$= \frac{\ell\pi}{2}\, w\, w'\, d\approx$$

The total mode volume between two-mirror is

$$V = \frac{\ell\pi}{2} \int_{-1}^{1} w\, w'\, d\tilde{z}$$

$$= \frac{\ell^2\lambda}{2\beta\beta'} \int_{0}^{1} \gamma\, \gamma'\, d\tilde{z} \qquad (4.41)$$

The integration of equation 4.41 cannot be performed analytically except when $\alpha = 0$ (refer Sections 5.1e and 5.3e).

4.1.3f Numerical Solutions

Numerical values for the diffraction losses and phase shifts in multi-reflector resonators may be obtained by making use of the computed results for standard two mirror cavities. A simple re-scaling of these data transforms them into results applicable to geometries using more than two mirrors.

The data presented here are for resonators in which the mirrors are concave and rectangular in cross-section with dimensions 2a perpendicular to the plane of the resonator and $\frac{2a}{\cos\alpha}$ in the plane of the resonator. In computing these results it was assumed that to a good approximation the eigenvalues for finite mirrors could be expressed as products of the eigenvalues of infinite strip mirrors.

Figures 4.4a and 4.4b, 4.5a and 4.5b and 4.6a and 4.6b illustrate the diffraction loss per side and per circuit for resonators with two, three and four mirrors. The limiting values of $\frac{\ell}{b}$ predicted by the geometrical optics approach of Section 2.3 are indicated.

As the number of mirrors is increased the spacing for minimum

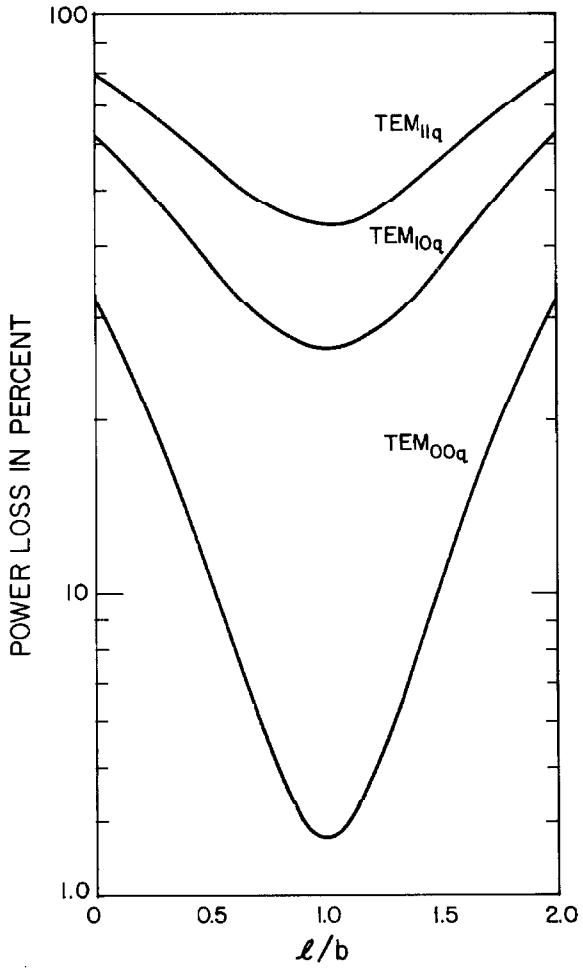

Fig. 4.4a

Power loss/transit for a symmetric two-mirror cavity $(\frac{a^2}{\ell\lambda} = 0.5)$.

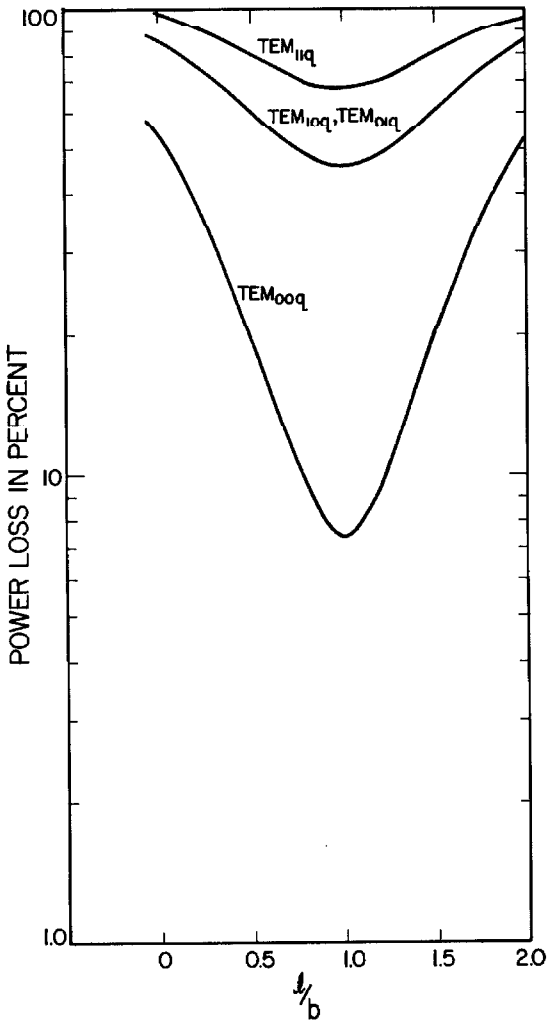

Fig. 4.4b

Power loss/circuit for a symmetric two-mirror cavity $(\frac{a^2}{\ell\lambda} = 0.5)$.

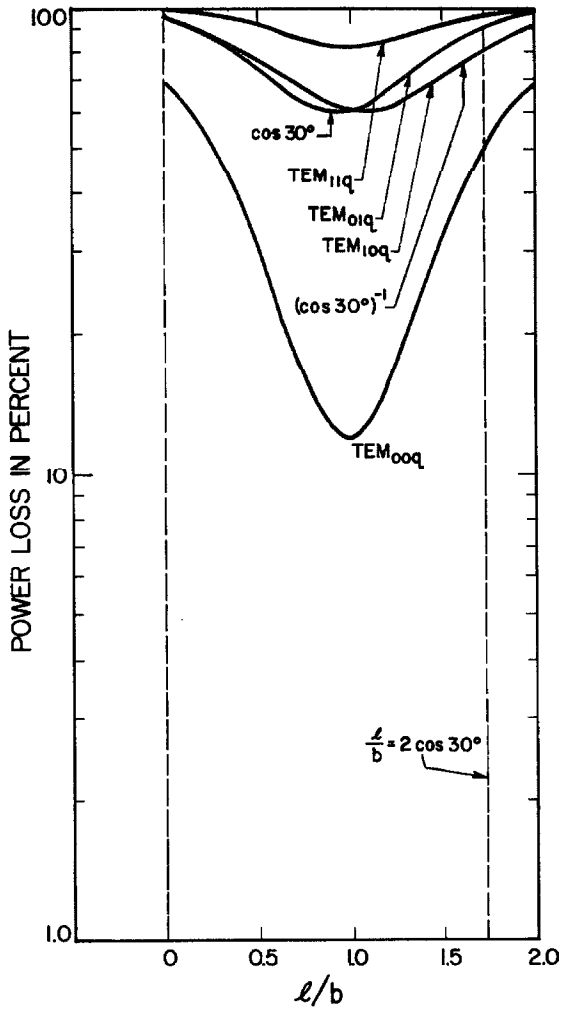

Fig. 4.5a Power loss/side for a symmetric three-mirror cavity ($\frac{a^2}{\ell\lambda} = 0.5$).

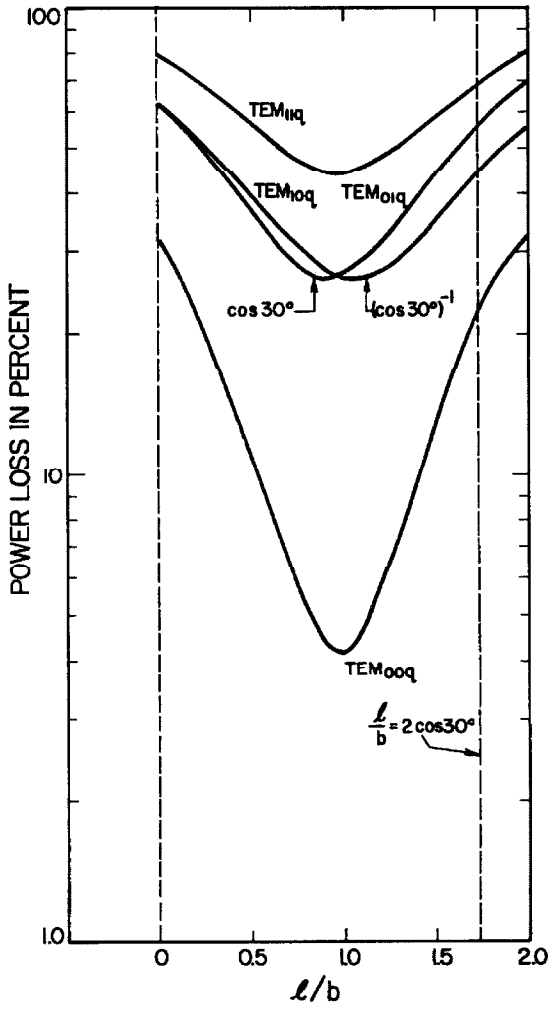

Fig. 4.5b Power loss/circuit for a symmetric three-mirror cavity ($\frac{a^2}{\ell\lambda} = 0.5$).

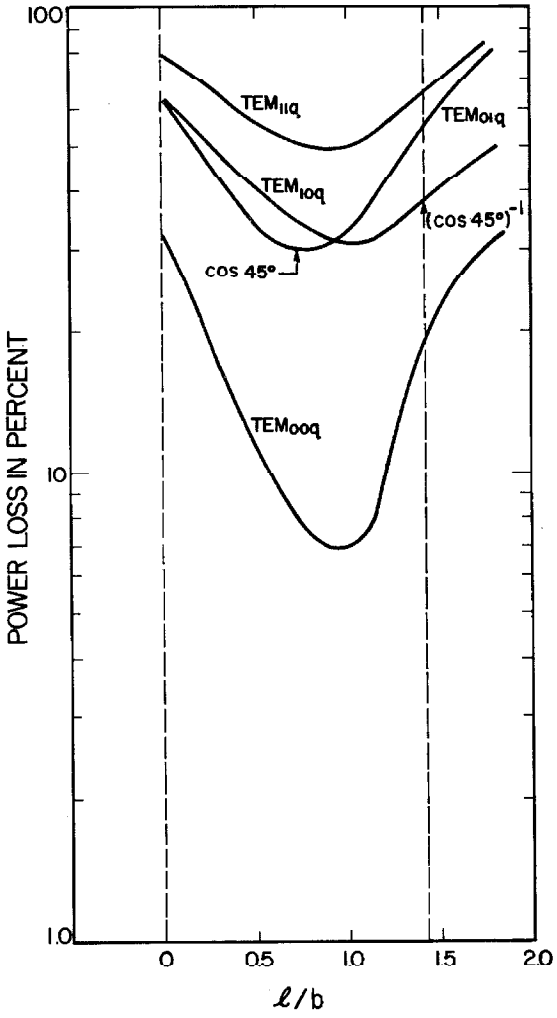

Fig. 4.6a

Power loss/side for a symmetric four-mirror cavity ($\frac{a^2}{\ell\lambda} = 0.5$).

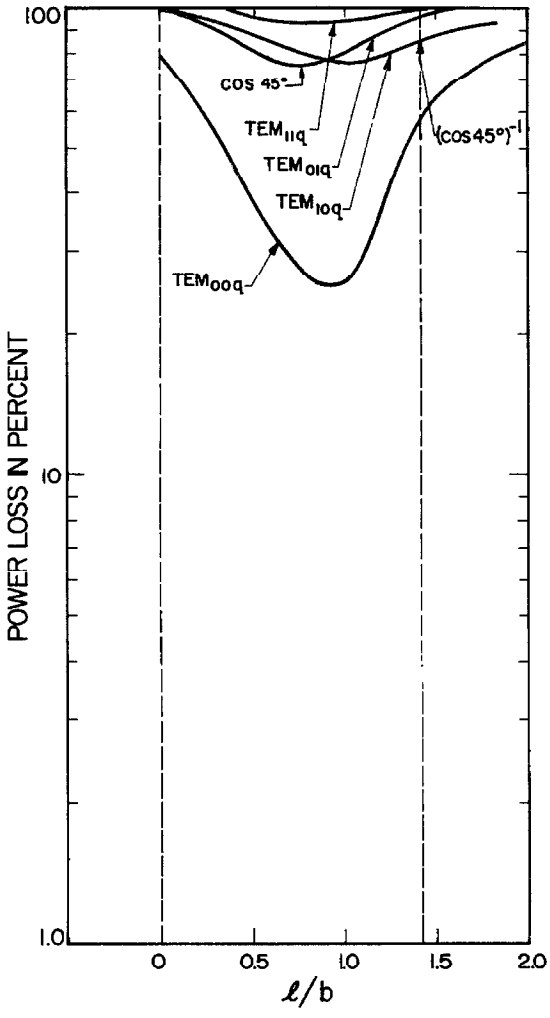

Fig. 4.6b

Power loss/circuit for a symmetric four-mirror cavity ($\frac{a^2}{\ell\lambda} = 0.5$).

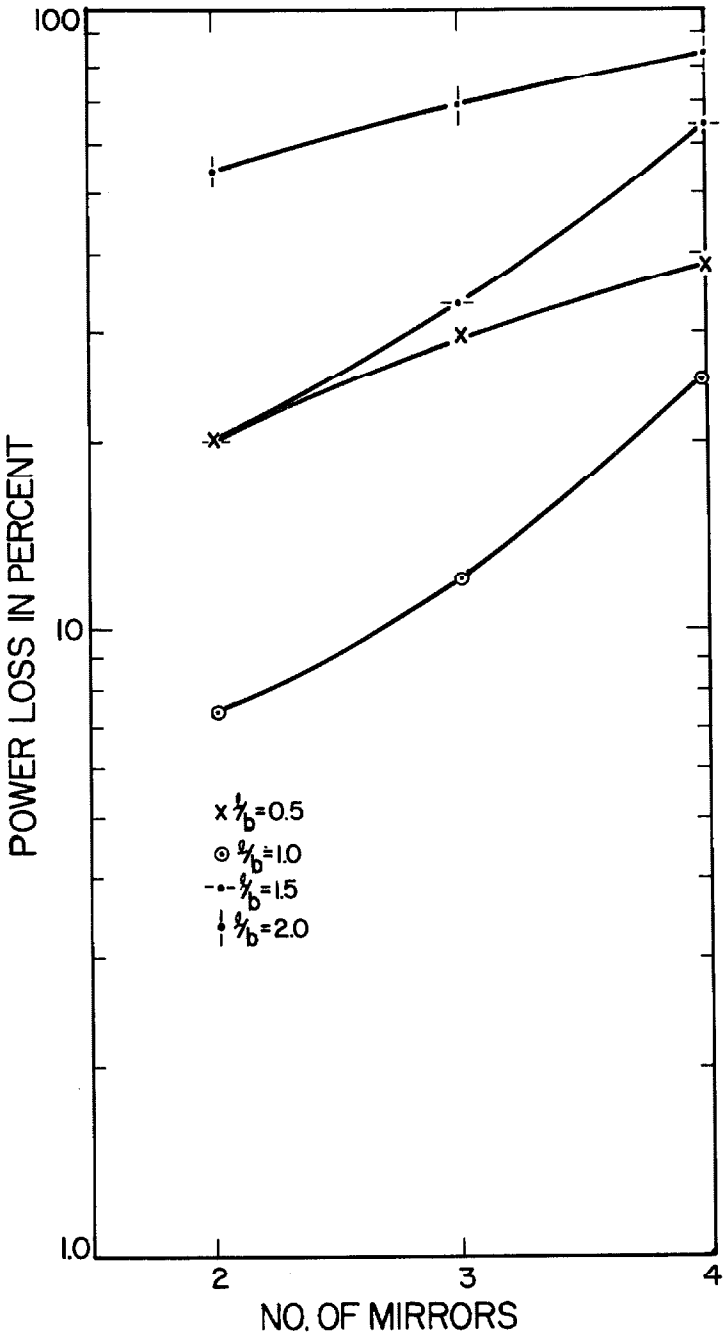

Fig. 4.7 Comparison of the power loss/circuit in the TEM_{00q} mode for two, three and four-mirror resonators.

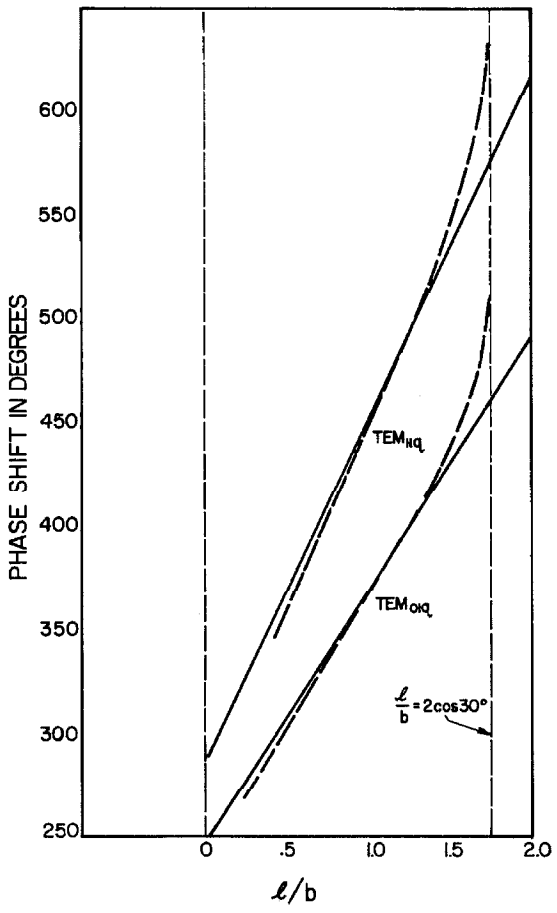

Fig. 4.8a Phase shift/side (leading relative to geometrical phase shift) for a symmetric three-mirror cavity; TEM_{00q} and TEM_{10q} modes $(\frac{a^2}{\ell\lambda} = 0.5)$.

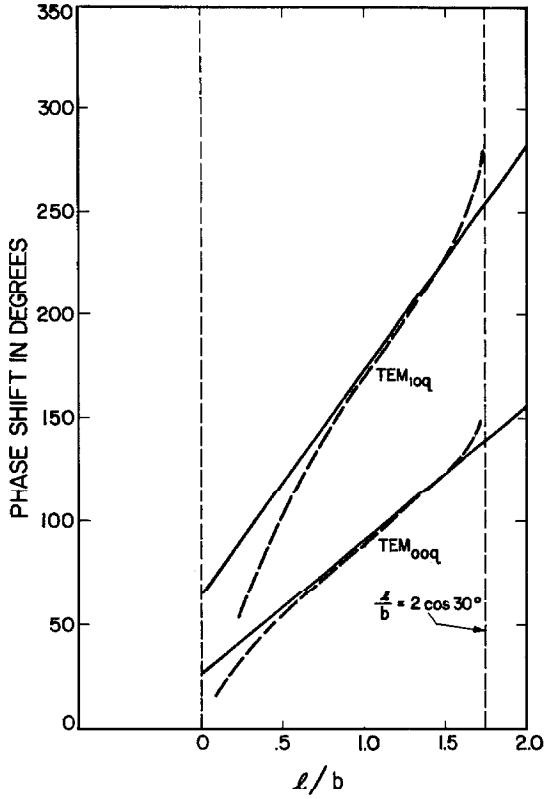

Fig. 4.8b Phase shift/side (leading relative to geometrical phase shift) for a symmetric three-mirror cavity; TEM_{01q} and TEM_{11q} modes $(\frac{a^2}{\ell\lambda} = 0.5)$.

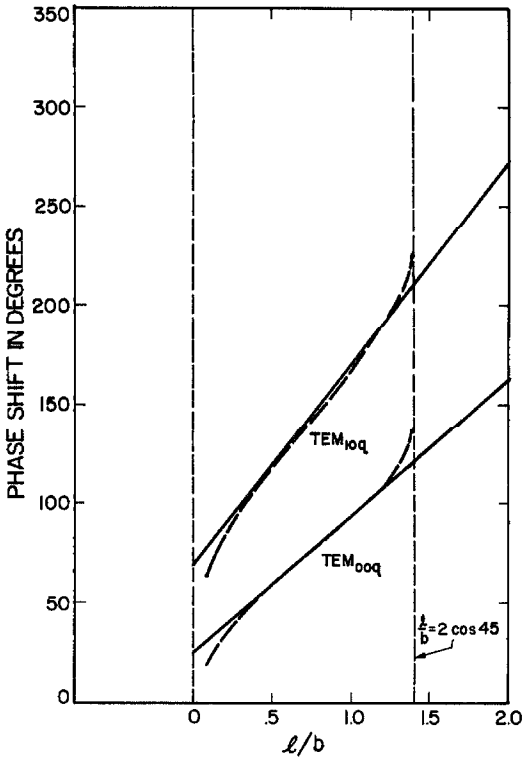

Fig. 4.9a

Phase shift/side (leading relative to geometrical phase shift) for a symmetric four-mirror cavity: TEM_{00q} and TEM_{10q} modes $(\frac{a^2}{\ell\lambda} = 0.5)$.

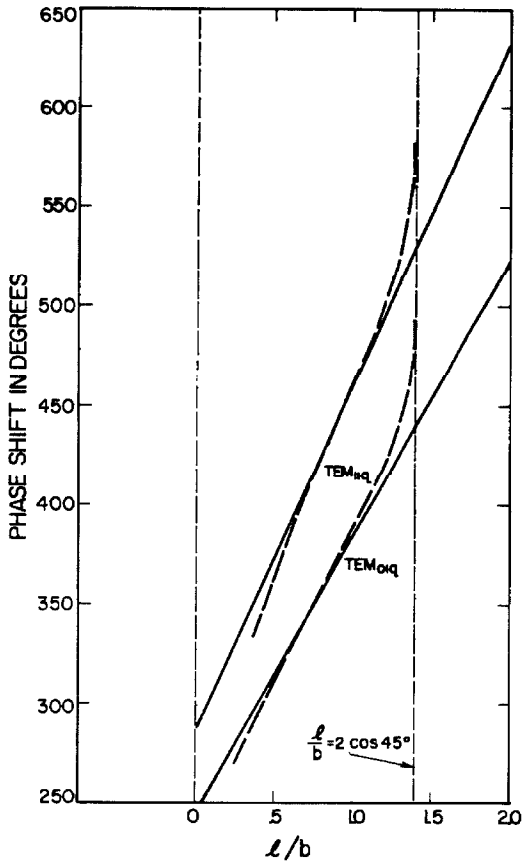

Fig. 4.9b

Phase shift/side (leading relative to geometrical phase shift) for a symmetric four-mirror cavity; TEM_{01q} and TEM_{11q} modes $(\frac{a^2}{\ell\lambda} = 0.5)$.

diffraction loss in the TEM_{00q} and TEM_{11q} modes shifts slowly to values of $\frac{\ell}{b} < 1$. For the TEM_{10q} mode minimum loss occurs at $\frac{\ell}{b} > 1$, while within the accuracy of the calculations the condition for minimum diffraction loss in the TEM_{01q} mode is $\frac{\ell}{b} = \cos \alpha$. As expected the total energy loss is weighted more heavily by diffraction at mirror edges perpendicular to the plane of the resonator than parallel to it and this effect increases rapidly with the degree of field variation in the resonator plane. In fact the optimum ratio of $\frac{\ell}{b}$ for the TEM_{01q} mode corresponds to the "pseudo-confocal" spacing in the resonator plane discussed in Section 4.1.3b.

Figure 4.7 indicates how the power loss per circuit in the TEM_{00q} mode increases as the number of reflectors.

Computed phase shifts for the TEM_{00q}, TEM_{10q}, TEM_{01q} and TEM_{11q} modes in the three and four-mirror cavities are shown in Figures 4.8a and 4.8b, and 4.9a and 4.9b. The dashed curves indicate the values computed from equation 4.31.

4.2 The NonSymmetric Four-Mirror Resonator

4.2a Modes of the Resonator

The coordinate systems on which the self-consistent field analysis of the four-mirror or parrallelogram resonator is based are illustrated in Figure 4.10. Mirrors 1 and 3 have radius of curvature b_1, 2 and 4 have radius of curvature b_2. The 1 to 2 and 3 to 4 center-to-center spacing is ℓ_1, the 2 to 3 and 4 to 1 spacing is ℓ_2. All the reflectors are rectangular in cross-section with dimensions $2a_1$

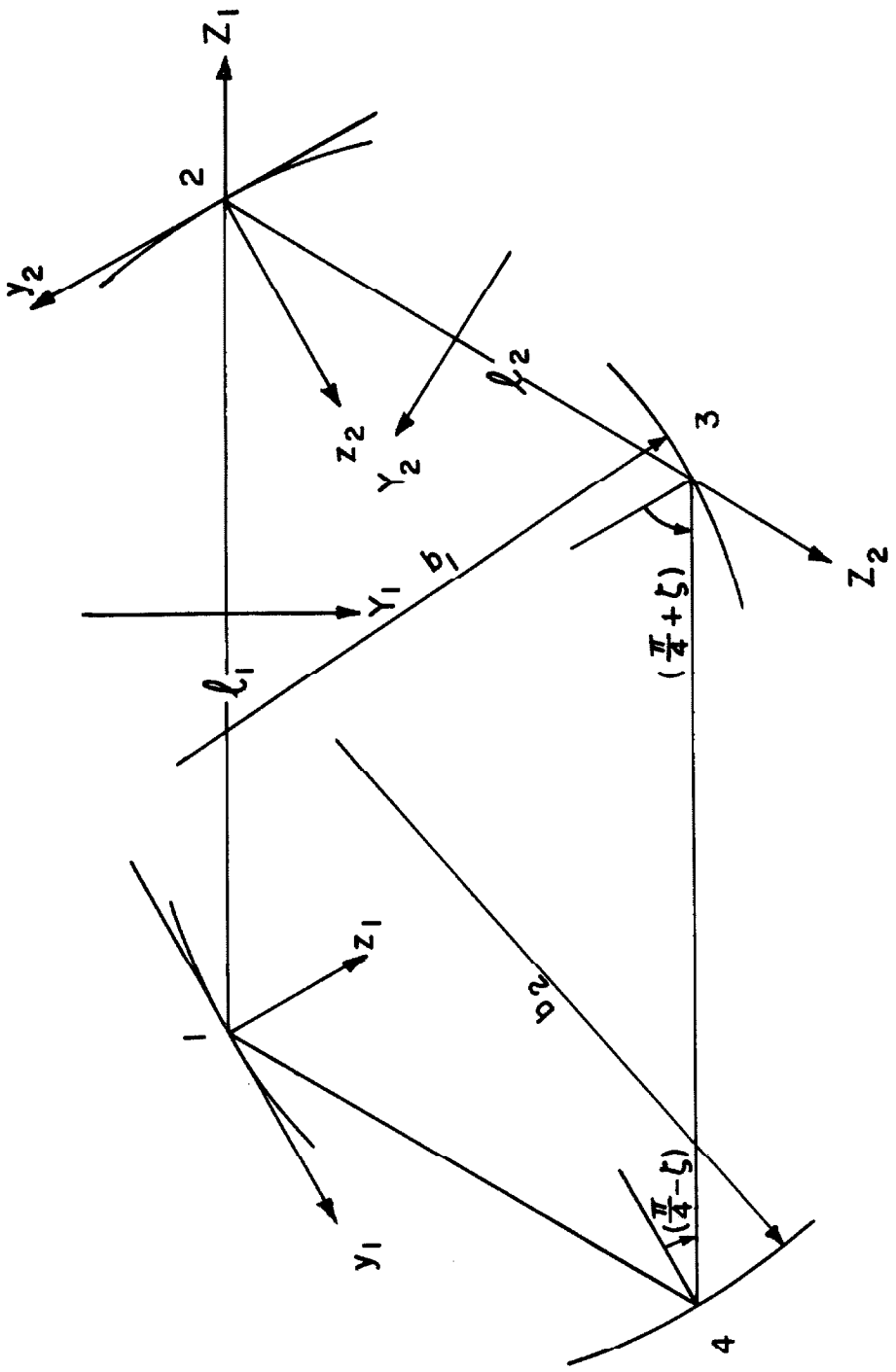

Fig. 4.10 Coordinate system for the analysis of the nonsymmetric four-mirror resonator.

perpendicular to the plane of the resonator and $2a_2$ in the plane of the resonator.

Due to the lack of complete symmetry in the cavity the electric field distribution reflected from mirror 1 will not be identical to that reflected from mirror 2. However the symmetry about the resonator diagonals indicates that the fields reflected from mirrors 1 and 3 (or 2 and 4) will be equal within a constant if modes exist in the resonator. It is assumed that the fields are linearly polarized with the electric vector perpendicular to the plane of the resonator and that the distributions can be written as the products of functions of x and of y, i.e.

$$E_x^{r(\pm)}(x,y) = -E_x^{i(\pm)}(x,y) = f_m^{(\pm)}(x)\, g_n^{(\pm)}(y) \tag{4.42}$$

Then it follows from equation 3.13b that the integral equation for the electric field of the clockwise travelling wave immediately after reflection from mirrors 1 and 3 is

$$\sigma_m^{(+)}\sigma_n^{(+)} f_m^{(+)}(x_3)\, g_n^{(+)}(y_3) = \left|\frac{-jk}{2\pi}\right|^2 \cos\left(\frac{\pi}{4}+\delta\right)\cos\left(\frac{\pi}{4}-\delta\right)\int_{-a_1}^{a_1} dx_1 \int_{-a_2}^{a_2} dy_1\, f_m^{(+)}(x_1)\, g_n^{(+)}(y_1)$$

$$K(x_1,y_1;x_3,y_3) \tag{4.43}$$

where

$$K(x_1,y_1;x_3,y_3) = \int_{-a_1}^{a_1} dx_2 \int_{-a_2}^{a_2} dy_2 \; \frac{e^{-jk(r_{12}+r_{23})}}{r_{12}\, r_{23}}$$

To the accuracy of the Fraunhofer approximation

$$r_{12}+r_{23} \simeq (\ell_1+\ell_2) - x_2\left(\frac{x_1}{\ell_1}+\frac{x_3}{\ell_2}\right) + y_2 \cos\left(\frac{\pi}{4}+\delta\right)\cos\left(\frac{\pi}{4}-\delta\right)\left(\frac{y_1}{\ell_1}+\frac{y_3}{\ell_2}\right)$$

$$+ y_1 \sin\left(\frac{\pi}{4}+\delta\right) - y_3 \sin\left(\frac{\pi}{4}+\delta\right) - x_1^2\left(\frac{\ell_1 \cos\left(\frac{\pi}{4}+\delta\right)-b_1}{2\ell_1 b_1}\right)$$

$$- y_1^2 \cos^2\left(\frac{\pi}{4}+\delta\right)\left(\frac{\ell_1 - b_1 \cos\left(\frac{\pi}{4}+\delta\right)}{2\ell_1 b_1 \cos\left(\frac{\pi}{4}+\delta\right)}\right) - x_3^2\left(\frac{\ell_2 \cos\left(\frac{\pi}{4}+\delta\right)-b_1}{2\ell_2 b_1}\right)$$

$$- y_3^2 \cos^2\left(\frac{\pi}{4}+\delta\right)\left(\frac{\ell_2 - b_1 \cos\left(\frac{\pi}{4}+\delta\right)}{2\ell_2 b_1 \cos\left(\frac{\pi}{4}+\delta\right)}\right) - x_2^2\left(\frac{2\ell_1\ell_2 \cos\left(\frac{\pi}{4}-\delta\right)-b_2(\ell_1+\ell_2)}{2\ell_1\ell_2 b_2}\right)$$

$$- y_2^2 \cos^2\left(\frac{\pi}{4}-\delta\right)\left(\frac{2\ell_1\ell_2 - b_2 \cos\left(\frac{\pi}{4}-\delta\right)(\ell_1+\ell_2)}{2\ell_1\ell_2 b_2 \cos\left(\frac{\pi}{4}-\delta\right)}\right) \qquad (4.44)$$

In the denominator of the integrand $r_{12}r_{23}$ may be replaced by $\ell_1\ell_2$.

The integral equation 4.43 cannot be solved with finite limits of integration. With substitutions similar to those of Section 4.1.1 and in the limit of zero wavelength the kernel may be integrated and 4.43 reduces to

$$\chi_m^{(+)}\chi_n^{(+)}F_m^{(+)}(\xi_3)G_n^{(+)}(\zeta_3) = \frac{1}{2\pi}\int_{-\infty}^{\infty}d\xi_1\int_{-\infty}^{\infty}d\zeta_1\, F_m^{(+)}(\xi_1)\, G_n^{(+)}(\zeta_1)$$

$$e^{j\left[\delta_1\xi_1^2 + \delta_2\xi_3^2 + \delta_1'\zeta_1^2 + \delta_2'\zeta_3^2 - \xi_1\xi_3 - \zeta_1\zeta_3\right]} \qquad (4.45)$$

where

$$\sigma_m^{(+)}\sigma_n^{(+)} = je^{-jk(\ell_1+\ell_2)}\chi_m^{(+)}\chi_n^{(+)}$$

$$\xi = \left[\frac{kb_2}{2\ell_1\ell_2\cos(\frac{\pi}{4}-\delta) - b_2(\ell_1+\ell_2)}\right]^{\frac{1}{2}} x$$

$$\zeta = \left[\frac{kb_2\cos(\frac{\pi}{4}-\delta)}{2\ell_1\ell_2 - b_2\cos(\frac{\pi}{4}-\delta)(\ell_1+\ell_2)}\right]^{\frac{1}{2}} y\cos(\frac{\pi}{4}+\delta)$$

$$\delta_1 = \frac{\ell_1\ell_2\cos 2\delta - (\ell_1+\ell_2)b_2\cos(\frac{\pi}{4}+\delta) - 2\ell_2 b_1\cos(\frac{\pi}{4}-\delta) + b_1b_2}{2b_1b_2}$$

$$\delta_2 = \frac{\ell_1\ell_2\cos 2\delta - (\ell_1+\ell_2)b_2\cos(\frac{\pi}{4}+\delta) - 2\ell_1 b_1\cos(\frac{\pi}{4}-\delta) + b_1b_2}{2b_1b_2}$$

$$\delta_1' = \frac{2\ell_1\ell_2 - (\ell_1+\ell_2)b_2\cos(\frac{\pi}{4}-\delta) - 2\ell_2 b_1\cos(\frac{\pi}{4}+\delta) + \frac{1}{2}b_1b_2\cos 2\delta}{b_1b_2\cos 2\delta}$$

$$\delta_2' = \frac{2\ell_1\ell_2 - (\ell_1+\ell_2)b_2 \cos\left(\frac{\pi}{4}-\delta\right) - 2\ell_1 b_1 \cos\left(\frac{\pi}{4}+\delta\right) + \frac{1}{2} b_1 b_2 \cos 2\delta}{b_1 b_2 \cos 2\delta}$$

with

$$\overset{(+)}{F}_m(\xi) \equiv \overset{(+)}{f}_m(x)$$

and

$$\overset{(+)}{G}_n(\zeta) \equiv \overset{(+)}{g}_n(y)\, e^{-jky \sin\left(\frac{\pi}{4}+\delta\right)}$$

Equation 4.45 is obviously separable, i.e.

$$\overset{(+)}{\chi}_m \overset{(+)}{F}_m(\xi_3) = \frac{1}{\sqrt{2\pi}} \int_{-\infty}^{\infty} d\xi_1 \overset{(+)}{F}_m(\xi_1)\, e^{j\left[\delta_1\xi_1^2 + \delta_2\xi_2^2 - \xi_1\xi_3\right]} \qquad (4.46a)$$

$$\overset{(+)}{\chi}_n \overset{(+)}{G}_n(\zeta_3) = \frac{1}{\sqrt{2\pi}} \int_{-\infty}^{\infty} d\zeta_1 \overset{(+)}{G}_n(\zeta_1)\, e^{j\left[\delta_1'\zeta_1^2 + \delta_2'\zeta_3^2 - \zeta_1\zeta_3\right]} \qquad (4.46b)$$

The solutions of Appendix 4 apply to equations 4.46a and 4.46b. This is easily seen by rewriting them as

$$\overset{(+)}{\chi}_m \overset{(+)}{\overline{F}}_m(\xi_3) = \frac{1}{\sqrt{2\pi}} \int_{-\infty}^{\infty} d\xi_1 \overset{(+)}{\overline{F}}_m(\xi_1)\, e^{j\left[\frac{(\delta_1+\delta_2)}{2}(\xi_1^2+\xi_3^2) - \xi_1\xi_3\right]} \qquad (4.47a)$$

$$\overset{(+)}{\chi}_n \overset{(+)}{\overline{G}}_n(\zeta_3) = \frac{1}{\sqrt{2\pi}} \int_{-\infty}^{\infty} d\zeta_1 \overset{(+)}{\overline{G}}_n(\zeta_1)\, e^{j\left[\frac{(\delta_1'+\delta_2')}{2}(\zeta_1^2+\zeta_2^2) - \zeta_1\zeta_2\right]} \qquad (4.47b)$$

where

$$\overline{F}_m^{(+)}(\xi)\, e^{-j\frac{(\delta_1 - \delta_2)}{2}\xi^2} \equiv f_m^{(+)}(x)$$

$$\overline{G}_n^{(+)}(\zeta)\, e^{-j\frac{(\delta_1' - \delta_2')}{2}\zeta^2} \equiv g_n^{(+)}(y)\, e^{-jky \sin(\frac{\pi}{4} + \delta)}$$

The integral equations for the counter-clockwise travelling wave are identical with equations 4.47a and 4.47b with the functions given by

$$\overline{F}_m^{(-)}(\xi)\, e^{j\frac{(\delta_1 - \delta_2)}{2}\xi^2} \equiv f_m^{(-)}(x)$$

$$\overline{G}_n^{(-)}(\zeta)\, e^{j\frac{(\delta_1' - \delta_2')}{2}\zeta^2} \equiv g_n^{(-)}(y)\, e^{jky \sin(\frac{\pi}{4} + \delta)}$$

After some simplification the field distribution reflected from mirrors 1 and 3 for clockwise travelling-wave modes is found to be

$$E_x^{r(+)}(x,y)_{1,3} = E_{13} \frac{\Gamma(\frac{m}{2}+1)\Gamma(\frac{n}{2}+1)}{\Gamma(m+1)\Gamma(n+1)} He_m\left[\left(\frac{k}{\sqrt{\ell_1 \ell_2}}\right)^{\frac{1}{2}} \beta_{13}\, x\right]$$

$$He_n\left[\left(\frac{k}{\sqrt{\ell_1 \ell_2}}\right)^{\frac{1}{2}} \beta_{13}'\, y \cos(\frac{\pi}{4} + \delta)\right]$$

$$e^{-\frac{k}{2\sqrt{\ell_1 \ell_2}}(\beta_{13}^2 x^2 + \beta_{13}'^2 y^2 \cos^2(\frac{\pi}{4} + \delta))}$$

$$e^{jk(y \sin(\frac{\pi}{4} + \delta) + \rho_{13} x^2 + \rho_{13}' y^2 \cos^2(\frac{\pi}{4} + \delta))} \qquad (4.48)$$

where

$$\beta_{13} = \left[\frac{\sqrt{\ell_1\ell_2}\,b_2}{2\ell_1\ell_2\cos(\frac{\pi}{4}-\delta) - b_2(\ell_1+\ell_2)}\right]^{\frac{1}{2}}$$

$$\times\left\{1-\left[\frac{\ell_1\ell_2\cos 2\delta - (\ell_1+\ell_2)\left(b_1\cos(\frac{\pi}{4}-\delta)+b_2\cos(\frac{\pi}{4}+\delta)\right)+b_1b_2}{b_1b_2}\right]^2\right\}^{\frac{1}{4}}$$

$$\beta'_{13} = \left[\frac{\sqrt{\ell_1\ell_2}\,b_2\cos(\frac{\pi}{4}-\delta)}{2\ell_1\ell_2 - b_2\cos(\frac{\pi}{4}-\delta)(\ell_1+\ell_2)}\right]^{\frac{1}{2}}$$

$$\times\left\{1-\left[\frac{2\ell_1\ell_2-(\ell_1+\ell_2)\left(b_1\cos(\frac{\pi}{4}+\delta)+b_2\cos(\frac{\pi}{4}-\delta)\right)+\frac{1}{2}b_1b_2\cos 2\delta}{\frac{1}{2}b_1b_2\cos 2\delta}\right]^2\right\}^{\frac{1}{4}}$$

$$\rho_{13} = \frac{(\ell_2-\ell_1)\cos(\frac{\pi}{4}-\delta)}{2\ell_1\ell_2\cos(\frac{\pi}{4}-\delta) - b_2(\ell_1+\ell_2)}$$

$$\rho'_{13} = \frac{(\ell_2-\ell_1)}{2\ell_1\ell_2 - b_2\cos(\frac{\pi}{4}-\delta)(\ell_1+\ell_2)}$$

The usual gamma function normalization has been chosen so that $E_x(0_1 0)_{1,3} = \pm E_{13}$ for m and n even.

The field distribution reflected in a counter-clockwise direction from mirrors 1 and 3 is obtained by changing the sign of the complex exponential in equation 4.48. In a non-rotating cavity the field distribution observed at a slightly transmitting mirror would have the form of equation 4.48 with the complex exponential replaced by the sine or cosine of its argument. Both circular functions are allowable since the two travelling waves are independent.

The electric field reflected from mirrors 2 and 4 for the clockwise travelling-wave modes results from interchanging ℓ_1 and ℓ_2, b_1 and b_2, and $(\frac{\pi}{4}+\delta)$ and $(\frac{\pi}{4}-\delta)$ in equation 4.48. Hence

$$E_x^{r(+)}(x,y)_{2,4} = E_{24}\,\frac{\Gamma(\frac{n}{2}+1)\Gamma(\frac{n}{2}+1)}{\Gamma(m+1)\Gamma(n+1)}\,He_m\left[\left(\frac{k}{\sqrt{\ell_1\ell_2}}\right)^{\frac{1}{2}}\beta_{24}\,x\right]$$

$$He_n\left[\left(\frac{k}{\sqrt{\ell_1\ell_2}}\right)^{\frac{1}{2}}\beta'_{24}\,y\cos\left(\tfrac{\pi}{4}-\delta\right)\right]$$

$$e^{-\frac{1}{2}\frac{k}{\sqrt{\ell_1\ell_2}}\left(\beta_{24}^2 x^2 + \beta_{24}'^2 y^2\cos^2\left(\frac{\pi}{4}-\delta\right)\right)}$$

$$e^{jk\left(y\sin\left(\frac{\pi}{4}-\delta\right) + \rho_{24}\,x^2 + \rho'_{24}\,y^2\cos^2\left(\frac{\pi}{4}-\delta\right)\right)} \qquad (4.49)$$

where

$$\beta_{24} = \left[\frac{\sqrt{\ell_1\ell_2}\, b_1}{2\ell_1\ell_2\cos(\frac{\pi}{4}+\delta) - b_1(\ell_1+\ell_2)}\right]^{\frac{1}{2}}$$

$$x\left\{1-\left[\frac{\ell_1\ell_2\cos 2\delta - (\ell_1+\ell_2)\left|b_1\cos(\frac{\pi}{4}-\delta) + b_2\cos(\frac{\pi}{4}+\delta)\right| + b_1 b_2}{b_1 b_2}\right]^2\right\}^{\frac{1}{4}}$$

$$\beta'_{24} = \left[\frac{\sqrt{\ell_1\ell_2}\, b_2\cos(\frac{\pi}{4}+\delta)}{2\ell_1\ell_2 - b_1\cos(\frac{\pi}{4}+\delta)(\ell_1+\ell_2)}\right]^{\frac{1}{2}}$$

$$x\left\{1-\left[\frac{2\ell_1\ell_2 - (\ell_1+\ell_2)\left|b_1\cos(\frac{\pi}{4}+\delta) + b_2\cos(\frac{\pi}{4}-\delta)\right| + \frac{1}{2}\, b_1 b_2\cos 2\delta}{\frac{1}{2}\, b_1 b_2\cos 2\delta}\right]^2\right\}^{\frac{1}{4}}$$

$$\rho_{24} = \frac{(\ell_2-\ell_1)\cos(\frac{\pi}{4}+\delta)}{2\ell_1\ell_2\cos(\frac{\pi}{4}+\delta) - b_2(\ell_1+\ell_2)}$$

$$\rho'_{24} = \frac{(\ell_2-\ell_1)}{2\ell_1\ell_2 - b_2\cos(\frac{\pi}{4}+\delta)(\ell_1\ell_2)}$$

The relation between the constants E_{13} and E_{24} is obtained by calculating $E_x^{i(+)}(x_2,y_2)$ from a knowledge of $E_x^{r(+)}(x_1,y_1)$ (refer equation 3.11). It is easily shown that

$$\left|\frac{E_{13}}{E_{24}}\right| = \left\{\frac{b_2^2\cos(\frac{\pi}{4}-\delta)}{b_1^2\cos(\frac{\pi}{4}+\delta)} \; \frac{2\ell_1\ell_2\cos(\frac{\pi}{4}+\delta)-b_1(\ell_1+\ell_2)}{2\ell_1\ell_2\cos(\frac{\pi}{4}-\delta)-b_2(\ell_1+\ell_2)} \; \frac{2\ell_1\ell_2-b_1\cos(\frac{\pi}{4}+\delta)(\ell_1+\ell_2)}{2\ell_1\ell_2-b_2\cos(\frac{\pi}{4}-\delta)(\ell_1+\ell_2)}\right\}^{\frac{1}{4}} \tag{4.50}$$

In order that the field distribution decay rapidly towards the edges of the mirrors it is necessary that

$$\beta_{13},\ \beta_{24} > 0$$

$$\beta'_{13},\ \beta'_{24} > 0$$

This second requirement leads to the stability condition derived by geometrical optics (refer Section 2.2b),

$$0 \leq \left[1-\frac{\ell_1}{b_1\cos(\frac{\pi}{4}+\delta)}\right]\left[1-\frac{\ell_2}{b_2\cos(\frac{\pi}{4}-\delta)}\right]+\left[1-\frac{\ell_1}{b_2\cos(\frac{\pi}{4}-\delta)}\right]\left[1-\frac{\ell_2}{b_1\cos(\frac{\pi}{4}+\delta)}\right] \leq 2 \tag{2.28}$$

The relation resulting from the first requirement is less rigorous and may be neglected.

4.2b Resonance Conditions

The eigenvalues corresponding to the solutions of equation 4.45 are purely imaginary, i.e.

$$\sigma_m^{(+)}\sigma_n^{(+)} = (-j)^{m+n+1} e^{-jk(\ell_1+\ell_2)+ j(m+\frac{1}{2})\tan^{-1}\frac{(\delta_1+\delta_2)}{\beta_{13}^2}+ j(n+\frac{1}{2})\tan^{-1}\frac{(\delta_1'+\delta_2')}{\beta_{13}'^2}} \tag{4.51}$$

For resonance the total phase shift around the resonator must be an integral q times 2π. Thus from equation 4.51 the resonance condition is

$$2q\pi = 2\left|k(\ell_1+\ell_2) - (m+n+1)\frac{3\pi}{2} - (m+\frac{1}{2})\tan^{-1}\frac{(\delta_1+\delta_2)}{\beta_{13}^2} - (n+\frac{1}{2})\tan^{-1}\frac{(\delta_1'+\delta_2')}{\beta_{13}'^2}\right| \tag{4.52}$$

or

$$\frac{4(\ell_1+\ell_2)}{\lambda} = 2q + (m+n+1)+ \frac{2}{\pi}(m+\frac{1}{2})\tan^{-1}\frac{(\delta_1+\delta_2)}{\beta_{13}^2}+ \frac{2}{\pi}(n+\frac{1}{2})\tan^{-1}\frac{(\delta_1'+\delta_2')}{\beta_{13}'^2} \tag{4.53}$$

The phase shift between two mirrors separated by ℓ_1 is obtained from the calculation of $E_x^{i(+)}(x_2,y_2)$ from a knowledge of $E_x^{r(+)}(x_1,y_1)$. It is found to be

$$\left|\Delta \text{ phase}\right|_{\ell_1} = \left|k\ell_1 - (m+3n+1)\frac{\pi}{2} - (m+\frac{1}{2})\theta_1 - (n+\frac{1}{2})\theta_1'\right| \tag{4.54}$$

where

$$\theta_1 = \tan^{-1} \frac{2\ell_1^2 \cos(\frac{\pi}{4} - \delta)\left[\ell_2 \cos(\frac{\pi}{4} + \delta) - b_1\right] - b_2(\ell_1 + \ell_2)\left[\ell_1 \cos(\frac{\pi}{4} + \delta) - b_1\right]}{\ell_1\left\{b_1^2 b_2^2 - \left[\ell_1\ell_2 \cos 2\delta - (\ell_1+\ell_2)\left(b_1 \cos(\frac{\pi}{4} - \delta) + b_2 \cos(\frac{\pi}{4} + \delta)\right) + b_1 b_2\right]^2\right\}^{\frac{1}{4}}}$$

$$\theta_1' = \tan^{-1} \frac{2\ell_1^2\left[\ell_2 - b_1 \cos(\frac{\pi}{4} + \delta)\right] - b_2 \cos(\frac{\pi}{4} - \delta)\ (\ell_1+\ell_2)\left[\ell_1 - b_1 \cos(\frac{\pi}{4} + \delta)\right]}{\ell_1\left\{\frac{1}{4} b_1^2 b_2^2 \cos^2 2\delta - \left[2\ell_1\ell_2 - (\ell_1+\ell_2)\left(b_1 \cos(\frac{\pi}{4} + \delta) + b_2 \cos(\frac{\pi}{4} - \delta)\right) + \frac{1}{2} b_1 b_2 \cos 2\delta\right]^2\right\}^{\frac{1}{4}}}$$

The change in phase corresponding to propagation between two reflectors of spacing ℓ_2 is

$$\left| \Delta \text{ phase} \right|_{\ell_2} = \left| k\ell_2 - (m+3n+1)\frac{\pi}{2} - (m+\tfrac{1}{2})\,\theta_2 - (n+\tfrac{1}{2})\,\theta_2' \right| \qquad (4.55)$$

where

$$\theta_2 = \tan^{-1} \frac{2\ell_2^2 \cos(\frac{\pi}{4} + \delta)\left[\ell_1 \cos(\frac{\pi}{4} - \delta) - b_2\right] - b_1(\ell_1+\ell_2)\left[\ell_2 \cos(\frac{\pi}{4} - \delta) - b_2\right]}{\ell_2\left\{b_1^2 b_2^2 - \left[\ell_1\ell_2 \cos 2\delta - (\ell_1+\ell_2)\left(b_1 \cos(\frac{\pi}{4} - \delta) + b_2 \cos(\frac{\pi}{4} + \delta)\right) + b_1 b_2\right]^2\right\}^{\frac{1}{4}}}$$

$$\theta_2' = \tan^{-1} \frac{2\ell_2^2\left[\ell_1 - b_2 \cos(\frac{\pi}{4} - \delta)\right] - b_1 \cos(\frac{\pi}{4} + \delta)\ (\ell_1+\ell_2)\left[\ell_2 - b_2 \cos(\frac{\pi}{4} - \delta)\right]}{\ell_2\left\{\frac{1}{4} b_1^2 b_2^2 \cos 2\delta - \left[2\ell_1\ell_2 - (\ell_1+\ell_2)\left(b_1 \cos(\frac{\pi}{4} + \delta) + b_2 \cos(\frac{\pi}{4} - \delta)\right) + \frac{1}{2} b_1 b_2 \cos 2\delta\right]^2\right\}^{\frac{1}{4}}}$$

4.2c Electric Field at an Arbitrary Point in the Resonator

The electric field travelling in a clockwise direction at some arbitrary point in the resonator between mirrors 1 and 2 is calculated from the distribution reflected from mirror 1 (refer equation 4.48) using the integral of equation 3.10. The result of the integration is

$$E_x^{(+)}(X_1,Y_1,Z_1) = E_{13}\frac{\Gamma(\frac{m}{2}+1)\,\Gamma(\frac{n}{2}+1)}{\Gamma(m+1)\,\Gamma(n+1)}\sqrt{\frac{2}{r_1 r_1'}}\,He_m\left[\left(\frac{2k}{\sqrt{\ell_1\ell_2}}\right)^{\frac{1}{2}}\frac{\beta_{13}}{r_1}X_1\right]$$

$$He_n\left[\left(\frac{2k}{\sqrt{\ell_1\ell_2}}\right)^{\frac{1}{2}}\frac{\beta_{13}'}{r_1'}Y_1\right]e^{-\frac{k}{\sqrt{\ell_1\ell_2}}\left(\frac{\beta_{13}^2}{r_1^2}X_1^2+\frac{\beta_{13}'^2}{r_1'^2}Y_1^2\right)}$$

$$e^{-j\left[\frac{k\ell_1}{2}(1+\approx_1)+\frac{k}{\ell_1}\frac{(X_1^2+Y_1^2)}{(1+\approx_1)}+\frac{2k}{\sqrt{\ell_1\ell_2}}\left(\frac{\eta_1 X_1^2}{r_1^2}+\frac{\eta_1' Y_1^2}{r_1'^2}\right)\right]}$$

$$e^{j(m+\frac{1}{2})(\frac{\pi}{2}+\varphi_1)+j(n+\frac{1}{2})(\frac{\pi}{2}+\varphi_1')} \qquad (4.56)$$

where

$$\approx_1 = \frac{2Z_1}{\ell_1}$$

$$r_1 = \sqrt{2}\,(1+\approx_1)\left[\frac{1}{4}\left(\frac{\ell_1}{\ell_2}\right)\beta_{13}^4+\eta_1^2\right]^{\frac{1}{2}}$$

$$r_1' = \sqrt{2}\,(1+\approx_1)\left[\frac{1}{4}\left(\frac{\ell_1}{\ell_2}\right)\beta_{13}^4 + \eta_1'^2\right]^{\frac{1}{2}}$$

$$\varphi_1 = \tan^{-1}\frac{2\eta_1}{\left(\frac{\ell_1}{\ell_2}\right)^{\frac{1}{2}}\beta_{13}^2}$$

$$\varphi_1' = \tan^{-1}\frac{2\eta_1'}{\left(\frac{\ell_1}{\ell_2}\right)^{\frac{1}{2}}\beta_{13}'^2}$$

$$\eta_1 = \frac{\ell_1(\ell_2-\ell_1)\cos(\frac{\pi}{4}-\delta)}{2\ell_1\ell_2\cos(\frac{\pi}{4}-\delta) - b_2(\ell_1+\ell_2)} + \frac{\ell_1\cos(\frac{\pi}{4}+\delta)}{2b_1} - \frac{1}{1+\approx_1}$$

$$\eta_1' = \frac{\ell_1(\ell_2-\ell_1)}{2\ell_1\ell_2 - b_2\cos(\frac{\pi}{4}-\delta)(\ell_1+\ell_2)} + \frac{\ell_1}{2b_1\cos(\frac{\pi}{4}+\delta)} - \frac{1}{1+\approx_1}$$

For the situation in which waves of equal amplitude are propagating in both directions around a non-rotating cavity the transverse standing wave existing along ℓ_1 in the far zone of the mirrors is obtained by replacing the exponential phase function in 4.56 by the corresponding sine or cosine function. As in Section 4.1.3c a sine distribution is assumed, viz.

$$E_x(X_1,Y_1,Z_1) = E'_{13}\frac{\Gamma(\frac{m}{2}+1)\Gamma(\frac{n}{2}+1)}{\Gamma(m+1)\Gamma(n+1)}\sqrt{\frac{2}{r_1 r'_1}}\,He_m\left[\left(\frac{2k}{\sqrt{\ell_1\ell_2}}\right)^{\frac{1}{2}}\frac{\beta_{13}}{r_1}X_1\right]$$

$$He_n\left[\left(\frac{2k}{\sqrt{\ell_1\ell_2}}\right)^{\frac{1}{2}}\frac{\beta'_{13}}{r'_1}Y_1\right]\,e^{-\frac{k}{\sqrt{\ell_1\ell_2}}\left(\frac{\beta_{13}^2}{r_1^2}X_1^2+\frac{\beta'^2_{13}}{r'^2_1}Y_1^2\right)}$$

$$\sin\left\{\frac{k\ell_1}{2}(1+\approx_1)\frac{k}{\ell_1}\frac{(X_1^2+Y_1^2)}{(1+\approx_1)}+\frac{2k}{\sqrt{\ell_1\ell_2}}\left(\frac{\eta_1 X_1^2}{r_1^2}+\frac{\eta'_1 Y_1^2}{r'^2_1}\right)\right.$$

$$\left.-(m+\tfrac{1}{2})(\tfrac{\pi}{2}+\varphi_1)-(n+\tfrac{1}{2})(\tfrac{\pi}{2}+\varphi'_1)\right\} \qquad (4.57)$$

This can be shown by calculating the travelling-wave distribution for a field moving counter-clockwise from mirror 2. Using equations 4.50 and 4.54 the result of this calculation can be combined with equation 4.56 to give the result of equation 4.57.

The corresponding transverse standing wave along ℓ_2 in the far zone of the mirrors is

$$E_x(X_2,Y_2,Z_2) = E'_{24}\frac{\Gamma(\frac{m}{2}+1)\Gamma(\frac{n}{2}+1)}{\Gamma(m+1)\Gamma(n+1)}\sqrt{\frac{2}{r_2 r'_2}}\,He_m\left[\left(\frac{2k}{\sqrt{\ell_1\ell_2}}\right)^{\frac{1}{2}}\frac{\beta_{24}}{r_2}X_2\right]$$

$$\mathrm{He}_n\left[\left(\frac{2k}{\sqrt{\ell_1\ell_2}}\right)^{\frac{1}{2}}\frac{\beta'_{24}}{r'_2}\,Y_2\right]e^{-\frac{k}{\sqrt{\ell_1\ell_2}}\left(\frac{\beta_{24}^2}{r_2^2}X_2^2+\frac{\beta_{24}'^2}{r_2'^2}Y_2^2\right)}$$

$$\sin\left\{\frac{k\ell_2}{2}(1+\approx_2)+\frac{k}{\ell_2}\frac{(X_2^2+Y_2^2)}{(1+\approx_2)}+\frac{2k}{\sqrt{\ell_1\ell_2}}\left(\frac{\eta_2X_2^2}{r_2^2}+\frac{\eta'_2Y_2^2}{r_2'^2}\right)\right.$$

$$\left.-(m+\tfrac{1}{2})(\tfrac{\pi}{2}+\varphi_2)-(n+\tfrac{1}{2})(\tfrac{\pi}{2}+\varphi'_2)\right\} \qquad (4.58)$$

where

$$\approx_2 = \frac{2Z_2}{\ell_2}$$

$$r_2 = \sqrt{2}\,(1+\approx_2)\left[\tfrac{1}{4}\left(\frac{\ell_2}{\ell_1}\right)\beta_{24}^4+\eta_2^2\right]^{\frac{1}{2}}$$

$$r'_2 = \sqrt{2}\,(1+\approx_2)\left[\tfrac{1}{4}\left(\frac{\ell_2}{\ell_1}\right)\beta_{24}'^4+\eta_2'^2\right]^{\frac{1}{2}}$$

$$\varphi_2 = \tan^{-1}\frac{2\eta_2}{\left(\frac{\ell_2}{\ell_1}\right)^{\frac{1}{2}}\beta_{24}^2}$$

$$\varphi_2' = \tan^{-1} \frac{2\eta_2'}{\left(\frac{\ell_2}{\ell_1}\right)^{\frac{1}{2}} \beta_{24}'^2}$$

$$\eta_2 = \frac{\ell_2(\ell_1-\ell_2)\cos(\frac{\pi}{4}+\delta)}{2\ell_1\ell_2\cos(\frac{\pi}{4}+\delta) - b_1(\ell_1+\ell_2)} + \frac{\ell_2\cos(\frac{\pi}{4}-\delta)}{2b_2} - \frac{1}{1+\approx_2}$$

$$\eta_2' = \frac{\ell_2(\ell_1-\ell_2)}{2\ell_1\ell_2 - b_1\cos(\frac{\pi}{4}+\delta)(\ell_1+\ell_2)} + \frac{\ell_2}{2b_2\cos(\frac{\pi}{4}-\delta)} - \frac{1}{1+\approx_2}$$

4.2d Nodal Surfaces

The requirement that the total electric field be zero at points along ℓ_1 and along ℓ_2 leads to two sets of nodal surfaces. To a good approximation these surfaces are defined by the condition that the line of intersection between them and a plane containing the Z_1 or Z_2-axis be a circular arc.

Along ℓ_1 the radius of the curve of intersection is

$$\rho_1 = \frac{\ell_1}{2} \left| \frac{(1+\approx_{10})}{1+2\sqrt{\frac{\ell_1}{\ell_2}} \frac{\eta_{10}}{r_{10}^2}(1+\approx_{10})} \right| \qquad (4.59a)$$

in the X_1-Z_1 plane, and

$$\rho_1' = \frac{\ell_1}{2}\left|\frac{(1+\approx_{10})}{1+2\sqrt{\frac{\ell_1}{\ell_2}}\frac{\eta'_{10}}{r'^2_{10}}(1+\approx_{10})}\right| \tag{4.59b}$$

in the Y_1-Z_1 plane.

The corresponding radii along ℓ_2 are

$$\rho_2 = \frac{\ell_2}{2}\left|\frac{(1+\approx_{20})}{1+2\sqrt{\frac{\ell_2}{\ell_1}}\frac{\eta_{20}}{r^2_{20}}(1+\approx_{20})}\right| \tag{4.60a}$$

and

$$\rho_2' = \frac{\ell_2}{2}\left|\frac{(1+\approx_{20})}{1+2\sqrt{\frac{\ell_2}{\ell_1}}\frac{\eta'_{20}}{r'^2_{20}}(1+\approx_{20})}\right| \tag{4.60b}$$

The nodal surfaces intersect the Z_1 and Z_2-axis at Z_{10} and Z_{20} respectively. The additional subscript 0 indicates that $\approx_1$ and $\approx_2$ have been replaced by $\approx_{10} = \frac{2Z_{10}}{\ell_1}$ and $\approx_{20} = \frac{2Z_{20}}{\ell_2}$ in the various parameters involved.

4.2e Mode Dimensions and Mode Volume

As in Section 4.1.3c the mode dimensions are defined as those distances along the axes at which the arguments of the exponential factors in equations 4.57 and 4.58 become -1. Thus the nonsymmetric four-mirror resonator is characterized by four mode dimensions. From

equation 4.57 the mode dimensions along ℓ_1 are

$$w_1 = \left(\frac{\sqrt{\ell_1 \ell_2}}{k}\right)^{\frac{1}{2}} \frac{r_1}{\beta_{13}} \quad \text{in the } X_1 \text{ direction} \tag{4.61a}$$

$$w_1' = \left(\frac{\sqrt{\ell_1 \ell_2}}{k}\right)^{\frac{1}{2}} \frac{r_1'}{\beta_{13}'} \quad \text{in the } Y_1 \text{ direction} \tag{4.61b}$$

From equation 4.58 those along ℓ_2 are

$$w_2 = \left(\frac{\sqrt{\ell_1 \ell_2}}{k}\right) \frac{r_2}{\beta_{24}} \quad \text{in the } X_2 \text{ direction} \tag{4.62a}$$

$$w_2' = \left(\frac{\sqrt{\ell_1 \ell_2}}{k}\right) \frac{r_2'}{\beta_{24}'} \quad \text{in the } Y_2 \text{ direction} \tag{4.62b}$$

The corresponding mode volumes are

$$V_1 = \frac{\ell_1 \ell_2 \lambda}{2\beta_{13}\beta_{13}'} \int_0^1 r_1 r_1' \, d\xi_1 \tag{4.63}$$

between mirrors 1 and 2 or 3 and 4

$$V_2 = \frac{\ell_1 \ell_2 \lambda}{2\beta_{24}\beta_{24}'} \int_0^1 r_2 r_2' \, d\xi_2 \tag{4.64}$$

between mirrors 2 and 3 or 1 and 4.

CHAPTER V

THE SELF-CONSISTENT FIELD ANALYSIS OF THE TWO-MIRROR RESONATOR

The properties of the standard two-mirror resonator will be summarized in this chapter. In the case of the symmetric cavity these may be obtained by setting $\alpha = 0$ $(N = 2)$ in the results of Section 4.1. The analysis of the nonsymmetric resonator is similar to that followed in Section 4.2.

5.1 Symmetric, Nonconfocal Resonator

5.1a Modes of the Resonator

The symmetric, nonconfocal resonator is illustrated schematically in Figure 5.1. Unlike the multimirror resonators both mirrors can be represented in the same coordinate system. The reflector spacing is ℓ and the mirror curvature b. Both mirrors are square in cross-section with side dimension 2a.

Setting $\alpha = 0$ in equation 4.28 gives the distribution of the reflected electric field for the normal modes of the resonator, viz.

$$E_x^r(x,y) = E_o \frac{\Gamma(\frac{m}{2}+1)\,\Gamma(\frac{n}{2}+1)}{\Gamma(m+1)\,\Gamma(n+1)} \, He_m\left(\sqrt{\frac{k}{\ell}}\,\beta x\right) \, He_n\left(\sqrt{\frac{k}{\ell}}\,\beta y\right)$$

$$e^{-\frac{k}{2\ell}\beta^2(x^2+y^2)} \qquad (5.1)$$

where

$$\beta = \left(2\frac{\ell}{b} - \frac{\ell^2}{b^2}\right)^{\frac{1}{4}}$$

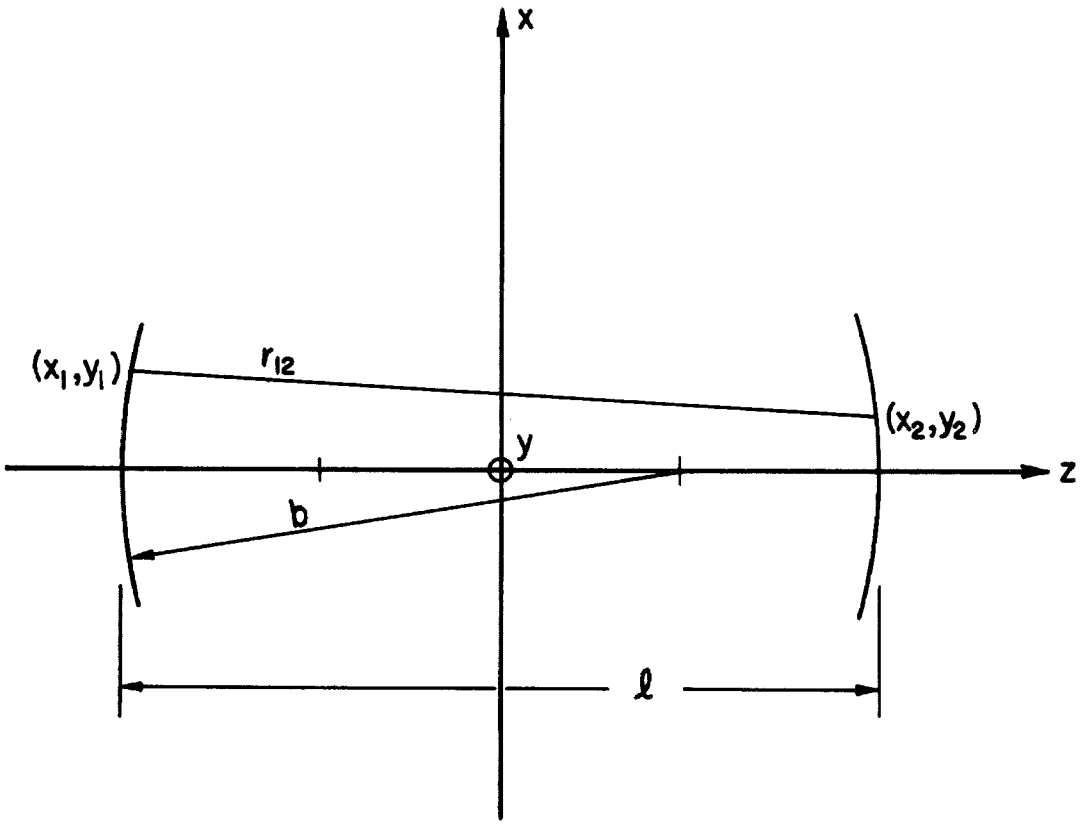

Fig. 5.1 A symmetric, nonconfocal two-mirror resonator.

From the expression for β it is evident that this approximate analysis fails when $\ell \geq 2b$.

5.1b Resonance Conditions and Diffraction Losses

The resonance condition for the symmetric, nonconfocal resonator does not follow directly from equation 4.31 with $\alpha = 0$ and $N = 2$. This results from the fact that the modes are defined differently for resonators in which a travelling wave reflects back on itself and resonators in which the travelling wave circulates. It is easily shown that this difference appears as a factor $(-1)^n$ in the expression 4.30 for the eigenvalues $\sigma_m^{(+)}\sigma_n^{(+)}$. With this correction the resonance condition becomes

$$\frac{4\ell}{\lambda} = 2q + (m+n+1)\left[1+\frac{2}{\pi}\tan^{-1}\frac{2\delta}{\beta^2}\right] \qquad (5.2)$$

where $\delta = \frac{\ell-b}{2b}$.

It is evident from equation 5.2 that no frequency degeneracy exists. The spectral range or mode separation is

$$\Delta\left(\frac{1}{\lambda}\right) = \frac{1}{4\ell}\left\{2\Delta q + \left[1+\frac{2}{\pi}\tan^{-1}\frac{2\delta}{\beta^2}\right]\Delta(m+n)\right\} \qquad (5.3)$$

The results given by equation 5.2 and 5.3 differ slightly from those obtained using the concept of the equivalent confocal resonator (19) namely

$$\frac{4\ell}{\lambda} = 2q + (m+n+1)\left[1-\frac{4}{\pi}\tan^{-1}\frac{(1-\frac{\ell}{b})}{(1+\frac{\ell}{b})}\right] \qquad (5.4)$$

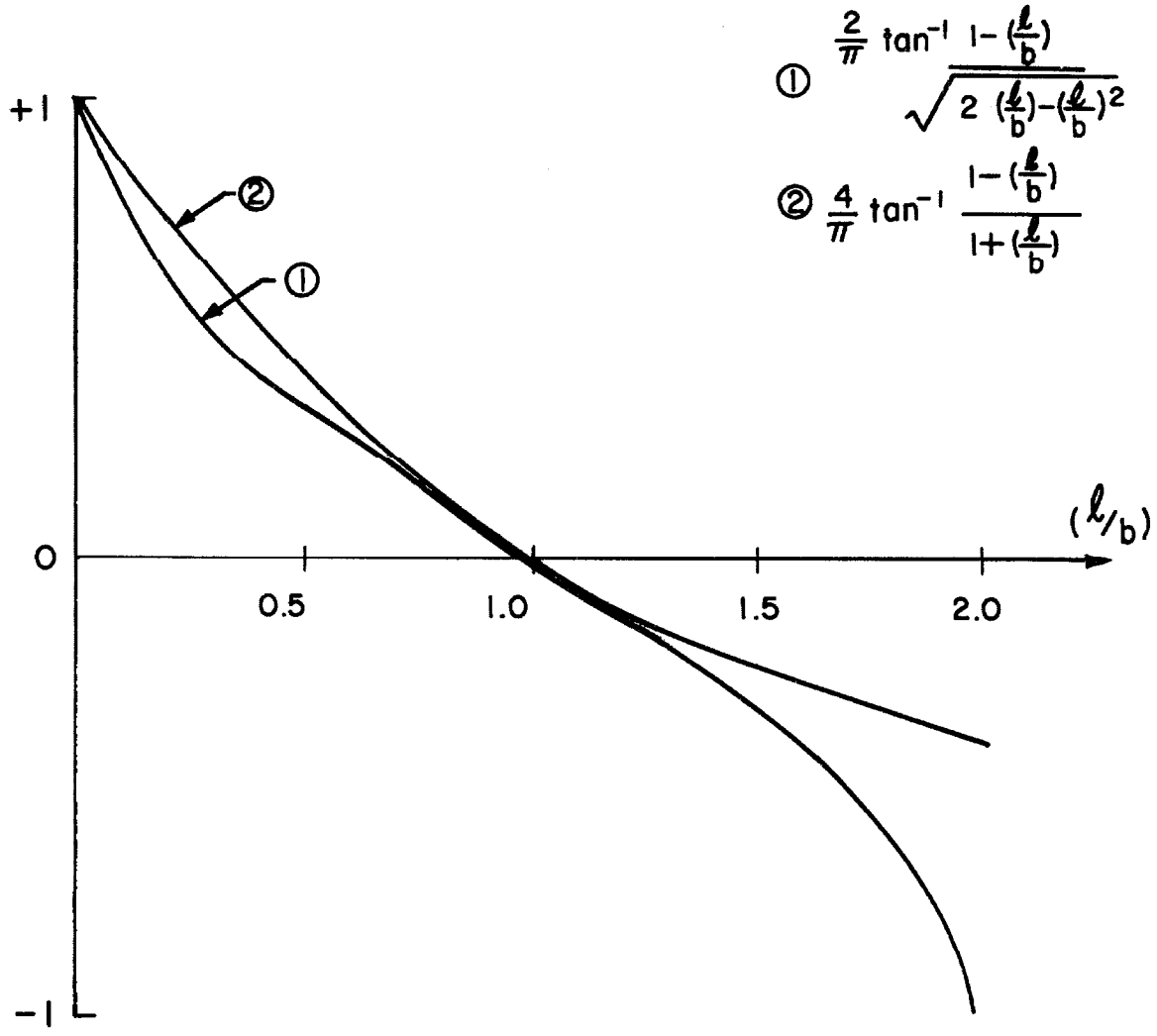

Fig. 5.2 Difference in resonance conditions for the symmetric, non-confocal resonator.

and

$$\left(\frac{1}{\lambda}\right) = \frac{1}{4\ell}\left\{2\Delta q + \left[1 - \frac{4}{\pi}\tan^{-1}\frac{\left(1-\frac{\ell}{b}\right)}{\left(1+\frac{\ell}{b}\right)}\right]\Delta(m+n)\right\} \qquad (5.5)$$

The difference in the last terms of equations 5.2 and 5.4 is illustrated in Figure 5.2 as a function of $\left(\frac{\ell}{b}\right)$.

The properties of the integral equation for the modes of the resonator were discussed in Section 3.2 There it was indicated that with a complex, symmetric but non-Hermitian kernel there is no guarantee that variational techniques will give a result which approaches the lowest order eigenvalue. However in Appendix 5 it is shown that at optical wavelengths an approximation to the lowest order eigenvalue is

$$\left|\sigma_o\right| \simeq \operatorname{erf}\left\{\sqrt{\frac{k}{\ell}}\,\beta a\right\} \qquad (5.6)$$

The fractional energy loss per reflection due to diffraction effects for an infinite cylindrical mirror, i.e.

$$\alpha_D = 1 - \operatorname{erf}^2\left\{\sqrt{\frac{k}{\ell}}\,\beta a\right\} \qquad (5.7)$$

is shown in Figure 5.3. Also shown are the results obtained by Boyd and Gordon (19) using their concept of the equivalent resonator and the results obtained by Fox and Li (24) using numerical iteration.

5.1c Electric Field at an Arbitrary Point in the Resonator

The transverse field travelling in the positive z-direction at an arbitrary point in the resonator is obtained from equation 4.34 with

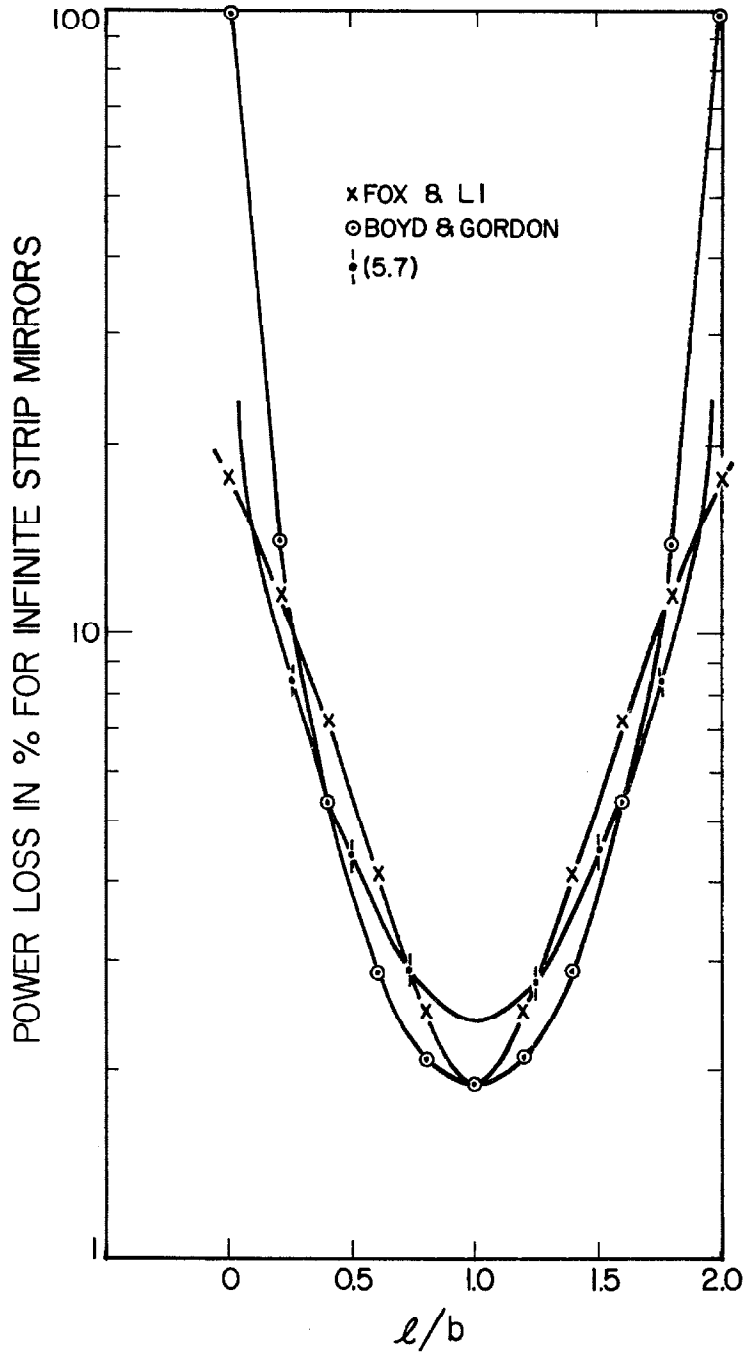

Fig. 5.3 Diffraction loss for the TEM_{00q} mode in a symmetric two-mirror resonator with infinite cylindrical reflectors ($\frac{a^2}{\ell\lambda} = 0.5$).

$\alpha = 0$, thus

$$E_x^{(+)}(x,y,z) = E_o \frac{\Gamma(\frac{m}{2}+1)\Gamma(\frac{n}{2}+1)}{\Gamma(m+1)\Gamma(n+1)} \frac{\sqrt{2}}{\gamma} He_m\left(\sqrt{\frac{2k}{\ell}} \frac{\beta}{\gamma} x\right)$$

$$He_n\left(\sqrt{\frac{2k}{\ell}} \frac{\beta}{\gamma} y\right) e^{-\frac{k}{\ell}\frac{\beta^2}{\gamma^2}(x^2+y^2)}$$

$$e^{j\left[\frac{k\ell}{2}(1+\xi)+\frac{k}{b}(x^2+y^2)\frac{\xi}{\gamma^2}-(m+n+1)(\frac{\pi}{2}-\varphi)\right]} \tag{5.8}$$

with

$$\xi = \frac{2z}{\ell}$$

$$\gamma = \left[2 - \frac{\ell(1-\xi^2)}{b}\right]^{\frac{1}{2}}$$

$$\varphi = \tan^{-1} \frac{2 - \frac{\ell}{b}(1+\xi)}{\beta^2(1+\xi)}$$

Similarly from equation 4.35 the negatively directed wave is

$$E_x^{(-)}(x,y,z) = -E_o \frac{\Gamma(\frac{m}{2}+1)\Gamma(\frac{n}{2}+1)}{\Gamma(m+1)\Gamma(n+1)} \frac{\sqrt{2}}{\gamma} He_m\left(\sqrt{\frac{2k}{\ell}} \frac{\beta}{\gamma} x\right)$$

$$He_n\left(\sqrt{\frac{2k}{\ell}} \frac{\beta}{\gamma} y\right) e^{-\frac{k}{\ell}\frac{\beta^2}{\gamma^2}(x^2+y^2)}$$

$$e^{j\left[\frac{k\ell}{2}(1-\xi)-\frac{k}{b}(x^2+y^2)\frac{\xi}{\gamma^2}-(m+n+1)(\frac{\pi}{2}-\chi)\right]} \tag{5.9}$$

with

$$\chi = \tan^{-1}\frac{2-\frac{\ell}{b}(1-\xi)}{\beta^2(1-\xi)}$$

Equations 5.8 and 5.9 may also be considered as the travelling-wave field distributions outside the resonator providing that the loss on transmission through the mirrors is accounted for.

The transverse standing wave is equation 5.8 with the exponential phase function replaced by the sine function. The variation in amplitude of the TEM_{00q} mode is illustrated in Figure 5.4

5.1d Nodal Surfaces

The nodal surfaces are obtained from the condition that

$$\frac{k\ell}{2}(1+\xi)+\frac{k}{b}(x^2+y^2)\frac{\xi}{\gamma^2}-(m+n+1)(\frac{\pi}{2}-\varphi) = p\pi \tag{5.10}$$

They intersect the axis at points z_o which satisfy the relation

$$\frac{k\ell}{2}(1+\xi_o)-(m+n+1)(\frac{\pi}{2}-\varphi) = p\pi \tag{5.11}$$

If the variation of φ with ξ is neglected as well as the small error involved in replacing ξ by ξ_o in γ^2, then equations 5.10 and 5.11 may be combined to give

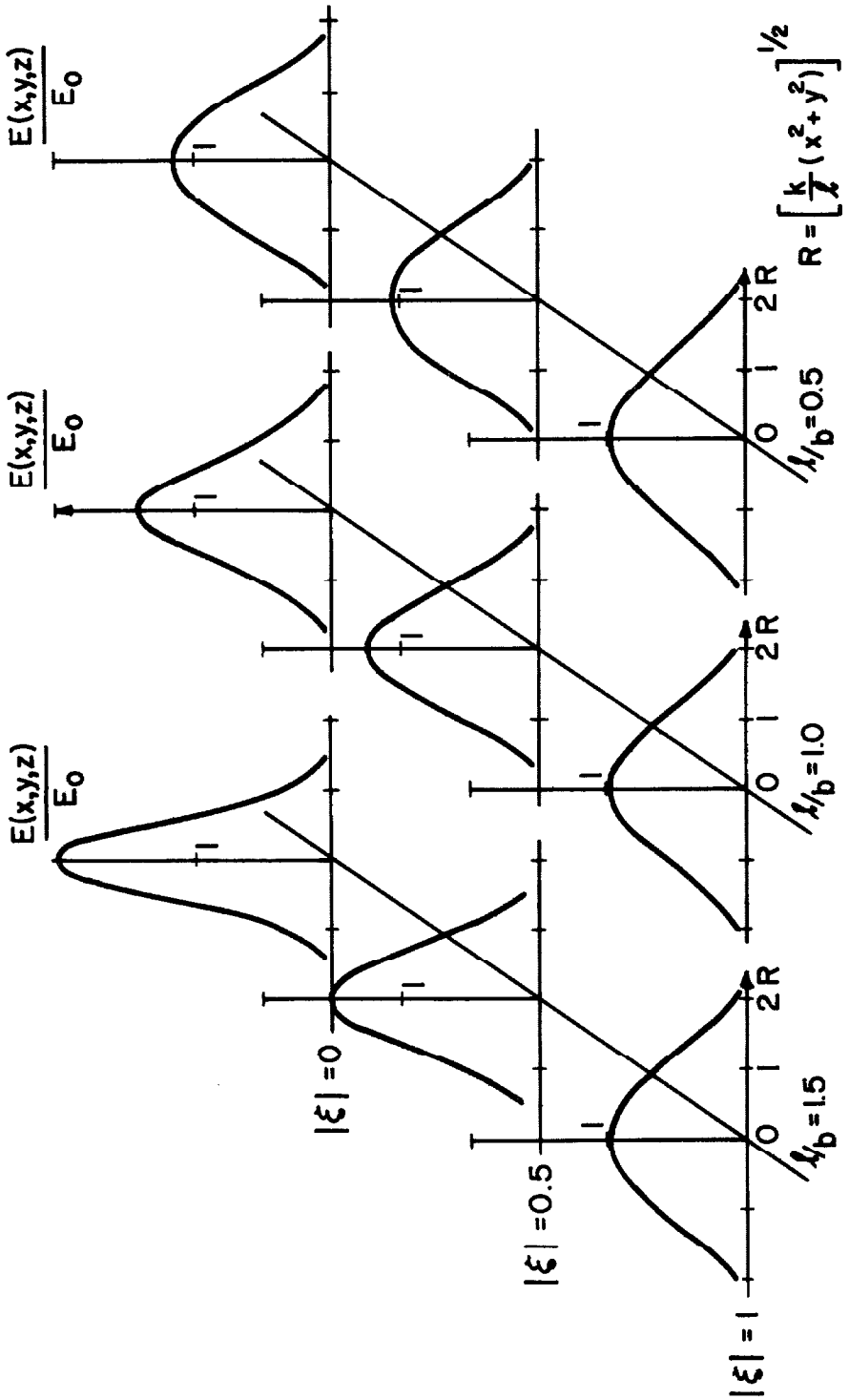

Fig. 5.4 Variation in amplitude of the TEM_{00q} mode in the symmetric, nonconfocal resonator.

$$z - z_o = - \frac{(x^2 + y^2)}{b} \frac{\xi_o}{r_o^2} \tag{5.12}$$

Within these approximations 5.12 represents a spherical surface with radius of curvature

$$\rho = \frac{b}{2} \left| \frac{r_o^2}{\xi_o} \right| \tag{5.13}$$

The variation of ρ as a function of ξ_o is plotted in Figure 5.5. ℓ is chosen equal to unity.

When the fields in the resonator are approached from the travelling wave point of view the equiphase surfaces correspond to the standing-wave nodal surfaces. At optical wavelengths the geometrical wavefronts correspond to these surfaces and moreover it is easily shown that the average Poynting vector is directed along a normal to the geometrical wavefront (56). Since the radii of curvature of the equiphase surfaces do not become zero for $\frac{\ell}{b} \leq 2$ it is clear that as a point in the field distribution propagates from one reflector to the other it does not cross the axis of the resonator. This does not agree with the picture presented by ray-tracing techniques where the rays reflected from the mirrors cross the resonator axis. However this latter treatment is incorrect since it completely neglects diffraction effects which occur when the dimensions concerned approach the order of a wavelength. This would be the case if the radius of curvature of the wavefront were to approach zero at some focal point in the resonator.

Although the radius of curvature of a nodal or equiphase

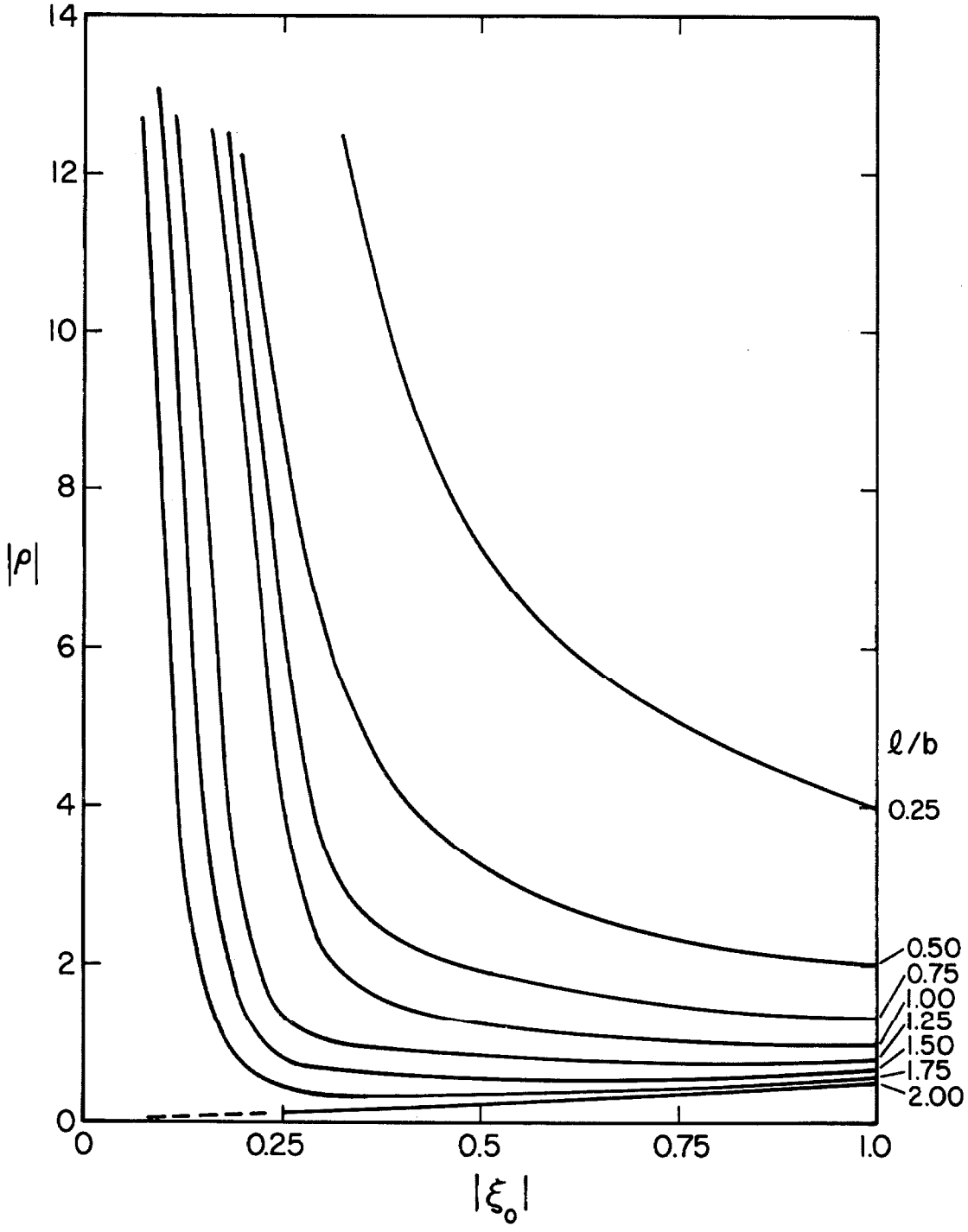

Fig. 5.5 Variation of the nodal surface radius of curvature for the symmetric, nonconfocal resonator.

surface does not become zero for $\frac{\ell}{b} < 2$ it is not generally a monotonically increasing function of ξ_o (refer Figure 5.5). For some values of $\frac{\ell}{b}$ ρ passes through a minimum for $0 \leq |\xi_o| \leq 1$. The minimum value of ρ and the point where the corresponding surface intersects the resonator axis are easily obtained by differentiating equation 5.13.

$$\rho_{min} = \left| \sqrt{2\ell b - \ell^2} \right| \tag{5.14}$$

$$(z_o)_{min} = \frac{\rho_{min}}{2} \tag{5.15}$$

For equations 5.14 and 5.15 it appears that any symmetric resonator is characterized by a pair of confocal equiphase (or nodal) surfaces and that these surfaces are those at which the field distribution is the most highly convergent.

Properties of the resonator may now be investigated by considering those of a confocal resonator whose mirror curvature and spacing are given by 5.14. This is the concept of the equivalent confocal resonator arrived at by Boyd and Gordon (19) through a consideration of equiphase surfaces in the confocal resonator.

5.1e Mode Dimensions and Mode Volume

Due to the rotational symmetry of the field distributions about the resonator axis the locus at which the field amplitude decreases to e^{-1} of its value on the axis is a circle with radius of

$$w = \sqrt{\frac{\ell}{k}} \sqrt{\frac{r}{\beta}} \tag{5.16}$$

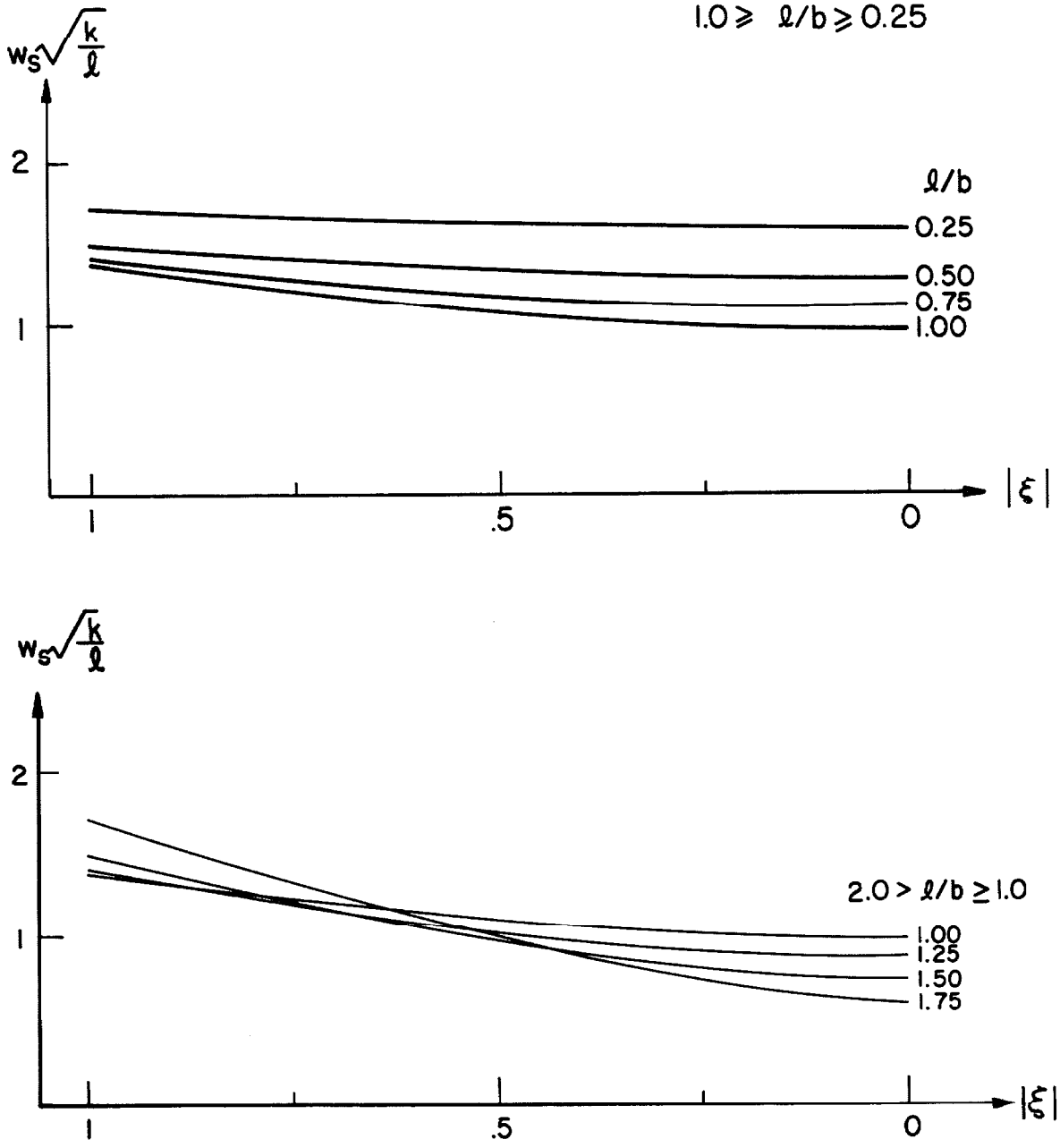

Fig. 5.6 Variation of the characteristic mode radius for the symmetric, nonconfocal resonator.

The variation of the characteristic mode radius w is shown in Figure 5.6.

When $\alpha = 0$ (or $N = 2$) equation 4.41 can be integrated. Hence the mode volume for the symmetric, nonconfocal, two-mirror resonator is

$$V = \frac{\ell^2 \lambda \left[1 - \frac{1}{3}\left(\frac{\ell}{b}\right)\right]}{\sqrt{2\frac{\ell}{b} - \frac{\ell^2}{b^2}}} \qquad (5.17)$$

The mode volume is presented in Figure 5.7 as a function of $\frac{\ell}{b}$. It is interesting to note that the minimum mode volume

$$V_{min} = \frac{\ell^2 \lambda}{3}$$

occurs for $\frac{\ell}{b} = 1.5$ and not $\frac{\ell}{b} = 1$ as was previously indicated (19).

In a resonator with mirrors which are not perfectly reflecting the Q due to reflection will increase with separation when the diffraction losses are small. Soohoo (25) has shown that with a reflection loss of 1% the maximum Q occurs at a spacing of $\frac{\ell}{b} = 1.5$.

5.2 Confocal Resonator

5.2a Approximate Solution

The properties of the confocal resonator may be obtained by placing $\ell = b$ in the results of Section 5.1.

The resonance condition 5.2 becomes

$$\frac{4b}{\lambda} = 2q + (m+n+1) \qquad (5.19)$$

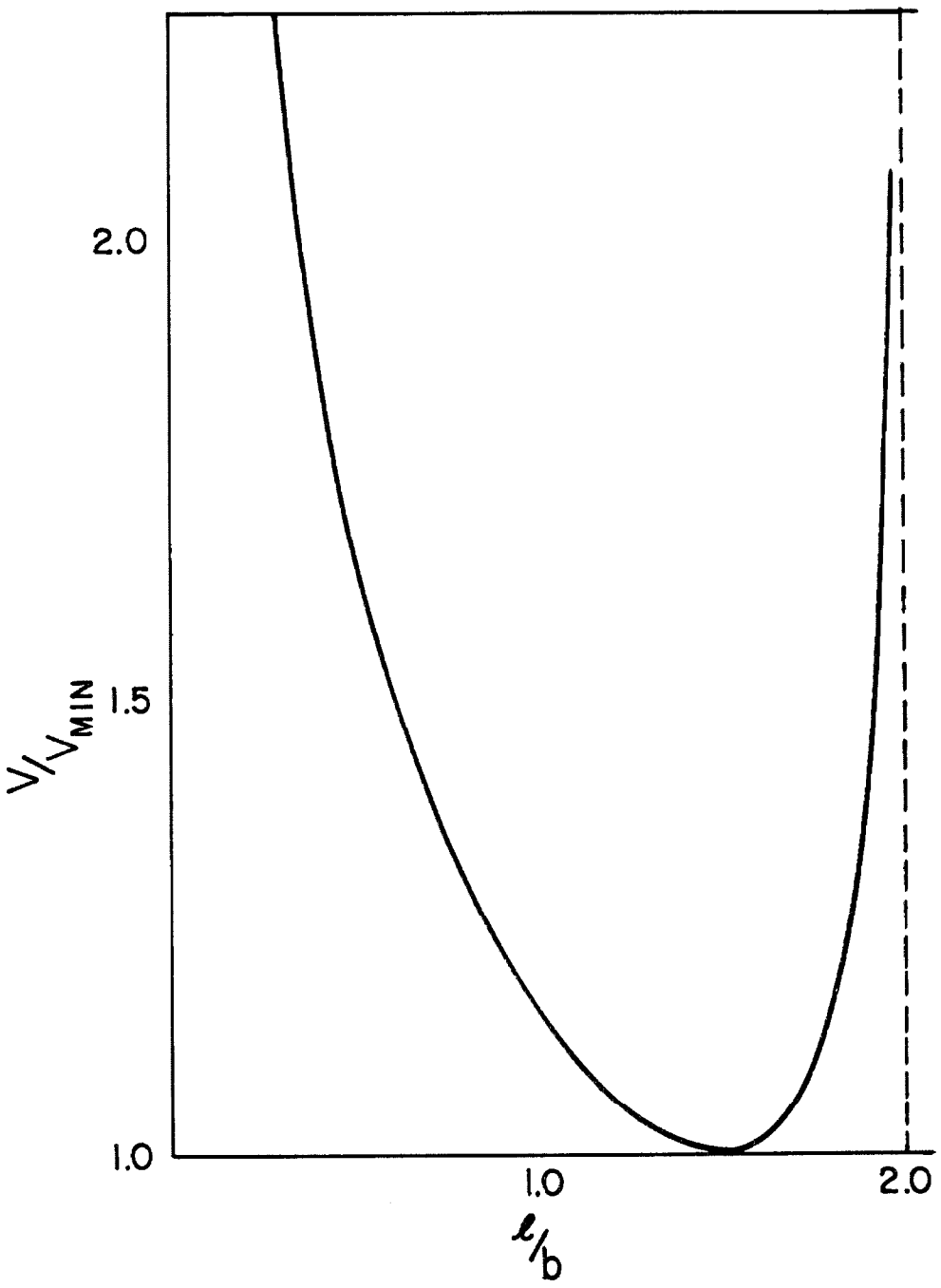

Fig. 5.7 Variation in mode volume for the symmetric, nonconfocal resonator.

From equation 5.19 it is evident that unlike the nonconfocal case the confocal cavity is resonant only for integral values of $\frac{4b}{\lambda}$. Considerable degeneracy exists since the resonance condition may be satisfied by different combinations of m, n and q. Thus the modes of the confocal resonator form a complete set of orthogonal functions but due to their frequency degeneracy they are not unique. Unless the diffraction losses of the various modes are considered any linear combination of degenerate eigenfunctions is still a mode of the resonator.

The radius of curvature of nodal surfaces in the confocal resonator is

$$\rho = \frac{b}{2}\left|\frac{1+\xi_o^2}{\xi_o}\right| \tag{5.20}$$

The concept of the equivalent confocal resonator (19) stems from this equation. Since equation 5.20 describes nodal surfaces on which the total electric field is zero it also describes surfaces on which the boundary condition for perfect reflection is satisfied. Thus the properties of a symmetric, nonconfocal resonator with mirror spacing ℓ and mirror curvature b' may be approximately described by considering a confocal resonator whose mirror separation and curvature b satisfies the relation

$$b^2 = 2\ell b' - \ell^2 \tag{5.21}$$

As noted previously in Section 5.1b the equivalent confocal

resonator concept gives a resonance condition for the symmetric, non-confocal resonator which is very close to the correct result.

An approximation to the diffraction loss of a symmetric, non-confocal resonator with square mirrors of dimension 2a' is obtained by assuming that its loss is equal to that of its equivalent confocal resonator with reflector dimensions scaled up by the ratio of their characteristic mode radii at the mirrors. Thus the equivalent confocal resonator has a reflector dimension

$$2a = 2a' \frac{w}{w'} = 2a' \sqrt{2 - \frac{\ell}{b'}} \tag{5.22}$$

The important parameter in determining losses is the Fresnel number

$$\frac{a^2}{b\lambda} = \frac{a'^2}{\ell\lambda} \sqrt{2\frac{\ell}{b'} - \frac{\ell^2}{b'^2}} \tag{5.23}$$

Hence the diffraction losses for a nonconfocal resonator characterized by ℓ, b' and a' is approximately that of a confocal resonator whose Fresnel number is given by equation 5.23. It will be seen in Section 5.2b that the diffraction loss for a finite aperture confocal resonator may be found exactly.

5.2b Exact Solution (19)

The properties of the confocal resonator resulting from the non-zero wavelength solution to the problem are arrived at by putting $\alpha = 0$ in the equations of Section 4.1.2b.

The normal mode field distributions reflected from the mirrors are

$$E_x^r(x,y) = E_o\, S_{Om}\left(\frac{a^2k}{b},\ \frac{x}{a}\right) S_{On}\left(\frac{a^2k}{b},\ \frac{y}{a}\right) \quad m,n = 0,1,2 \ldots \qquad (5.24)$$

where S_{Om} is an angular prolate spheroidal wave function (50). The realness of the eigenfunctions indicates that the reflectors are surfaces of constant phase.

The fractional energy loss per reflection due to diffraction effects is

$$\alpha_D = 1 - \left[\frac{4a^2}{b\lambda} R_{Om}^{(1)}\left(\frac{a^2k}{b},1\right) R_{On}^{(1)}\left(\frac{a^2k}{b},1\right)\right]^2 \qquad (5.25)$$

where $R_{Om}^{(1)}$ is a radial prolate spheroidal wave function (50).

5.3 Nonsymmetric, Nonconfocal Resonator

5.3a Modes of the Resonator

The eigenfunctions of the nonsymmetric, nonconfocal two-mirror resonator illustrated in Figure 5.8 do not follow directly from the results of Section 4.2. However they are determined in a similar manner, that is to say by the solution of an integral equation similar to 4.43.

The self-consistent fields found to be reflected from mirror 1 are

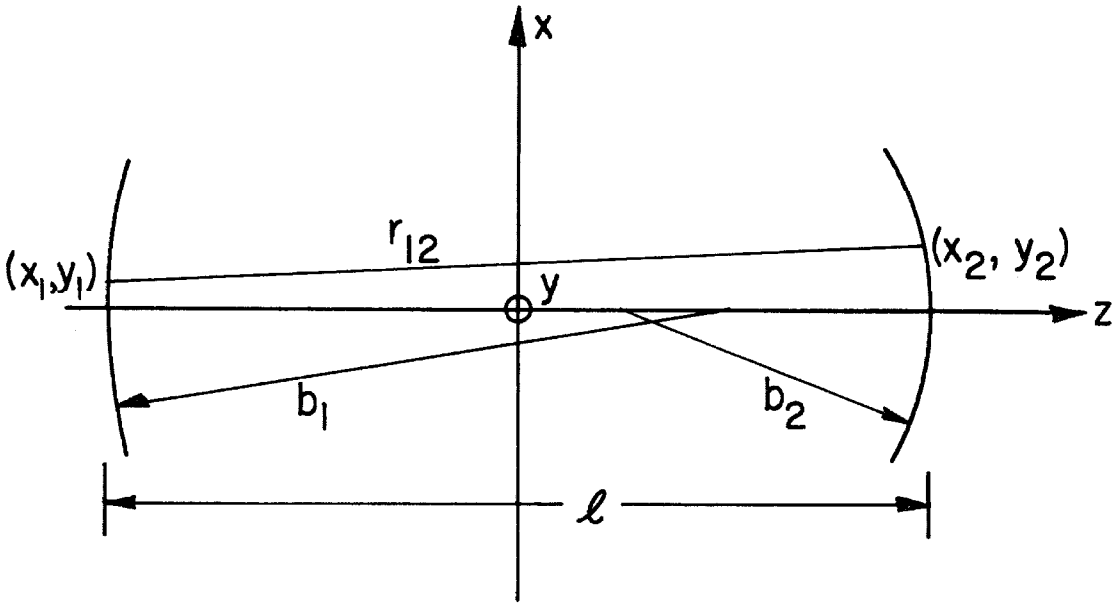

Fig. 5.8 A nonsymmetric, nonconfocal two-mirror resonator.

$$E_x^r(x_1, y_1) = E_1 \frac{\Gamma(\frac{m}{2}+1)\,\Gamma(\frac{n}{2}+1)}{\Gamma(m+1)\,\Gamma(n+1)} He_m\left(\sqrt{\frac{k}{\ell}}\,\beta_1 x_1\right) He_n\left(\sqrt{\frac{k}{\ell}}\,\beta_1 y_1\right) e^{-\frac{k}{2\ell}\beta_1^2(x_1^2+y_1^2)} \tag{5.26}$$

where

$$\beta_1 = \left[\frac{(b_1-\ell)}{(b_2-\ell)}\,\frac{\ell(b_1+b_2)-\ell^2}{b_1^2}\right]^{\frac{1}{4}}$$

In addition the modes reflected from mirror 2 are

$$E_x^r(x_2, y_2) = E_2 \frac{\Gamma(\frac{m}{2}+1)\Gamma(\frac{n}{2}+1)}{\Gamma(m+1)\Gamma(n+1)} He_m\left(\sqrt{\frac{k}{\ell}}\,\beta_2 x_2\right) He_n\left(\sqrt{\frac{k}{\ell}}\,\beta_2 y_2\right) e^{-\frac{k}{2\ell}\beta_2^2(x_2^2+y_2^2)} \tag{5.27}$$

where

$$\beta_2 = \left[\frac{(b_2-\ell)}{(b_1-\ell)}\,\frac{\ell(b_1+b_2)-\ell^2}{b_2^2}\right]^{\frac{1}{4}}$$

and

$$\left|\frac{E_1}{E_2}\right| = \left[\frac{b_2(b_1-\ell)}{b_1(b_2-\ell)}\right]^{\frac{1}{2}}$$

Examination of the quantities β_1 and β_2 and the ratio $\left|\frac{E_1}{E_2}\right|$ reveals that the values of ℓ, b_1 and b_2 may not vary indiscriminately. The limiting condition is

$$0 \le \left(\frac{\ell}{b_1} - 1\right)\left(\frac{\ell}{b_2} - 1\right) \le 1 \tag{5.29}$$

This expression is the two-mirror analogue to equation 2.28. It was previously derived by Boyd and Kogelnik (22) from a geometrical optics viewpoint based on the equivalence of the resonator and a periodic sequence of parallel lenses.

5.3b Resonance Conditions

The eigenvalues corresponding to the eigenfunctions given by equations 5.26 and 5.27 are

$$\sigma_m\sigma_n = e^{-j\left\{2k\ell-(m+n+1)\left[\frac{\pi}{2}-\tan^{-1}\frac{2\delta}{\sqrt{1-4\delta^2}}\right]\right\}} \qquad (5.30)$$

with

$$\delta = \frac{2\ell(b_1+b_2)-2\ell^2-b_1b_2}{2b_1b_2}$$

The round-trip phase shift equals the phase angle of $\sigma_m\sigma_n$ and for resonance must be an integer q times 2π, i.e.

$$2\pi q = \left|2k\ell-(m+n+1)\left[\frac{\pi}{2}-\tan^{-1}\frac{2\delta}{\sqrt{1-4\delta^2}}\right]\right| \qquad (5.31)$$

or

$$\frac{4\ell}{\lambda} = 2q+(m+n+1)\left[1-\frac{2}{\pi}\tan^{-1}\frac{2\delta}{\sqrt{1-4\delta^2}}\right]$$

The spectral range or mode separation is

$$\Delta\left(\frac{1}{\lambda}\right) = \frac{1}{4\ell}\left\{2\Delta q+\left[1-\frac{2}{\pi}\tan^{-1}\frac{2\delta}{\sqrt{1-4\delta^2}}\right]\Delta(m+n)\right\} \qquad (5.32)$$

5.3c Electric Field at an Arbitrary Point in the Resonator

The field distribution travelling in the positive z-direction is computed directly from the electric field at mirror 1 (refer equation 3.10), viz.

$$E_x^{(+)}(x,y,z) = E_1 \frac{\Gamma(\frac{m}{2}+1)\Gamma(\frac{n}{2}+1)}{\Gamma(m+1)\Gamma(n+1)} \frac{\sqrt{2}}{r_1} He_m\left(\sqrt{\frac{2k}{\ell}} \frac{\beta_1}{r_1} x\right)$$

$$He_n\left(\sqrt{\frac{2k}{\ell}} \frac{\beta_1}{r_1} y\right) e^{-\frac{k}{\ell} \frac{\beta_1^2}{r_1^2} (x^2+y^2)}$$

$$e^{-j\left\{\frac{k\ell}{2}(1+\xi) + \frac{k}{\ell}\left(\frac{1}{1+\xi} + \frac{2\eta_1}{r_1^2}\right)(x^2+y^2) - (m+n+1)\left(\frac{\pi}{2} + \varphi_1\right)\right\}} \tag{5.31}$$

where

$$\xi = \frac{2z}{\ell}$$

$$r_1 = \sqrt{2}\,(1+\xi)\left[\frac{\beta_1^4}{4} + \eta_1^2\right]^{\frac{1}{2}}$$

$$\varphi_1 = \tan^{-1} \frac{2\eta_1}{\beta_1^2}$$

$$\eta_1 = \frac{\ell}{2b_1} - \frac{1}{1+\xi}$$

In a similar manner the negatively-directed travelling wave is

$$E_x^{(-)}(x,y,z) = -E_2 \frac{\Gamma(\frac{m}{2}+1)\Gamma(\frac{n}{2}+1)}{\Gamma(m+1)\Gamma(n+1)} \frac{\sqrt{2}}{r_2} He_m\left(\sqrt{\frac{2k}{\ell}} \frac{\beta_2}{r_2} x\right)$$

$$He_n\left(\sqrt{\frac{2k}{\ell}} \frac{\beta_2}{r_2} y\right) \quad e^{-\frac{k}{\ell} \frac{\beta_2^2}{r_2^2} (x^2+y^2)}$$

$$e^{-j\left\{\frac{k\ell}{2}(1-\xi) + \frac{k}{\ell}\left(\frac{1}{1-\xi} + \frac{2\eta_2}{r_2^2}\right)(x^2+y^2) - (m+n+1)\left(\frac{\pi}{2} + \varphi_2\right)\right\}} \tag{5.32}$$

where

$$r_2 = \sqrt{2}\,(1-\xi)\left[\frac{\beta_2^4}{4} + \eta_2^2\right]^{\frac{1}{2}}$$

$$\varphi_2 = \tan^{-1} \frac{2\eta_2}{\beta_2^2}$$

$$\eta_2 = \frac{\ell}{2b_2} - \frac{1}{1-\xi}$$

The minus sign in equation 5.32 has been assigned arbitrarily so that boundary condition for perfect reflection at the mirror will be satisfied.

The transverse standing wave in the cavity is obtained by replacing the exponential phase function in 5.31 by the corresponding sine function. The variation in amplitude of $\left|\frac{E_x^{(+)}(x,y,z)}{E_1}\right|$ for the TEM_{00q} mode is illustrated in Figure 5.9.

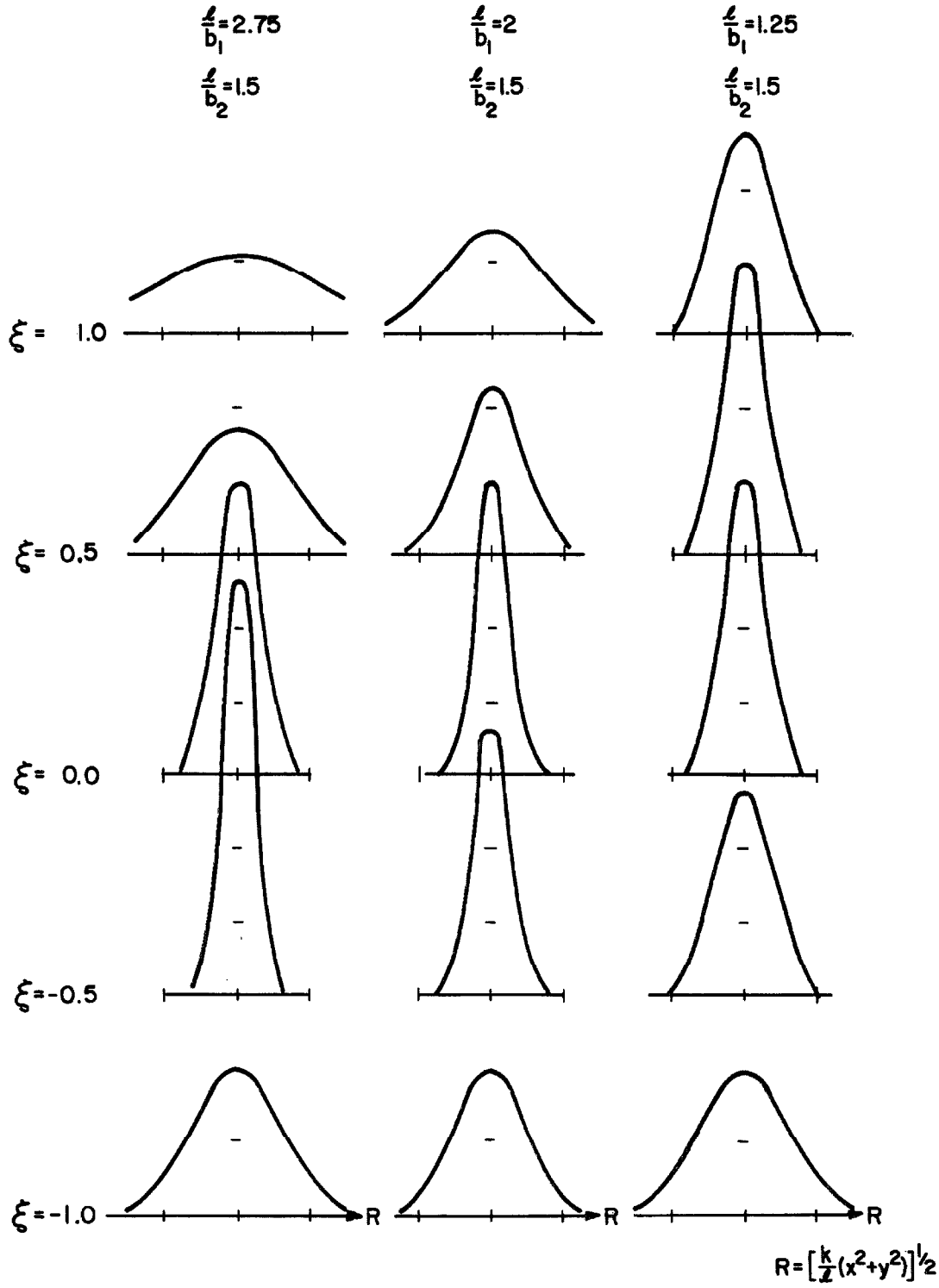

Fig. 5.9 Variation in amplitude of the TEM_{00q} mode in the nonsymmetric, nonconfocal resonator.

5.3d Nodal Surfaces

From the requirement that the total electric field be zero on the nodal surfaces it is easily shown that these surfaces are approximately spherical with radius of curvature

$$\rho \simeq \frac{\ell}{2}\left|\frac{(1+\xi_o)}{1+\frac{2\eta_{10}(1+\xi_o)}{r_{10}^2}}\right| \tag{5.33}$$

The surfaces intersect the axis at z_o and η_{10} and r_{10} correspond to η_1 and r_1 with ξ replaced by ξ_o. Figure 5.10 show the variation of ρ as a function of ξ_o.

From Figure 5.10 it is evident that the field does not "cross" the axis in propagating from one reflector to the other. Differentiation of equation 5.33 leads to the minimum values of ρ and the points where the corresponding surfaces intersect the resonator axis, viz.

$$\rho_{min} = \ell\left|\frac{(1-\frac{b_2}{\ell})-(1-\frac{b_1}{\ell}) \pm 2\sqrt{(1-\frac{b_1}{\ell})(1-\frac{b_2}{\ell})(\frac{b_1}{\ell}+\frac{b_2}{\ell}-1)}}{(1-\frac{b_1}{\ell})+(1-\frac{b_2}{\ell})}\right| \tag{5.34}$$

$$(z_o)_{min} = \frac{\rho_{min}}{2} \tag{5.35}$$

In equation 5.34 the + and - signs are associated with the phase fronts leaving mirrors 1 and 2 respectively. Unlike the

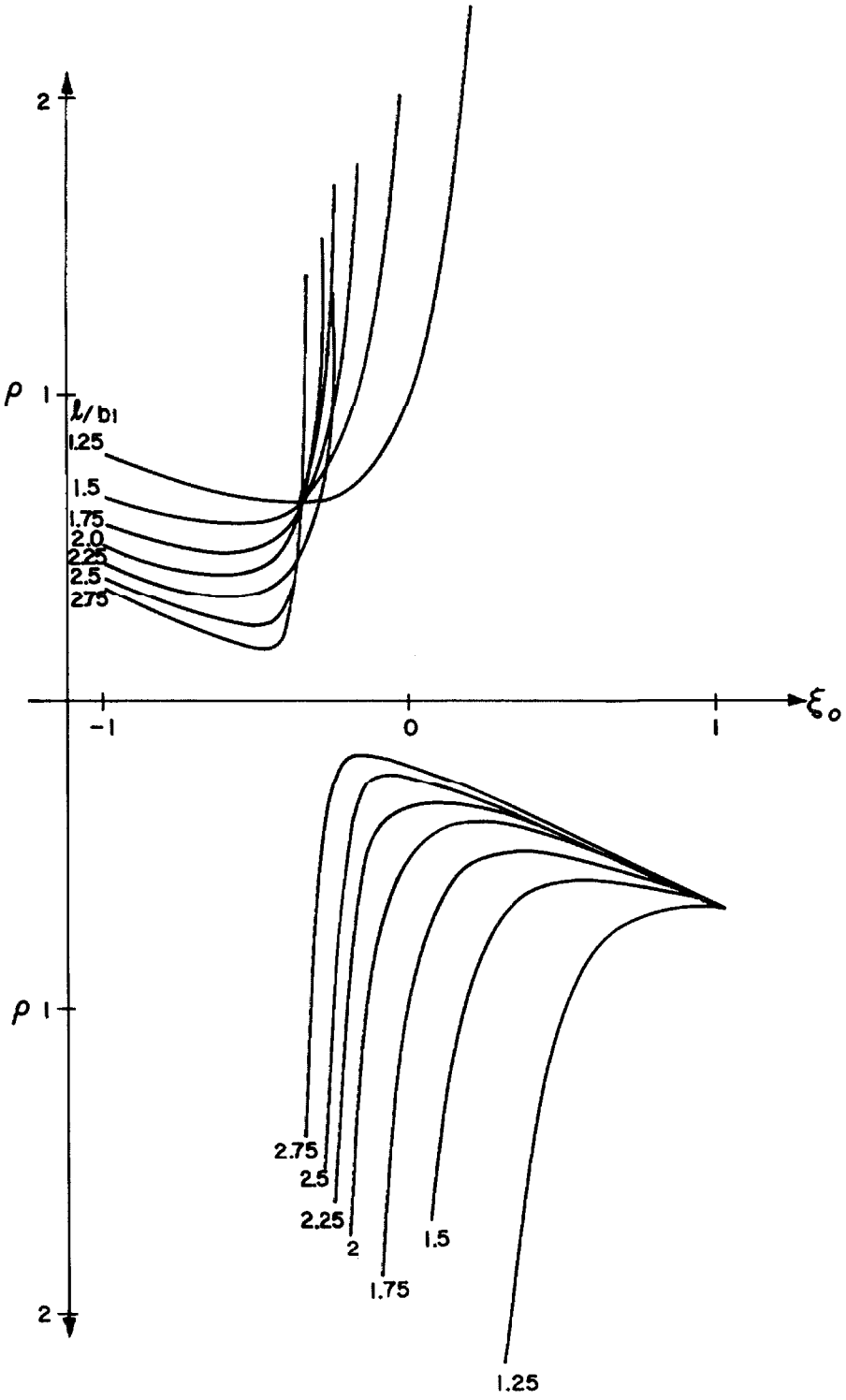

Fig. 5.10 Variation of the nodal surface radius of curvature for the nonsymmetric, nonconfocal resonator ($\frac{\ell}{b_2} = 1.5$, $\ell = 1$).

symmetric, nonconfocal cavity this resonator is not characterized by a single equivalent confocal configuration.

5.3e Mode Dimensions and Mode Volume

Following the usual definition the characteristic mode radius for a two-mirror resonator with reflectors of different radii of curvature is

$$w = \sqrt{\frac{\ell}{k}\frac{r_1}{\beta_1}} = \sqrt{\frac{\ell}{k}\frac{r_2}{\beta_2}} \tag{5.36}$$

In Figure 5.11 equation 5.36 is plotted as a function of ξ for $\frac{\ell}{b_2} = 1.5$ and several values of $\frac{\ell}{b_1}$. The ratio of the spot sizes at the two mirrors is

$$\frac{w^2(\xi=-1)}{w^2(\xi=+1)} = \frac{b_1(b_2-\ell)}{b_2(b_1-\ell)} = \frac{E_2^2}{E_1^2} \tag{5.37}$$

The mode volume for this cavity is

$$V = \frac{\ell^2\lambda}{3}\,\frac{\ell(\ell-b_1)-(2\ell-3b_1)(\ell-b_2)}{\left\{(\ell-b_1)(\ell-b_2)\left[\ell(b_1+b_2)-\ell^2\right]\right\}^{\frac{1}{2}}} \tag{5.38}$$

With b_2 and ℓ fixed the mode volume is a minimum for

$$b_1 = \ell\,\frac{4b_2^2-5b_2\ell+2\ell^2}{3b_2^2-4b_2\ell+2\ell^2} \tag{5.39}$$

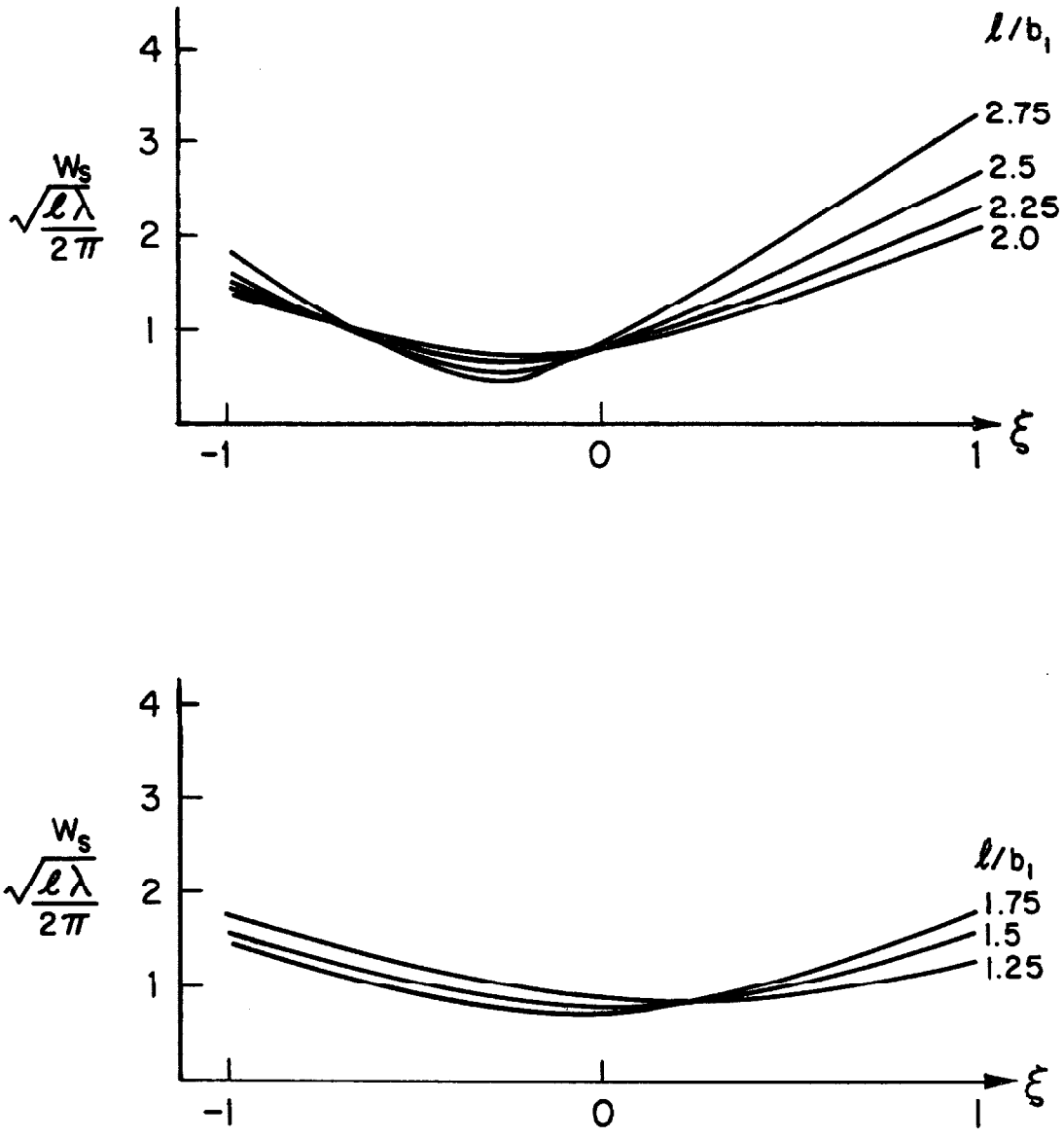

Fig. 5.11 Variation of the characteristic mode radius for the non-symmetric, nonconfocal resonator ($\frac{\ell}{b2} = 1.5$).

The corresponding value of V is

$$V = \frac{2}{3}\ell^2\lambda\,\frac{(3b_2^2 - 3b_2\ell + \ell^2)^{\frac{1}{2}}}{b_2} \qquad (5.40)$$

5.4 Plane-Parallel and Concentric Resonators

5.4a Equivalence of the Plane-Parallel and Concentric Resonators

The variation of β^4 as a function of b with ℓ fixed is illustrated in Figure 5.12. At $b = \frac{\ell}{2}$ (concentric) and $b = \infty$ (plane-parallel) $\beta^4 = 0$ and the description of the fields obtained in Section 5.1 collapses. In both situations the failure of the theory results from a neglect of the effects which determine the characteristic radial extent of the field distributions.

This approximate theory does not take into account diffraction effects at the mirrors. This is the dominant mechanism producing finite spot sizes when the mirror curvature becomes small with respect to the spacing, i.e. $b < \frac{\ell}{2}$. In the planar case the zero wavelength or infinite aperture approximation fails to provide the resonator with any mechanism for field confinement.

The fact that the difficulties involved in treating these two resonators stem from the same basic problem indicates that a solution of one configuration may lead to that of the other.

The integral equation to be solved for the x-component of the field reflected from a mirror in the concentric cavity is

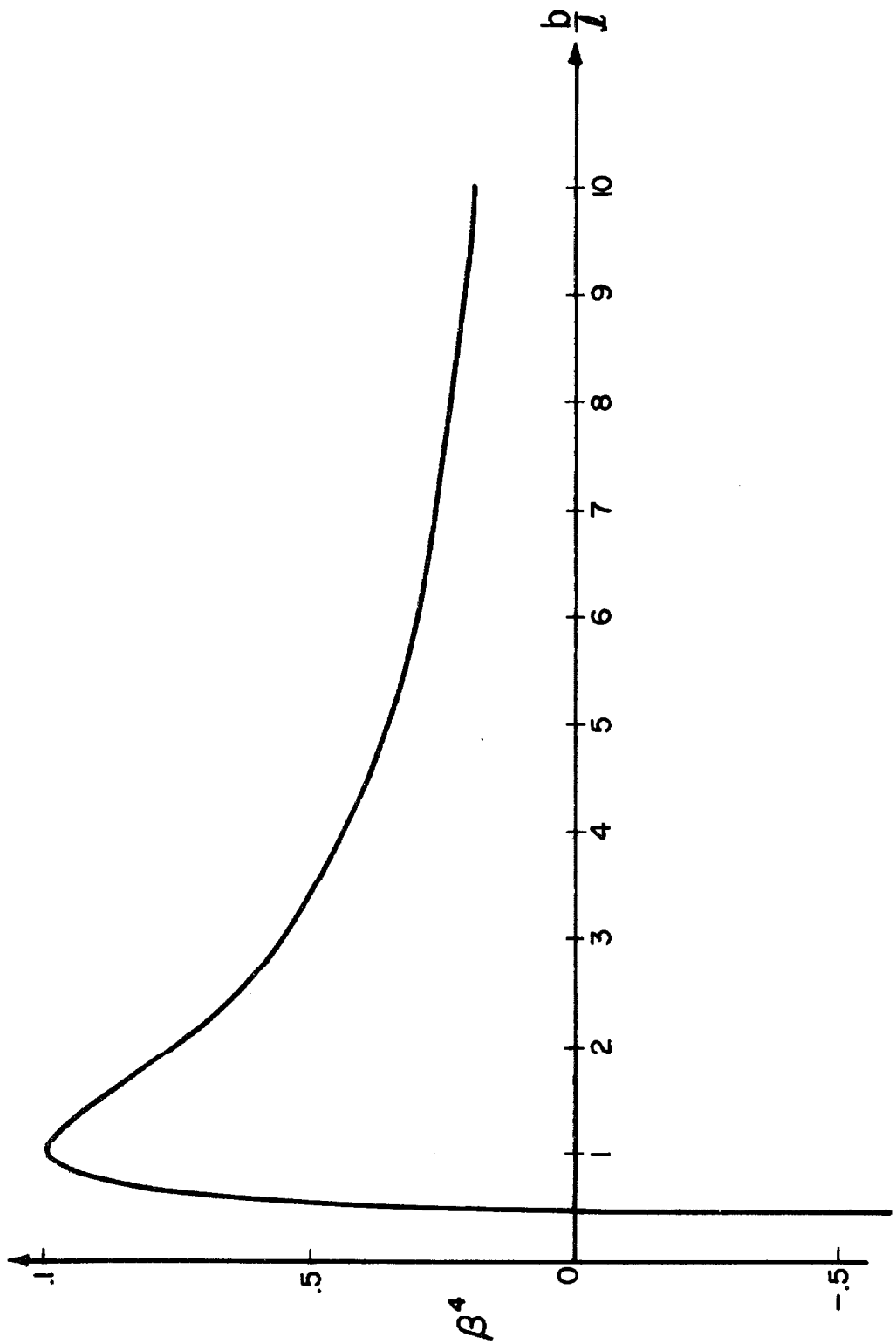

Fig. 5.12 Variation of $\beta^4 = 2\left(\frac{\ell}{b}\right) - \left(\frac{\ell}{b}\right)^2$.

$$\chi_m F_m(s_2) = \frac{1}{\sqrt{2\pi}} \int_{-\sqrt{c}}^{\sqrt{c}} ds_1 \, F_m(s_1) \, e^{\frac{j}{2}(s_1+s_2)^2} \tag{5.41}$$

The corresponding equation for the planar case is

$$\chi_m F_m(s_2) = \frac{1}{\sqrt{2\pi}} \int_{-\sqrt{c}}^{\sqrt{c}} ds_1 \, F_m(s_1) \, e^{-\frac{j}{2}(s_1-s_2)^2} \tag{5.42}$$

The Hermitian adjoint of equation 5.42 is

$$\chi_m^* F_m^*(s_2) = \frac{1}{\sqrt{2\pi}} \int_{-\sqrt{c}}^{\sqrt{c}} ds_1 \, F_m^*(s_1) \, e^{\frac{j}{2}(s_2-s_1)^2} \tag{5.43}$$

This may be rewritten as

$$\pm \chi_m^* F_m^*(s_2) = \frac{1}{\sqrt{2\pi}} \int_{-\sqrt{c}}^{\sqrt{c}} ds_1 \, F_m(s_1) \, e^{\frac{j}{2}(s_1+s_2)^2} \tag{5.44}$$

where + applies to even eigenfunctions and - to odd.

Comparing equations 5.41 and 5.44 it is evident that the eigenfunctions and eigenvalues for the concentric resonator are the complex conjugates of those in the plane-parallel configuration. This equivalence has been demonstrated numerically by Fox and Li (24).

5.4b Electric Field in the Plane-Parallel Resonator

For a plane-parallel resonator in which the reflectors are circular in cross-section the integral equation for the self-consistent

electric field at a mirror is

$$\lambda_{mn} f_{mn}(\rho_2,\varphi_2) = \frac{jke^{-jk\ell}}{2\pi\ell} \int_o^a \rho_1 d\rho_1 \int_o^{2\pi} d\varphi_1 \; f_{mn}(\rho_1,\varphi_1) \; e^{-\frac{jk}{\ell}\left[\frac{(\rho_1^2+\rho_2^2)}{2} - \rho_1\rho_2\cos(\varphi_1-\varphi_2)\right]} \tag{5.45}$$

This equation may be simplified by using the following identity (57)

$$e^{jm(\frac{\pi}{2}-\varphi_2)} J_m\left(\frac{k\rho_1\rho_2}{\ell}\right) = \frac{1}{2\pi}\int_o^{2\pi} d\varphi_1 \; e^{j\frac{k}{\ell}\rho_1\rho_2\cos(\varphi_1-\varphi_2) - jm\varphi_1} \tag{5.46}$$

It is evident that

$$f_{mn}(\rho,\varphi) = R_{mn}(\rho)\, e^{-jm\varphi} \tag{5.47}$$

where m is an integer and n is an index referring to the ρ-dependence of the field.

The function $R_{mn}(\rho)$ satisfies the reduced integral equation

$$\lambda_{mn} R_{mn}(\rho_2) = \frac{j^{m+1} k e^{-jk\ell}}{\ell} \int_o^a d\rho_1 \rho_1 R_{mn}(\rho_1)\, J_m\left(\frac{k\rho_1\rho_2}{\ell}\right) e^{-\frac{jk}{2\ell}(\rho_1^2+\rho_2^2)} \tag{5.48}$$

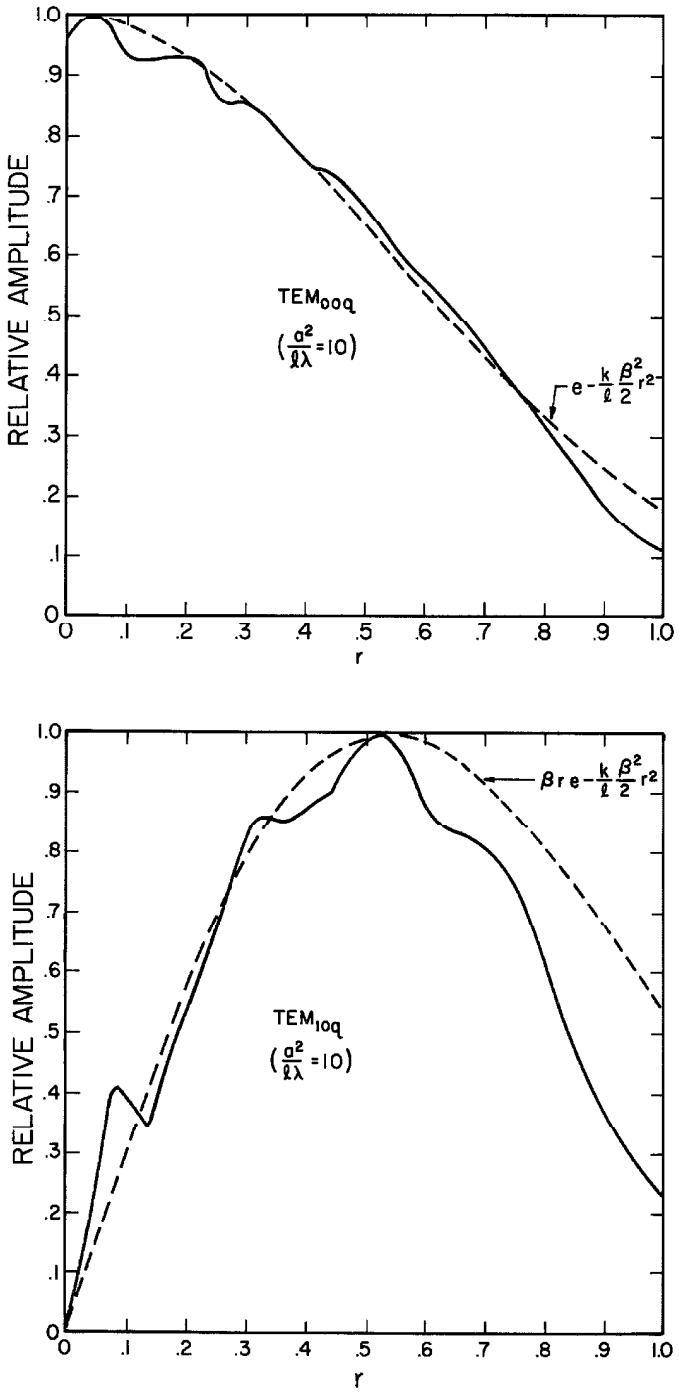

Fig. 5.13 Variation in amplitude of the reflected field distribution for the TEM_{00q} and TEM_{10q} modes in the plane-parallel resonator with circular mirrors (after Fox and Li).

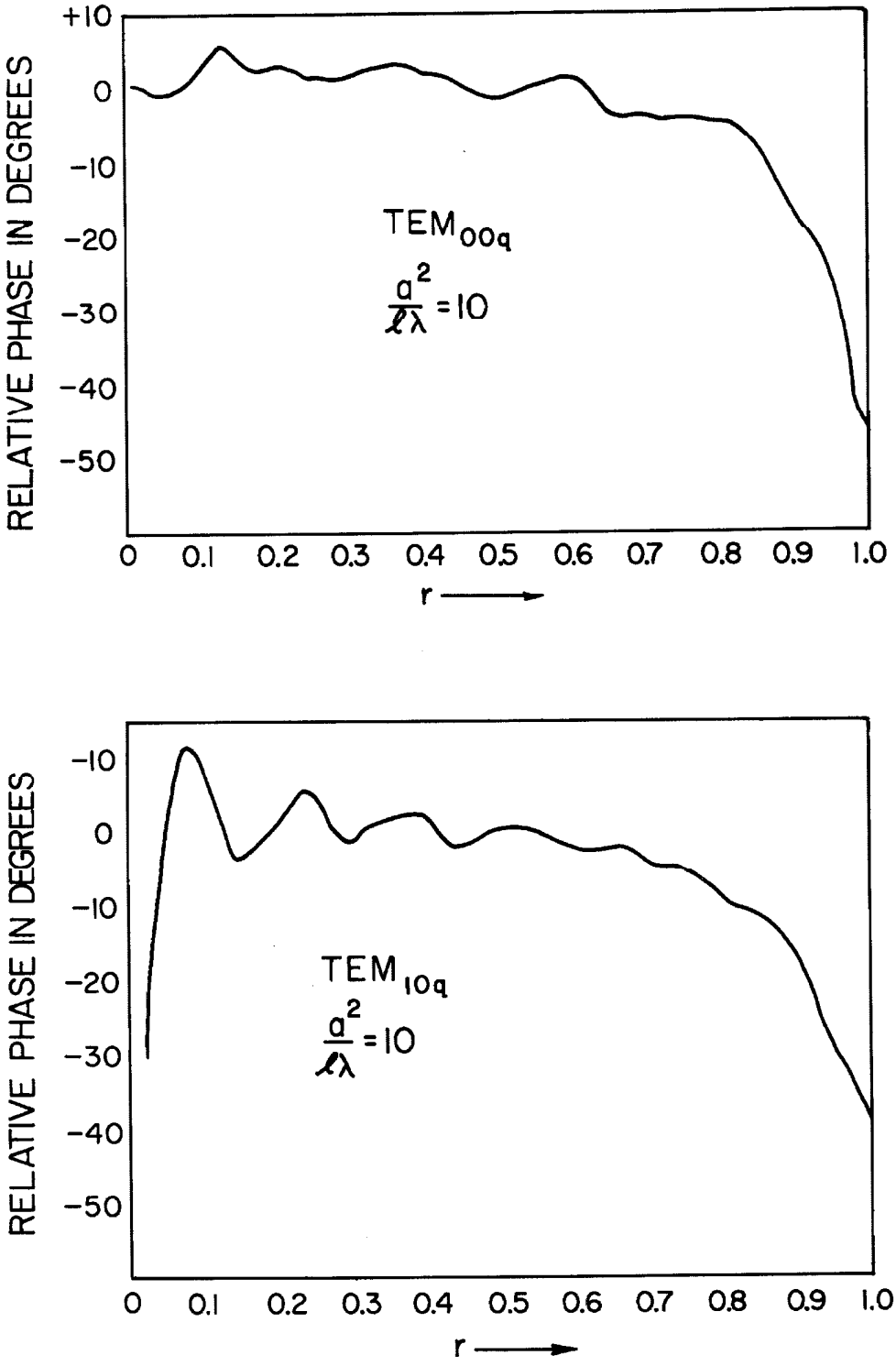

Fig. 5.14 Relative phase of the reflected field distribution for the TEM_{00q} and TEM_{10q} modes in the plane-parallel resonator with circular mirrors (after Fox and Li).

Equation 5.48 has been solved numerically for m = 0,1 by Fox and Li (18). The amplitudes of the reflected fields for the TEM_{00q} and TEM_{10q} modes are shown in Figure 5.13. The dashed curves represent normalized functions of the form

$$R_{mn}(r) \propto (\beta r)^m L_n^m \left(\frac{k}{\ell} \beta^2 r^2\right) e^{-\frac{k}{\ell}\frac{\beta^2}{2} r^2} \qquad (5.49)$$

where $L_n^m\left(\frac{k}{\ell}\beta^2 r^2\right)$ is the associated Laguerre polynomial (58) and $r = \frac{\rho}{a}$.

The corresponding phase distributions are illustrated in Figure 5.14.

The numerical results for the self-consistent fields reflected from the mirrors may be used as a basis from which the traveling-wave fields in the resonator may be calculated. In a cylindrical coordinate system in which two flat mirrors of radius a are located at $z = \pm \frac{\ell}{2}$ the positively directed field is computed from a knowledge of the distribution reflected from mirror at $z = -\frac{\ell}{2}$. For the TEM_{00q} mode the resulting integral (refer equation 3.10) is

$$E^{(+)}(r,\xi) = j\gamma e^{-jk\frac{\ell}{2}(1+\xi)} \int_0^1 dr_1 r_1 e^{-j\frac{\gamma}{2}(r^2+r_1^2)} J_0(\gamma r r_1) E^r(r_1) \qquad (5.50)$$

where

$$\xi = \frac{2z}{\ell}$$

$$r = \frac{\rho}{a}$$

$$\gamma = \frac{2ka^2}{\ell(1+\xi)}$$

$E^r(r_1)$ is the complex field reflected from the mirror at $z = -\frac{\ell}{2}$. Its amplitude and phase are obtained from Figures 5.13 and 5.14 respectively.

Equation 5.50 has been evaluated numerically on an IBM 7090 computer. The relative amplitude and phase distributions of the field at $\xi = 0, .25, .50, .75$ are shown in Figures 5.15 and 5.16. From the amplitude curves it is evident that near the edges of the cavity volume determined by the projected area of the mirrors the field varies smoothly and uniformly throughout the entire resonator. For $r \lesssim .4$ the amplitude varies rapidly and randomly. Part of this variation may be due to the nature of the numerical computation, however the curves are sufficiently smooth to imply that some of the variance is characteristic of a resonator with plane-parallel mirrors.

The plots of relative phase all exhibit a somewhat similar behavior: smooth but rapid variation near $r = 1$; rapid, random changes near $r = 0$; a fairly smooth "average" value for $.1 \lesssim r \lesssim .6$. The phase difference between the "average" and the value at $r = 1$ shows a definite variation with ξ. Starting with a lag of about 45° at $\xi = 1$ it dips to a minimum of approximately 35° at $\xi = .5$ and then increases nearly to initial value at $\xi = 0$.

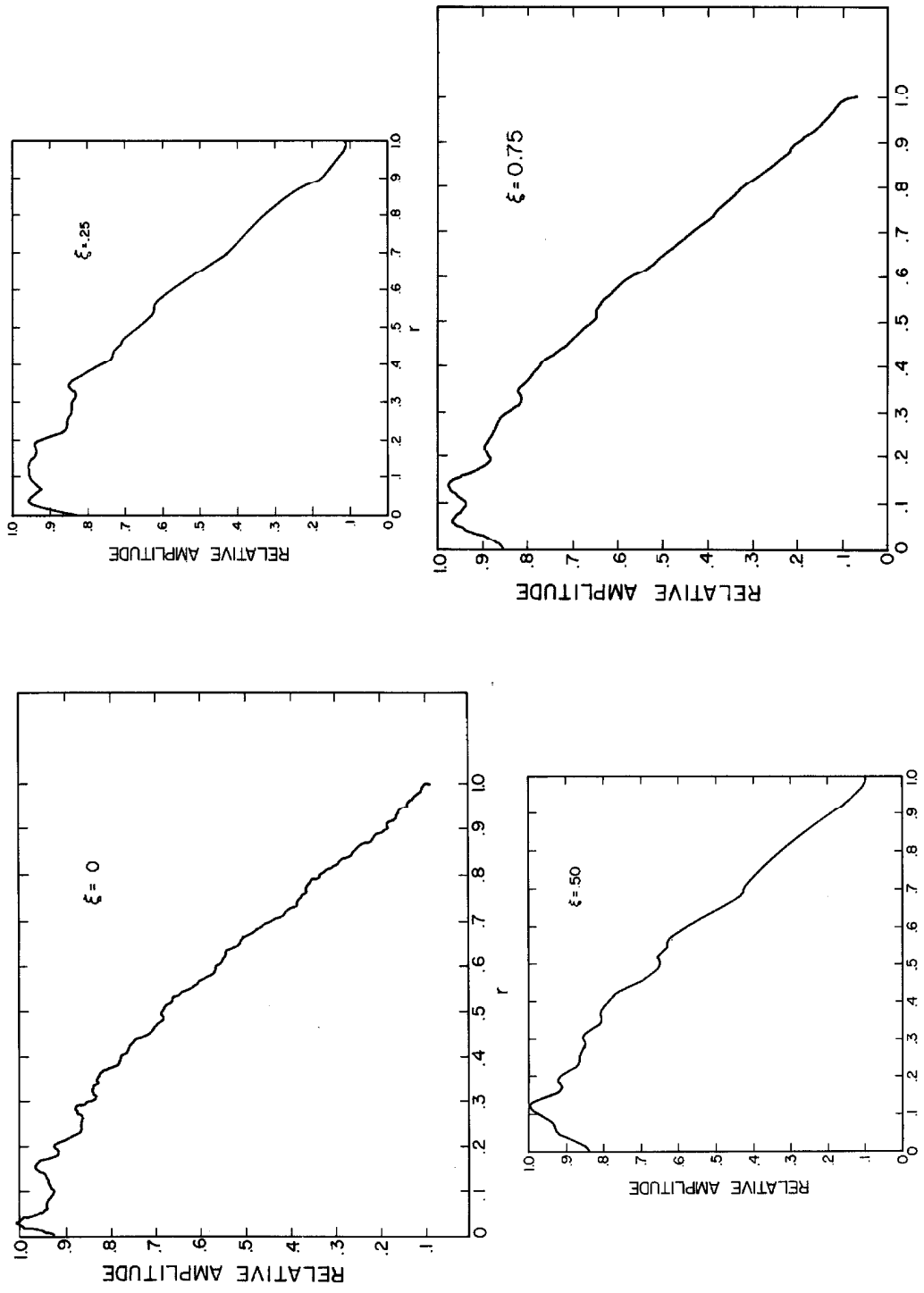

Fig. 5.15 Amplitude variation for the TEM_{00q} mode in the plane-parallel resonator at ξ = 0,.25,.50,.75.

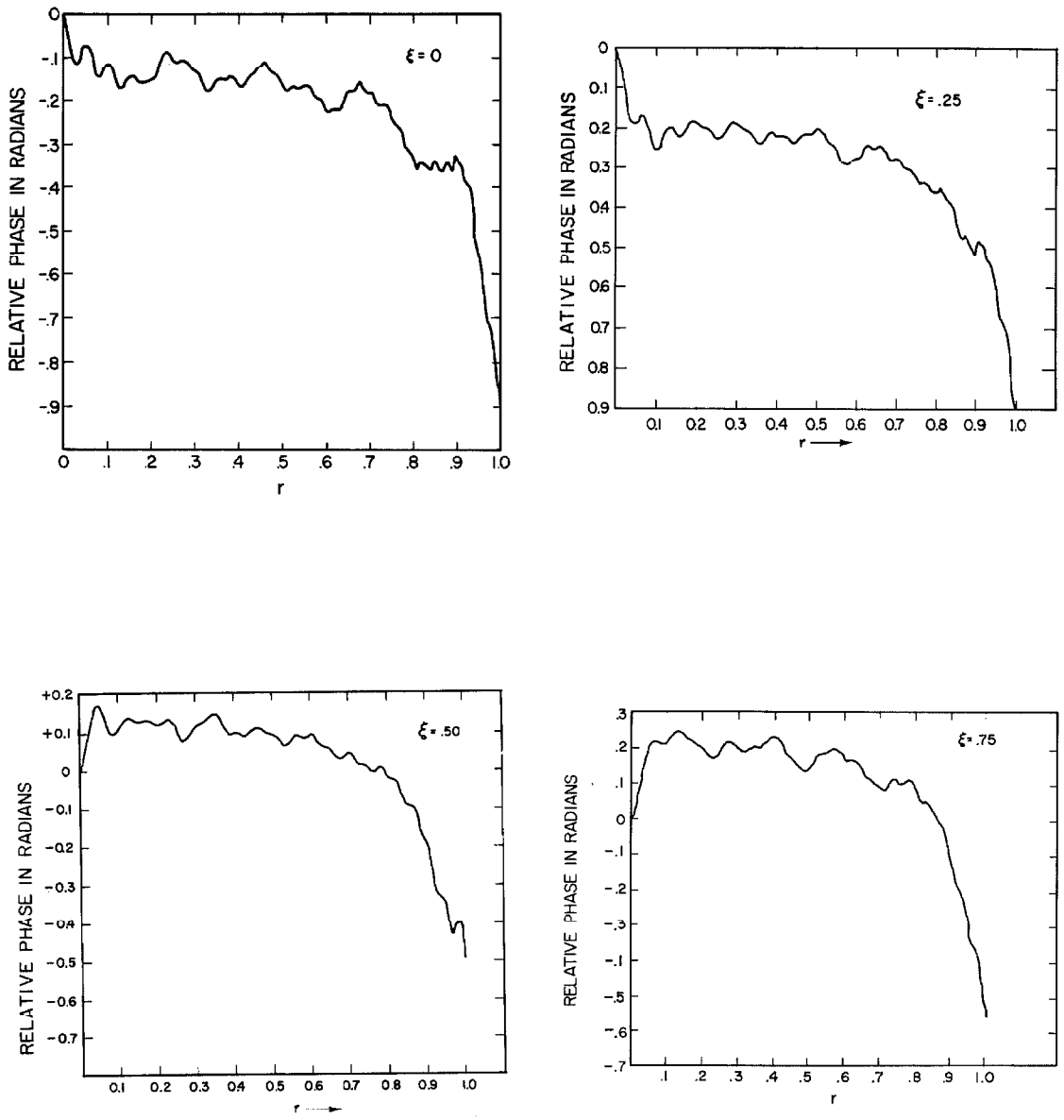

Fig. 5.16 Relative phase variation for the TEM_{00q} mode in the plane-parallel resonator at ξ = 0, .25, .50, .75.

CHAPTER VI

SUMMARY AND CONCLUSIONS

Detailed investigations of the field distributions in resonant structures with dimensions $>>\lambda$ and in which the fields are confined solely by the use of highly reflecting mirrors were motivated by the development of the optical maser. The initial analyses of Boyd and Gordon (19) and Boyd and Kogelnik (22) are only applicable to resonators formed by two mirrors in which the resultant field distribution is due to the interference of travelling waves reflected back upon themselves. This paper treats a different and more general type of resonator than that considered by previous authors. The cavity is formed by more than two mirrors so that the resultant field distribution is due to two independent, oppositely circulating travelling waves. Two resonators are examined in detail, a general symmetric N-mirror cavity and a particular nonsymmetric four-mirror cavity.

Using the methods of geometrical optics sets of simultaneous nonlinear difference equations are derived which describe the path of an optical ray in the symmetric and nonsymmetric resonators. Approximate solutions to these equations lead to relationships among the resonator parameters which must be satisfied if an optical ray is to remain inside the limits of the cavity. Such stability relationships may be interpreted as determining resonators with high and low energy loss.

A general integral equation for the mode distribution in a symmetric resonator is obtained. The same method of analysis is

extended to give a integral equation for the self-consistent fields in any arbitrary nonsymmetric resonator. Solutions to the integral equations are discussed for non-zero and zero wavelengths.

The self-consistent field analysis leads to a complete description of the field distributions in a symmetric N-mirror resonator. It is shown that when the mirror spacing is much greater than the mirror curvature only one field distribution rather than an infinite set can exist in the cavity and that this mode is characterized by high loss. Non-zero wavelength solutions are obtained for a symmetric "pseudo-confocal" resonator in which the mirrors are not spherical but are defined by the condition that the line of intersection between a mirror and a plane containing the mirror normal be a circular arc whose radius varies continuously between a maximum and minimum as the plane rotates from a position parallel to the plane of the resonator to a position perpendicular to the plane of the resonator. Unlike the two-mirror confocal cavity the modes of the symmetric pseudo-confocal multireflector resonator are not frequency degenerate. The mode distributions and resonance conditions for the symmetric N-mirror resonator with arbitrary spacing are considered in the case of very short wavelengths. The field distribution is described at any point in the resonator. It is shown that the oppositely circulating fields are entirely independent but when the resonator is not rotating may combine to form a standirg wave. The diffraction losses for three and four-mirror resonators are calculated numerically. It is found that for minimum diffraction loss the ratio of mirror spacing to mirror curvature (i.e. $\frac{\ell}{b}$)

is not constant but varies from mode to mode. The phase shifts between reflections in three and four-mirror resonators are computed and for $0 < \frac{\ell}{b} < 2 \cos \alpha$ are found to agree closely with those predicted by analytical solutions of the integral equations.

The self-consistent field analysis is applied to a particular nonsymmetric four-mirror resonator. In the limit of very short wavelength expressions are obtained for the resonance conditions and the field distribution everywhere in the cavity. The requirement that the fields be closely confined about the resonator axis leads to the stability relation among the resonator parameters previously obtained by the geometrical optics approach.

The analysis of two-mirror resonators is presented as a special case of the more general multireflector theory. The results of other authors (19,22) are obtained and extended. In general there is good agreement with previous work, however it is noted that the results obtained in this paper for the resonance condition and minimum mode volume of a symmetric nonconfocal cavity differ slightly from those of Boyd and Gordon.

The amplitude and phase distributions throughout the volume of a plane-parallel Fabry-Perot cavity are computed numerically for the TEM_{00q} mode. Except for some variation in the amount of fluctuation near the axis the amplitude curves are essentially identical at all points along the axis of the resonator. The phase distributions have a somewhat similar behavior except that the amount of phase lag between the center and edge of the field distribution is not constant throughout the resonator.

APPENDIX 1

FIRST ORDER ITERATIVE CORRECTIONS TO THE APPROXIMATE SOLUTIONS OF THE DIFFERENCE EQUATIONS GOVERNING THE PATH OF A RAY IN A SYMMETRIC N-MIRROR RESONATOR

As shown in Section 2.1c the approximate solutions to equations 2.3a to 2.3d are given by

$$r_n^{(o)} = c_1^{(o)} \cos n\theta + c_2^{(o)} \sin n\theta \qquad (2.7)$$

as well as the relations expressed by equations 2.10, 2.11 and 2.12. An inhomogeneous difference equation for $r_n^{(1)}$ is obtained by substituting these solutions into equation 2.22a with m = o:

$$r_{n+2}^{(1)} - 2\cos\theta\, r_{n+1}^{(1)} + r_n^{(1)} =$$

$$- \frac{\tan\alpha}{2\ell\cos\frac{\theta}{2}} \left[(r_{n+2}^{(o)2} - r_n^{(o)2})(1 - 2\cos\tfrac{\theta}{2}) + 2r_{n+1}^{(o)}(r_{n+2}^{(o)} - r_n^{(o)}) \right] \qquad (A1.1)$$

The substitution of the approximate solution given by equation 2.7 into A1.1 results in

$$r_{n+2}^{(1)} - 2\cos\theta\, r_{n+1}^{(1)} + r_n^{(1)} = A\cos 2n\theta + B\sin 2n\theta \qquad (A1.2)$$

where

$$A = -\frac{4 \tan \alpha}{\ell} \sin\theta \left(\cos\theta - \cos\frac{\theta}{2}\right) \left[\frac{c_1^{(o)2} - c_2^{(o)2}}{2} \sin 2\theta - c_1^{(o)} c_2^{(o)} \cos 2\theta\right] \tag{A1.3a}$$

$$B = -\frac{4 \tan \alpha}{\ell} \sin\theta \left(\cos\theta - \cos\frac{\theta}{2}\right) \left[\frac{c_1^{(o)2} - c_2^{(o)2}}{2} \cos 2\theta - c_1^{(o)} c_2^{(o)} \sin 2\theta\right] \tag{A1.3b}$$

The general solution of A1.2 consists of a complementary function and a particular solution (42). The former is simply

$$r_n^{(1)} = c_1^{(1)} \cos n\theta + c_2^{(1)} \sin n\theta \tag{A1.4}$$

The particular solution is found by the method of undetermined coefficients.

The resulting general solution for $r_n^{(1)}$ is

$$r_n^{(1)} = c_1^{(1)} \cos n\theta + c_2^{(1)} \sin n\theta + a_1 \cos 2n\theta + a_2 \sin 2n\theta \tag{A1.5}$$

where

$$a_1 = \frac{AC - BD}{C^2 + D^2}$$

$$a_2 = \frac{BC - AD}{C^2 + D^2}$$

$$C = \cos 4\theta - 2 \cos 2\theta \cos\theta + 1$$

$$D = \sin 4\theta - 2 \sin 2\theta \cos\theta$$

The first order general solution for $s_n^{(1)}$ follows from equation 2.22b, viz.

$$s_n^{(1)} = \frac{r_{n+1}^{(1)} + r_n^{(1)} - \frac{\tan \alpha}{\ell} \left(r_{n+1}^{(o)2} - r_n^{(o)2}\right)}{2 \cos \frac{\theta}{2}} \qquad \text{(A1.6)}$$

where $r_n^{(o)}$ is given by equation 2.13.

The unknown parameters $c_1^{(1)}$ and $c_2^{(1)}$ are obtained by substituting the initial conditions $r_o^{(1)} = r_o^{(o)} = d_1$ and $s_o^{(1)} = s_o^{(o)} = d_2$ into equations A1.5 and A1.6.

APPENDIX 2

AN EXPRESSION FOR THE VECTORS $\underline{E}$ AND $\underline{H}$ AT AN INTERIOR POINT IN TERMS OF THE VALUES OF $\underline{E}$ AND $\underline{H}$ OVER AN ENCLOSING SURFACE (45)

If $\underline{F}$ and $\underline{G}$ are two vector fields which are continuous and have continuous first and second derivatives everywhere within a volume V and on the bounding surface S they will satisfy a vector Green's theorem, i.e.

$$\int_V dV \ (\underline{F} \cdot \nabla x \ \nabla x \ \underline{G} - \underline{G} \cdot \nabla x \ \nabla x \ \underline{F}) = \int_S dS \ (\underline{G} \ x \ \nabla x \ \underline{F} - \underline{F} \ x \nabla x \ \underline{G}) \cdot \underline{n} \qquad (A2.1)$$

In equation A2.1 replace $\underline{F}$ by the electric field $\underline{E}$ and $\underline{G}$ by $\underline{a}\varphi = \underline{a}\,\frac{e}{r}^{-jkr}$ where $\underline{a}$ is an arbitrary constant vector and r is the distance from an arbitrary surface point to a fixed interior observation point P. In a source-free volume

$$\nabla x \nabla x \underline{E} = k^2 \underline{E} \text{ and } \nabla \cdot \underline{E} = 0.$$

With the vector identities

$$\nabla x \nabla x (\underline{a}\varphi) = \underline{a} k^2 \varphi + \nabla (\underline{a} \cdot \nabla \varphi)$$

$$\underline{E} \cdot \nabla (\underline{a} \cdot \nabla \varphi) = \nabla \cdot \left[\underline{E} (\underline{a} \cdot \nabla \varphi)\right]$$

equation A2.1 becomes

$$\int_S dS \left[a\varphi \times \nabla \times \underline{E} - \underline{E} \times \nabla \times \underline{a}\varphi - \underline{E} (\underline{a} \cdot \nabla\varphi) \right] \cdot \underline{n} = 0 \qquad \text{(A2.2)}$$

The additional relations

$$(\underline{a} \times \nabla \times \underline{E}) \cdot \underline{n} = -j\omega\mu \, \underline{a} \cdot (\underline{n} \times \underline{H})$$

$$(\underline{E} \times \nabla \times \underline{a}\varphi) \cdot \underline{n} = \underline{a} \cdot (\underline{n} \times \underline{E} \times \nabla\varphi)$$

allow A2.2 to be rewritten as

$$\int_S dS \, \underline{a} \cdot \left[j\omega\mu \, (\underline{n} \times \underline{H}) + (\underline{n} \times \underline{E}) \times \nabla\varphi + (\underline{n} \cdot \underline{E}) \nabla\varphi \right] = 0 \qquad \text{(A2.3)}$$

Since $\underline{a}$ is an arbitrary vector it may be dropped.

The validity of equation A2.3 is based on the assumption that the fields are continuous and possess continuous first and second derivatives. However $\underline{a}\varphi$ has a singularity at $r = o$ and consequently this point must be excluded. A sphere of radius r_1 is circumscribed about the point P, its normal directed out of V and consequently radially toward the center.

$$\nabla\varphi = \left(\frac{1}{r} + jk\right) \frac{e^{-jkr}}{r} \underline{r}_o$$

and on the sphere $\underline{n} = \underline{r}_o$. The area of the sphere vanishes with the radius as $4\pi r_1^2$ and, since

$$(\underline{n} \times \underline{E}) \times \underline{n} + (\underline{n} \cdot \underline{E}) \underline{n} = \underline{E}$$

the contribution of the spherical surface to the integral of equation A2.3 is $4\pi \underline{E}(P)$. Thus the value of $\underline{E}$ and any interior point P of V is

$$\underline{E}(P) = -\frac{1}{4\pi}\int_S dS \left[j\omega\mu (\underline{n} \times \underline{H})\varphi + (\underline{n} \times \underline{E}) \times \nabla\varphi + (\underline{n} \cdot \underline{E})\nabla\varphi \right] \quad (A2.4)$$

APPENDIX 3

PROPAGATION IN ROTATING SYSTEMS (47)

The motion of a particle on the surface of the earth is affected by two gravitational fields. The first of these is the static gravity field whose origin is not completely understood. The effect of this field on the solution of electromagnetic theory problems is generally neglected. The second gravitational field is due to the rotation of the earth. The second postulate of Einstein's general theory of relativity, the principle of equivalence, asserts the equality of gravitational and inertial mass. Thus the properties of motion in a noninertial system are the same as those in an inertial system in the presence of a gravitational field.

The consequences of this latter gravitational field are not completely negligible. Although the rotational effect is similar to gravity in that they are both constant (i.e. it is possible to choose a system of reference in which all components of the metric tensor are independent of time) it is different in that it is not produced by a body which is static but by one which is in motion.

Maxwell's equations in a uniformly rotating system may be written the usual three-dimensional form, viz.

$$\nabla \times \underline{E} = -\frac{1}{c}\frac{\partial \underline{B}}{\partial t} \qquad \nabla \cdot \underline{D} = 0$$

$$\nabla \times \underline{H} = \frac{1}{c}\frac{\partial \underline{D}}{\partial t} \qquad \nabla \cdot \underline{B} = 0 \tag{A3.1}$$

However the constitutive equations are no longer linear, i.e.

$$\underline{D} = \frac{\underline{E}}{\sqrt{h}} + \underline{H} \times \underline{g}$$

$$\underline{B} = \frac{\underline{H}}{\sqrt{h}} + \underline{g} \times \underline{E} \qquad \text{(A3.2)}$$

where in cylindrical coordinates for example

$$h = \left(1 - \frac{\omega^2 r^2}{c^2}\right) \qquad \text{(A3.3)}$$

$$g = \begin{pmatrix} 0 \\ \frac{\omega^2 r^2}{c} \\ 0 \end{pmatrix} \qquad \text{(A3.4)}$$

ω = rotation rate about the z-axis in radians per second.

Moreover the vector operations are performed in three-dimensional space with the metric

$$\gamma = \begin{pmatrix} 1 & 0 & 0 \\ 0 & r^2 + \frac{\omega^4 r^4}{hc^2} & 0 \\ 0 & 0 & 1 \end{pmatrix} \qquad \text{(A3.5)}$$

An additional property of the gravitational field due to uniform rotation is the difference in times in and opposite to the direction of rotation. A consequence of this property is that in travelling around a closed path light will experience a time delay per circuit of

$$t = \pm \frac{2\omega S\cos\theta}{c^2} \qquad \text{(A3.6)}$$

where S is the enclosed area of the circuit, θ is the angle between the normal to S and the axis of rotation, and $\pm$ refer to propagation in and opposite to the direction of rotation.

As far as multi-reflector resonators are concerned this time delay will require that the oppositely circulating fields have slightly different resonant frequencies. For mechanically stable structures this frequency difference is observed by mixing the two waves on a photosurface. With presently available gas lasers the beat frequency will be less than 100 cycles per second.

In the analysis presented in this paper the effect of rotation will be neglected in the description of the resonator fields.

APPENDIX 4

SOLUTION OF THE GENERAL INTEGRAL EQUATION

The type of integral equation which arises in this approach to the theory of optical resonators is homogeneous Fredholm equation of the second kind, i.e.

$$\sigma f(z) = \frac{1}{2\pi} \int_{-\sqrt{c}}^{\sqrt{c}} dz_o \, f(z_o) \, e^{j(\gamma z^2 + \gamma z_o^2 + z z_o)} \qquad (A4.1)$$

As noted in Section 3.2 little can be deduced about the solutions of an integral equation with a symmetric, complex but non-Hermitian kernel. Each case must be solved individually.

The existence of self-consistent fields in the resonator as shown by numerical iteration (18,24,25) implies that equation A4.1 may have several eigenfunctions and eigenvalues. Extrapolation of closed resonator theory to open resonators suggests that modes, if they exist, would be orthogonal. This indicates that an avenue to be explored in attempting to solve A4.1 is the expansion of the kernel as a sum of orthogonal functions. It is also intuitively obvious that the desired solutions must all decrease rapidly for increasing arguments.

A plane wave in λ-μ space may be expanded as a sum of cylindrical parabolic (or Weber) functions (51) i.e.

$$e^{j(\lambda \cos\varphi + \mu \sin\varphi)^2} = e^{\frac{j}{2}(\lambda^2+\mu^2)} \sec\varphi \sum_{n=0}^{\infty} \frac{j^n}{n!} \tan^n\varphi \, D_n(\lambda\sqrt{-2j}) D_n(\mu\sqrt{2j}) \qquad (A4.2)$$

In order that a solution of the Helmholtz equation in parabolic coordinates be single-valued over the $\lambda - \mu$ plane it is necessary that n be an integer (52). For integral values of n the cylindrical parabolic functions are expressible as Hermite polynomials (51), viz.

$$D_n(z) = z^{-\frac{n}{2}} e^{-z\frac{2}{4}} He_m\left(\frac{z}{\sqrt{2}}\right) \tag{A4.3}$$

Hence the plane wave expansion becomes

$$e^{j(\lambda^2 \frac{\cos 2\varphi}{2} - \mu^2 \frac{\cos 2\varphi}{2} + \mu\lambda \sin 2\varphi)} = e^{\frac{j}{2}(\lambda^2 - \mu^2)} \sum_{n=0}^{\infty} \left(\frac{j}{2}\right)^n \frac{\sin^n \varphi}{\cos^{n+1}\varphi} \frac{1}{n!} He_n(\lambda\sqrt{-j}) He_n(\mu\sqrt{j}) \tag{A4.4}$$

The kernel of integral equation A4.1 may be rewritten in a form similar to the left-hand side of equation A4.4,

$$e^{j(\gamma z + \gamma z + z z)} = e^{j\left\{\left[(4\gamma^2-1)^{\frac{1}{4}} z\right]^2 \frac{\gamma}{(4\gamma^2-1)^{\frac{1}{2}}} - \left[-j(4\gamma^2-1)^{\frac{1}{4}} z_o\right]^2 \frac{\gamma}{(4\gamma^2-1)^{\frac{1}{2}}} + \left[-j(4\gamma^2-1)^{\frac{1}{2}} z z_o\right] \frac{j}{(4\gamma^2-1)^{\frac{1}{2}}}\right\}} \tag{A4.5}$$

Thus by comparison with A4.4 the kernel in A4.1 may be replaced by a sum of Hermite-Gaussian functions.

$$\sigma_n f_n(z) = \frac{1}{\sqrt{\pi}} \int_{-\sqrt{c}}^{\sqrt{c}} dz_o \; f_n(z_o) \sum_{n=0}^{\infty} \frac{(-1)^n}{2^n n!} \beta \frac{(\beta^2+2j\gamma)^{\frac{n}{2}}}{(\beta^2-2j\gamma)^{\frac{n+1}{2}}}$$

$$He_n(\beta z_o)\, He_n(\beta z)\, e^{-\frac{\beta^2}{2}(z_o^2+z^2)} \qquad (A.46)$$

where

$$\beta = (1-4\gamma^2)^{\frac{1}{4}}$$

The orthogonality relation for Hermite polynomials is (53)

$$\int_{-\infty}^{\infty} He_m(z)\, He_n(z)\, e^{-z^2}\, dz = \delta_{mn}\, 2^n\, n!\, \sqrt{\pi} \qquad (A4.7)$$

Thus in the limit of $c = \infty$ it is obvious from inspection that the solutions of equation A4.6 are

$$f_n(z) \propto e^{-\frac{\beta^2}{2} z^2}\, He_n(\beta z) \qquad (A4.8)$$

The eigenvalues are obtained by substituting for $f_n(z)$, interchanging the order of integration and summation, and applying the orthogonality relations for Hermite polynomials. The result is

$$\sigma_n = (-1)^{\frac{n}{2}}\, e^{j\,(n+\frac{1}{2})\,\tan^{-1}\frac{2\gamma}{\beta^2}} \qquad (A4.9)$$

APPENDIX 5

APPROXIMATION TO THE LOWEST ORDER EIGENVALUE FOR THE SYMMETRIC, NONCONFOCAL TWO-MIRROR RESONATOR

It has been shown in Appendix 4 that a solution to the general integral equation arising from the self-consistent field analysis of optical resonators may be obtained in the limit of zero wavelength. One intuitively feels that these same functions will be a good approximation to the exact solution of the problem with $\lambda \neq 0$. Then from equation A4.6

$$\sigma_n \, He_n(\beta z) \, e^{-\frac{\beta^2 z^2}{2}} \simeq \frac{1}{\sqrt{\pi}} \int_{-\sqrt{c}}^{\sqrt{c}} dz_o \, \beta \, He_n(\beta z_o) \, e^{-\frac{\beta^2 z_o^2}{2}}$$

$$\sum_{m=0}^{\infty} \frac{(-1)^{\frac{m}{2}}}{2^m m!} \frac{(\beta^2+2j\gamma)^{\frac{m}{2}}}{(\beta^2-2j\gamma)^{\frac{m+1}{2}}} He_m(\beta z) \, He_m(\beta z_o) \, e^{-\frac{\beta^2}{2}(z^2+z_o^2)} \tag{A5.1}$$

For m and n = 0 equation A5.1 reduces to

$$\sigma_o \simeq \operatorname{erf}(\beta\sqrt{c}) \, e^{\frac{j}{2}\tan^{-1}\frac{2\gamma}{\beta^2}} \tag{A5.2}$$

The validity of equation A5.2 is based on the assumption that

$$\sum_{m=0}^{\infty} \frac{(-1)^{\frac{m}{2}}}{2^m m!} e^{j(m+\frac{1}{2})\tan^{-1}\frac{2\gamma}{\beta^2}} \int_{-\sqrt{c}}^{\sqrt{c}} dz_o \, \beta \, He_m(\beta z_o) \, e^{-\frac{\beta z_o^2}{2}} \tag{A5.3}$$

may be neglected for $m > o$.

The first few terms of equation A5.3 are

$$\operatorname{erf}(\beta\sqrt{c})\, e^{\frac{j}{2}\tan^{-1}\frac{2\gamma}{\beta^2}} - \frac{\beta\sqrt{c}}{2\sqrt{\pi}}\, e^{-\beta^2 c}\left[e^{j\frac{5}{2}\tan^{-1}\frac{2\gamma}{\beta^2}} - \frac{1}{8} e^{j\frac{9}{2}\tan^{-1}\frac{2\gamma}{\beta^2}} + \cdots \right]$$

$$- \frac{(\beta\sqrt{c})}{24\sqrt{\pi}}\, e^{-\beta^2 c}\left[e^{j\frac{9}{2}\tan^{-1}\frac{2\gamma}{\beta^2}} \cdots \right] \qquad \text{(A5.4)}$$

In the following example it is evident that only the first term of equation A5.4 need be retained.

$$c = \frac{ka^2}{\ell} = \pi, \quad 0 < \frac{\ell}{b} < 2$$

$\frac{\ell}{b}$	β	$\operatorname{erf}(\beta\sqrt{c})$	$\frac{\beta\sqrt{c}}{2\sqrt{\pi}} e^{-\beta^2 c}$	$\frac{(\beta\sqrt{c})^3}{24\sqrt{\pi}} e^{-\beta^2 c}$
1.75	0.824	0.961	0.060	0.010_7
1.50	0.930	0.980	0.032	0.007_3
1.25	0.984	0.986	0.024	0.006_0
1.00	1.000	0.988	0.022	0.005_7
0.75	0.984	0.986	0.024	0.006_0
0.50	0.930	0.980	0.032	0.007_3
0.25	0.824	0.961	0.060	0.010_7

The relative values of erf $(\beta\sqrt{c})$, $\frac{\beta\sqrt{c}}{2\sqrt{\pi}}\, e^{-\beta^2 c}$ and $\frac{(\beta\sqrt{c})^3}{24\sqrt{\pi}}\, e^{-\beta^2 c}$ demonstrate clearly that equation A5.2 is a good approximation to the lowest order eigenvalue of equation A4.1 with finite limits.

REFERENCES

1. A. L. Schawlow and C. H. Townes, "Infrared and Optical Masers", Phys. Rev. 112, pp. 1940-1949 (1958).

2. A. M. Prokhorov, "Molecular Amplifier and Generator for Submillimeter Waves", Soviet Physics JETP 7, pp. 1140-1141 (1958).

3. R. H. Dicke, U. S. Patent No. 2, 851, 652, (1958).

4. For example see J. R. Singer, Masers, John Wiley and Sons, New York (1959).

5. T. H. Maiman, "Optical Maser Action in Ruby", British Communications and Electronics 7, p. 674 (1960).

6. T. H. Maiman, "Stimulated Optical Radiation in Ruby", Nature 187, p. 493 (1960).

7. A. Javan, W. R. Bennett and D. R. Harriott, "Population Inversion and Continuous Optical Maser Oscillation in a Gas Discharge", Phys. Rev. Letters 6, pp. 106-110 (1961).

8. E. Snitzer, "Optical Maser Action of Nd^{+3} in Barium Crown Glass", Phys. Rev. Letters 7, pp. 444-446 (1961).

9. R. N. Hall et al, "Coherent Light Emission from GaAs Junctions", Phys. Rev. Letters 9, pp. 366-368 (1962).

10. M. I. Nathan et al, "Stimulated Emission of Radiation from GaAs p-n Junctions", Appl. Phys. Letters 1, pp. 62-64 (1962).

11. T. M. Quist et al, "Semiconductor Maser of GaAs", Appl. Phys. Letters 1, pp. 91-92 (1962).

12. E. V. Ashburn et al, "Bibliography of the Open Literature on Lasers I and II", J. Opt. Soc. 53, pp. 647-652 (1963) and 54, pp. 135-142, (1964).

13. J. F. Price and A. K. Dunlop, "Masers and Lasers, A Bibliography", STL Research Bibliography No. 41 (1962).

14. "Optical Masers", Appl. Optics Supplement (1962).

15. S. K. Poultney, "Bibliography on Optical Masers and Related Subjects", Solid State Design, p. 49 et seq. (Nov. 1963) and p. 36 et seq. (Jan. 1964).

16. F. J. McLung and R. W. Hellwarth, "Giant Optical Pulsations from Ruby", J. Appl. Phys. 33, pp. 828-830 (1962).

17. M. Born and E. Wolf, Principles of Optics, Pergamon Press (1959) pp. 322-340.

18. A. G. Fox and T. Li, "Resonant Modes in a Maser Interferometer", B.S.T.J. 40, pp. 453-488 (1961).

19. G. D. Boyd and J. P. Gordon, "Confocal Multimode Resonator for Millimeter Through Optical Wavelength Masers", B.S.T.J. 40, pp. 489-508 (1961).

20. P. Connes, "Augmentation du Produit Luminosité x Résolution des Interféromètres par L'Emploi d'une Différence des Marches Indépendante de L'Incidence", Revue d'Optique 35, pp. 37-43 (1956).

21. P. Connes, "L'Etalon de Fabry-Perot Spherique", J. Phys. Rad. 19, pp. 261-269 (1958).

22. G. D. Boyd and H. Kogelnik, "Generalized Confocal Resonator Theory", B.S.T.J. 41, pp. 1347-1369 (1962).

23. G. Goubau and F. Schwering, "On the Guided Propagation of Electromagnetic Wave Beams", IRE Trans. on Antennas and Propagation AP-9, pp. 248-256 (1961).

24. A. G. Fox and T. Li, "Modes in a Maser Interferometer with Curved and Tilted Mirrors", Proc. IRE 51, pp. 80-89 (1963).

25. R. F. Soohoo, "Nonconfocal Multimode Resonators for Masers", Proc. IRE 51, pp. 70-75 (1963).

26. C. L. Tang, "On Diffraction Losses in Laser Interferometers", Appl. Optics 1, pp. 768-770 (1962).

27. W. Culshaw, "Further Considerations on Fabry-Perot Type Resonators", IRE Trans. on Microwave Theory and Techniques MTT-10, pp. 331-339 (1962).

28. A. G. Fox et al, "On Diffraction Losses in Laser Interferometers", Appl. Optics 2, pp. 544-545 (1963).

29. S. P. Morgan, "On the Integral Equations of Laser Theory", IEEE Trans. on Microwave Theory and Techniques MTT-11, pp. 191-193 (1963)

30. J. Kotik and M. C. Newstein, "Theory of Laser Oscillations in Fabry-Perot Resonators", J. Appl. Phys. 32, pp. 178-186 (1961).

31. S. R. Barone, "Resonances of the Fabry-Perot Resonator", J. Appl. Phys. 34, pp. 831-843 (1963).

32. For example see G. Toraldo di Francia, Electromagnetic Waves, Interscience Publishers (1956), pp. 223-225.

33. L. A. Vainshtein, "Open Resonators for Lasers", Soviet Physics JETP 17, pp. 709-719 (1963).

34. R. W. Zimmerer, "Spherical Mirror Fabry-Perot Resonators", IEEE Trans. on Microwave Theory and Techniques MTT-11, pp. 371-379 (1963).

35. W. A. Specht, private communication.

36. V. Evtuhov, "Mode Structure of Laser Resonators and Problems of Mode Control", Invited paper presented at the 1963 Winter Meeting of the American Physical Society, Pasadena, California.

37. F. B. Hildebrand, Methods of Applied Mathematics, Prentice-Hall Inc. (1958), pp. 237-242.

38. Born and Wolf, op. cit., pp. 170-173.

39. J. R. Pierce, Theory and Design of Electron Beams, D. Van Nostrand and Co. (1954), pp. 194-196.

40. For example see L. Weinberg, Network Analysis and Synthesis, McGraw-Hill Book Co. (1962), pp. 22-24.

41. F. Abeles, "Recherches sur la Propagation des Ondes Electromagnetiques Sinusoidale dans les Milieux Stratifies. Application aux Couches Minces II", Ann. de Physique 5, pp. 777-781 (1950).

42. Hildebrand, op. cit., pp. 242-243.

43. P. O. Clark, "Multireflector Optical Resonators", Proc. IEEE (Correspondence) 51, pp. 949-950 (1963).

44. For example see F. E. Borgnis and C. H. Papas, Randwertprobleme Der Mikrowellenphysik, Springer-Verlag (1955), pp. 4-12.

45. For example see J. A. Stratton, Electromagnetic Theory, McGraw-Hill (1941), pp. 464-466.

46. W. R. Smythe, Static and Dynamic Electricity, McGraw-Hill (1950), pp. 495-496.

47. For example see L. D. Landau and E. M. Lifshitz, The Classical Theory of Fields (Second Edition), Addison-Wesley (1962), pp. 289-297.

48. Hildebrand, op. cit., pp. 411-413.

49. D. Slepian and H. O. Pollak, "Prolate Spheroidal Wave Functions, Fourier Analysis and Uncertainty I" B.S.T.J. 40, pp. 43-63 (1961).

50. C. Flammer, Spheroidal Wave Functions, Stanford Univ. Press (1957).

51. P. M. Morse and H. Feshback, Methods of Theoretical Physics, McGraw-Hill (1953), p. 1405.

52. Ibid. p. 1404.

53. Ibid. pp. 786-787.

54. Born and Wolf, op. cit., pp. 382-383.

55. W. Magnus and F. Oberhettinger, Functions of Mathematical Physics, Chelsea Publishing Co. (1954), p. 96.

56. Born and Wolf, op. cit., pp. 112-113.

57. Magnus and Oberhettinger, op. cit., p. 26.

58. Morse and Feshback, op. cit., pp. 784-785.